PACKING DENSITY LINKS CONCRETE MIXTURE, RHEOLOGY, AND COMPRESSIVE STRENGTH

By
Fayez Moutassem
M.Sc.

Faculty of Engineering
Department of Civil Engineering

A Thesis
Submitted to the School of Graduate Studies
In Partial Fulfillment of the Requirements
For the Degree

Doctor of Philosophy

McMaster University
Hamilton, Ontario, Canada
April 2010

PACKING DENSITY LINKS CONCRETE MIXTURE, RHEOLOGY, AND COMPRESSIVE STRENGTH

Doctor of Philosophy (2010) McMaster University

(Civil Engineering) Hamilton, Ontario

TITLE: **Packing Density Links Concrete Mixture, Rheology, and Compressive Strength**

AUTHOR: **Fayez Moutassem, M.Sc.**

SUPERVISOR: **Professor Samir E. Chidiac, Ph.D, P.Eng.**

NUMBER OF PAGES: **150 pages (i-vii, 1-142)**

Abstract

Concrete is a mixture of cement, aggregate and water, whose properties, both fresh and hardened, depend on its composition. Establishing a link between the concrete mixture, the rheological properties of fresh concrete, and the compressive strength of hardened concrete provides a predictive tool for designing the rheology and the compressive strength on the basis of its constituents. Research has shown that packing density, which is a function of the constituents, influences the rheological and the compressive strength properties of concrete. Accordingly, it is postulated that packing density, a fundamental property, is the link. On this basis, representative models for rheology and compressive strength that employ packing density as a central variable have been developed for the latter and adopted from literature for the former.

A fundamental approach was undertaken to develop a mathematical compressive strength model that is function of packing density and the concrete mixture. The proposed model accounts for the type of cement, cement degree of hydration, type and gradation of aggregates, mixture proportions and porosity. An experimental program was developed on the basis of fractional factorial design to implement, calibrate and validate the strength model. An evaluation of published models was then carried out in which the rational, limitations and potential use of these models were discussed. In addition, the applicability and accuracy of these models for different ages were investigated and compared to the proposed model using a large amount of data obtained from literature. Results reveal that the proposed model is one of the most representative and accurate models providing the highest predictability with a correlation factor of 0.93.

A methodology for the postulated link, which provides a quantitative approach to design concrete mixtures to meet specific strength requirements and rheology, was proposed. The strength model developed for this purpose and the adopted rheological models were identified. An experimental program was developed to assess the postulated link. Results reveal that packing density links concrete mixture, rheology and strength. This was confirmed through successful generation and application of correlation nomographs whose trends were found consistent with what has been reported in literature.

Acknowledgments

I am grateful to Professor Samir Chidiac for his role as my advisor and for his continuous support and encouragement. I am also appreciative of the interest and assistance I have received from my advisory committee members, Professor G. Razaqpur and Professor J. Vlachopoulos.

I would like to express my gratitude towards the Natural Science and Engineering Research Council of Canada and McMaster University for the financial support. I would also like to thank Lafarge Canada and BASF for providing us with the materials needed to conduct the experiments. Special thanks to Fathollah Mahmoodzadeh for his help in sharing ideas and conducting experiments in addition to Michael Stolle and Omar Daoud for their help with the experiments. Also, thanks are extended to Peter Koudys for his help with the test apparatuses and to Kent Wheeler and David Perrett for their help with operating the concrete mixer. Finally, I am indebted to my father Moutassem Moutassem and my mother Nadida Al Badawi for their moral support, continuous encouragement, and confidence in me.

Publication List

This thesis consists of the following papers:

Paper I

Chidiac S.E., Moutassem F., and Mahmoodzadeh F., 2010. "Compressive Strength Model for Concrete - I: Theory". To be submitted for publication.

Paper II

Chidiac S.E., Moutassem F., and Mahmoodzadeh F., 2010. "Compressive Strength Model for Concrete - II: Calibration and Validation". To be submitted for publication.

Paper III

Moutassem F. and Chidiac S.E., 2010. "Assessment of Concrete Compressive Strength Predictions Methods". To be submitted for publication.

Paper IV

Moutassem F. and Chidiac S.E., 2010. "Packing Density Links Concrete Mixture, Rheology, and Compressive Strength". To be submitted for publication.

Co-Authorship

The preparation of this thesis is in accordance with the regulations of a 'Sandwich' thesis format specified by the Faculty of Graduate Studies at McMaster University and has been co-authored.

Paper I: Compressive Strength Model for Concrete - I: Theory.
by: S.E. Chidiac, F. Moutassem, and F. Mahmoodzadeh

January 2008 – May 2009
Model was developed by F. Moutassem in consultation with Dr. S.E. Chidiac and F. Mahmoodzadeh. Paper was written by F. Moutassem and edited by Dr. S. E. Chidiac.

Paper II: Compressive Strength Model for Concrete - II: Calibration and Validation.
by: S.E. Chidiac, F. Moutassem, and F. Mahmoodzadeh

May 2006 – May 2009
The experimental program was designed by S.E. Chidiac. Experimental testing was conducted by F. Moutassem, F. Mahmoodzadeh, and O. Daoud. Data analysis was performed by F. Moutassem in consultation with Dr. S.E. Chidiac. Paper was written by F. Moutassem and edited by Dr. S. E. Chidiac.

Paper III: Assessment of Concrete Compressive Strength Predictions Methods.
by: F. Moutassem and S.E. Chidiac

September 2008 – May 2009
Data analysis and models evaluation was performed by F. Moutassem in consultation with Dr. S.E. Chidiac. Paper was written by F. Moutassem and edited by Dr. S. E. Chidiac.

Paper IV: Packing Density Links Concrete Mixture, Rheology, and Compressive Strength.
by: F. Moutassem and S.E. Chidiac

May 2006 – June 2009
The concept of linking the rheological properties of fresh concrete to the hardened properties of concrete was developed by Dr. S. E. Chidiac. Refinement of the concept was developed by F. Moutassem. Experimental program was developed by Dr. S. E. Chidiac. Experimental testing was conducted by F. Moutassem and F. Mahmoodzadeh, and O. Daoud. Data analysis was performed by F. Moutassem in consultation with Dr. S.E. Chidiac. Paper was written by F. Moutassem and edited by Dr. S. E. Chidiac.

Contents

Chapter 1: Thesis Summary

1.0 Introduction

This chapter presents a summary of the thesis starting with the research impetus. Background information is presented to brief the reader on the status of knowledge and to facilitate in following the development of the research presented thereafter. Research scope and objectives are then presented. Thesis contributions are presented in the form of technical journal papers. Summary of each paper in addition to the main conclusions are presented. Moreover, suggestions for potential future research are identified.

1.1 Research Impetus

Concrete mixture is proportioned to meet workability and compressive strength requirements. Workability is required to ensure proper mixing, placement and consolidation whereas compressive strength is a structural requirement. Current design of concrete mixture targets first the strength requirement, with the workability addressed by varying the amount of water added. The procedure tends to be iterative and requires experimental testing of the concrete properties. This research provides a new methodology for addressing the workability and strength requirements simultaneously using a fundamental approach. Specifically, this research seeks to develop a predictive tool for characterizing the workability of fresh concrete and strength of hardened concrete from the composition of the mixture. It is further postulated that packing density will provide the link between the concrete mixture, rheology and strength.

1.2 Background

1.2.1 Introduction

Concrete is a heterogeneous mixture of cement, aggregates and water. The composition of the mixture influences the workability of fresh concrete and the properties of hardened concrete [1]. Traditionally, concrete mixture design aims to meet workability and

compressive strength requirements [1]. The slump test has been the standard test for workability. However, it has been shown that it is not sufficient and that two rheological properties, namely yield stress and plastic viscosity, are deemed necessary to quantify the workability of normal slump concrete [2, 3, 4].

For the compressive strength, current design targets the cement content and water-to-cement ratio (w/c) [1]. Research has shown that accounting for these two factors only is not sufficient and that other factors need be considered [5]. In addition, the current mix design approach is not fundamental but is rather phenomenological and statistical. A fundamental approach may allow for establishing a continuous link between the concrete mixture, rheology and compressive strength and thus provide control over the design.

Packing density, which indicates how efficiently particles fill a certain volume, is a fundamental property that is function of the mixture and that is statistically significant for both strength and slump (rheology) [5]. Therefore, it is postulated that packing density can be the central variable linking mixture composition, rheological properties and compressive strength.

This section is divided into 4 subsections. First subsection presents background information on packing density, its significance on the properties, its experimental measurement and a review of proposed models that relate packing density to the mixture. Subsection two presents background information on workability / rheology in which its importance, experimental measurement, relation to packing density, and review of models that are function of packing density are given. Subsection three deals with the compressive strength of concrete in which background information on cement chemistry, stoichiometry, and hydration are given first. In addition, the importance of hydration, its relation to the concrete mixture and packing density, experimental measurement, and review of models are given. Subsection four presents a review of the attempts made to link the concrete mixture, the rheological properties and the compressive strength to each other. In addition, emphasis is placed on specific gaps that need filling throughout these subsections, in order to achieve the main goals of this study.

1.2.2 Packing Density

1.2.2.1 Definition and Significance

Packing density is defined as the ratio of the volume of the solid particles to the bulk volume occupied by these particles [6]. This fundamental property indicates how efficiently particles fill a certain volume. For concrete, the packing density of aggregates is defined as [5]:

$$\phi_{agg} = \frac{V_{agg}}{V_t} = \frac{V_{agg}}{V_{agg} + V_v} = 1 - e \tag{1.1}$$

where V_{agg} is the volume of aggregates, V_t the total volume, V_v the volume of voids, and e the voids ratio. The packing density of concrete, ϕ_{conc}, is the volume fraction of solids in the concrete mix.

An increase in the packing density of aggregates through improved aggregates gradation and proportions, which leads to reduction in the amount of voids, will yield an increase in the amount of excess paste beyond what is required to fill the voids between the aggregates. This results in further lubrication of the mix and dispersion of its particles which leads to an increase in the workability of fresh concrete. In addition, an increase in the packing density of aggregates yields an increase in the strength of hardened concrete by allowing for a reduction in the water to cement ratio for the same workability [5]. Research has shown that workability is a function of the ratio of packing density of fresh concrete to its maximum packing density, $(\phi/\phi^*)_{conc}$ [5, 7, 8]. Research has also shown that the compressive strength is function of the concrete mixture and the ratio of packing density of aggregates in a concrete mixture to its maximum packing density, $(\phi/\phi^*)_{agg}$ [5]. For a given mixture, the maximum packing density is function of the size, shape, surface texture, and volume fraction of solids in addition to the method of compaction [5, 6, 9-16]. Packing density of aggregates has been shown to correlate with the packing density of fresh concrete, i.e., for a given cement content, increasing the packing density of aggregates yields an increase in the packing density of fresh concrete [5]. Hence, one can

deduce that packing density is the common parameter and can be the key to linking the concrete mixture, workability and strength.

1.2.2.2 Experimental Measurement

In a mixture of fine and coarse aggregates, given the method of compaction and the volume fractions of the particles, the maximum packing density of dry aggregates can be measured using cylindrical steel containers whose height and diameter is greater than 5 times the maximum aggregate size. According to ASTM C29 [17], the container is filled in 3 layers with each layer compacted 25 times with a rod. The surplus aggregate is then removed and the surface finished by rolling a steel rod across the top. The maximum packing density is then calculated according to:

$$\phi^*_{agg} = \frac{V_{agg}}{V_c} = \frac{W_{agg}}{V_c \gamma_{agg}} \tag{1.2}$$

where W_{agg} is the weight of the aggregate, γ_{agg} the specific gravity of the aggregates, V_{agg} the volume of solid and V_c the volume of the container. On the other hand, maximum packing density of concrete, ϕ^*_{conc}, which also involves wet cement, is difficult to measure experimentally and there is no accepted method of measurement [6]. In addition, the optimum mixture proportions which would yield an optimum maximum packing density for optimum workability and strength cannot be measured experimentally. Accordingly, models developed to predict the packing density of dry particles are used to study the maximum packing density of concrete.

1.2.2.3 Review of Packing Density Models

Numerous packing density models have been reported in the literature [5, 10-16]. The Furnas and Aim and Goff (AGM) models assume that the amount of fine particles is either much less than the amount of coarse particles to fill the voids or much higher so as to act as a medium in which the coarse particles are embedded [10, 11]. These models are

expected to yield better estimates when the volume fraction of fine particles is either too large or too small. Therefore, they are not suitable to calculate the packing density of aggregates used in concrete. In addition, these models are more applicable to smaller diameter ratios i.e. when the ratio between the diameters of the sand and coarse particles is small. In the Modified Toufar Model (MTM) [12], it is assumed that the diameter ratios of particles greater than 0.22 will be too large to be situated within the interstices between the larger particles. The result is a packing of the matrix that may be considered as a mixture of packed areas mainly consisting of larger particles, and packed areas that mainly consist of smaller particles with larger particles distributed discretely throughout the matrix of smaller particles. Therefore, this model is expected to yield good estimates for large diameter ratios. The AGM and the MTM assume that fine and coarse aggregate are of different sizes, which may lead to problems when the two aggregates have overlapping fractions. However, this problem is not usually encountered in concrete.

The linear packing model (LPM) [13] considers the un-mixing mechanism because it always assumes that there is only one controlling component. Therefore, the predictions can be adequate when the diameter ratios are large. On the other hand, the mixture packing model (MPM) [15] only considers the mixing mechanism and cannot satisfactorily account for the packing formed by the un-mixing mechanism. Therefore, the resultant predictions may not match the measurements well if the size ratios involved are small. The linear-mixture packing model (LMPM) [15] is a combination of the two models since it considers both the un-mixing and mixing mechanisms and is therefore superior to both models. However, it fails to accurately predict the packing density when there is a large difference in the initial experimental packing densities of the sand and coarse aggregate particles. In other words, it can only be used for packing systems in which the maximum difference between the initial packing densities is relatively small, i.e. less than 0.1.

In the theory of particle mixtures model (TPM) [16], each mono-sized particle is assumed to be associated with a single corresponding void. However, in reality, each solid particle shares voids with other particles. This model is based on the sequence of combining the

finest materials before adding the coarsest material. It assumes that a graded material can be represented by a single sized material (characteristic diameter) having the same void ratio as the graded material. This would create problems if a material with a gap in its grading is to be combined with a material with a mean size within that gap. This is usually not a problem for concrete and it was shown to produce good estimates of packing density.

The CPM [5] is a refined version of the LPM where the virtual packing and compaction index concepts are introduced and the wall and loosening effects are accounted for. The CPM covers combinations of any number of individual aggregate fractions, having any type of size distribution. In addition, the CPM can be used to predict the maximum packing density of concrete [5]. Using the CPM, the maximum packing density, ϕ^*, can be calculated from the following equation [5]:

$$\Pi = \sum_{i=1}^{n} \frac{\frac{\theta_i}{\beta_i}}{\frac{1}{\phi^*} - \frac{1}{\gamma_i}} \tag{1.3}$$

where Π is the partial compaction index that depends on the method of compaction (4.1 for loose, 4.5 for rodding, 4.9 for vibration, and 9 for vibration + pressure); θ_i the volume fraction of particle i; β_i the residual packing density of particle i at infinite amount of packing energy, which is approximated from $\beta_i = \phi_i^*/\Pi + \phi_i^*$; γ_i the virtual packing density of component i in the mixture. γ_i is defined as the maximum value of ϕ^*, which is attainable by placing the grains one by one, without altering their shape. The virtual packing density is the maximum packing density attainable with the material considered with an infinite amount of packing energy and is expressed as follows [5]:

$$\gamma = \gamma_i = \frac{\beta_i}{1 - \sum_{j=1}^{i-1} \theta_j \left(1 - \beta_i + b_{i,j}\beta_i\left(1 - \frac{1}{\beta_j}\right)\right) - \sum_{j=i+1}^{n} \theta_j \left(1 - a_{i,j}\frac{\beta_i}{\beta_j}\right)} \tag{1.4}$$

$$a_{i.j} = \sqrt{1-\left(1-\frac{d_j}{d_i}\right)^{1.02}} \quad (1.5)$$

$$b_{i.j} = 1-\left(1-\frac{d_i}{d_j}\right)^{1.5} \quad (1.6)$$

where d_i and d_j are the diameters of the monosized grains i and j, respectively; $a_{i,j}$ describes the loosening effect exerted by the finer particles i.e. class j on the class i (if $d_i > d_j$); $b_{i,j}$ describes the wall effect exerted by the coarser grains i.e. class j on the class i (if $d_j > d_i$).

In order to account for the different sizes of fine aggregate, coarse aggregate and cement particles, a characteristic diameter concept corresponding to 63.2% passing was introduced [9]. Given the method of compaction and knowing the followings; volume fractions of cement, fine aggregate and coarse aggregate, their characteristic diameters, and their maximum packing densities; the CPM model can be employed to calculate ϕ^*_{agg} and ϕ^*_{conc}.

1.2.3 Workability and Rheology

1.2.3.1 Definition and Significance

Workability is defined by the American Concrete Institute as "the property of fresh mixed concrete or mortar that determine the ease with which it can be mixed, placed, consolidated, and finished to a homogeneous condition [18]. The slump test has been the most widely used standardized test for measurement of workability. However, research has shown that the slump test is not sufficient for field applications and that two rheological parameters, the yield stress and plastic viscosity, are needed to characterize the flow of normal slump concrete [2, 3, 4]. The current standard for the design of concrete mixtures does not account for the plastic viscosity. Plastic viscosity is needed to avoid problems with mixing, placing particularly pumping, consolidation, finishing, and

stability. Therefore the current standard is not adequate for characterizing workability and controlling the quality of concrete.

The flow of concrete is described using Bingham's model and is given by:

$$\tau = \tau_0 + \eta\ \dot{\gamma} \tag{1.7}$$

where τ is the shear stress, $\dot{\gamma}$ the shear strain rate, τ_o the yield stress, and μ the plastic viscosity. The yield stress is the stress needed to initiate flow of concrete whereas the plastic viscosity provides a measure of the resistance to changes in shape or arrangement of its constituents [3].

1.2.3.2 Experimental Measurement

Different apparatuses were developed to measure the rheological properties: Tattersall's Two Point Test, Bertta Apparatus, the Btrheom rheometer, the SLRM II, etc. [19]. Tattersall two-point test device measures the torque needed to turn an impeller in concrete. The BML viscometer, which is a coaxial cylinder rheometer that consists of internal vertical blades and an outer rotating cylinder, is intended for concrete with slump more than 120 mm [20]. The IBB rheometer, which consists of a rotating impeller and a fixed container, was developed as an adjustment to Tattersall two-point test to measure the rheology of shotcrete [20]. Btrheom rheometer, which consists of a fixed part and rotating part, controls the speed of the rotating part and measures the corresponding resultant torques. Results are then fitted to Bingham's model to determine the rheological properties. Btrheom measures the flow for slumps higher than 80 mm and may cause segregation for very high slump concretes due to the shear force applied. SLRM II is a modified slump test which introduces the variable of time to the standard slump test. This apparatus, which is based on free fall, can measure the rheological properties for any value of slump. SLRM II is used to measure the concrete slump as a function of time, the slump flow, S_f, the slump, S_l, and the time of slump, t_{slump}. Subsequently, the rheological properties are determined [21, 22]:

$$\tau_o = \frac{4gV\rho}{\sqrt{3}\pi S_f^{\,2}} = 0.0397\left(\frac{\rho}{S_f^{\,2}}\right) \tag{1.8}$$

$$\eta = \frac{\rho g H V}{150\pi S_l S_f^{\,2}} t_{slump} \tag{1.9}$$

where ρ is the concrete density, H the height of the slump cone, V the volume of slump cone, and g the gravitational acceleration.

1.2.3.3 Review of Rheological Models

Plastic Viscosity

Phenomenological and fundamental plastic viscosity models have been reported in literature. Phenomenological models are based on observation. One of the most promising phenomenological models was developed by De Larrard [5]. His empirical model predicts the plastic viscosity of concrete as a function of the ratio of the packing density to the maximum packing density of the concrete mixture. Unfortunately, the predictive capabilities of phenomenological models are limited by the type and range of experimental data used. Fundamental models on the other hand are based on scientific and engineering principles. Fundamental models have been developed for fresh concrete and others for dense suspensions.

Chidiac and Mahmoodzadeh [7] revised Zholkovskiy's [23] fundamental plastic viscosity model, which is based on the cell method. In the formulation, the cell size was modified to account for the maximum packing density. The cell method postulates that a spherical cell of fluid containing a particle in the center is the representative volume of the suspension at the microscopic level, and that the cell is subjected to actions at its boundary. Their model has been reported to provide a higher degree of correlation to the experimental data as well as a more consistent and reliable predictions in comparison to the models currently proposed in the literature [8]. According to Chidiac and Mahmoodzadeh [7], the plastic viscosity can be predicted using the following equation:

$$\eta_r \cong \eta_i y^3 \frac{4(1-y^7)}{4(1+y^{10})-25y^3(1+y^4)+42y^5} \tag{1.10}$$

where η_i is the dynamic intrinsic viscosity and is a function of the particle shape, and y the ratio of the radius of the cell to the radius of the particle and is given by:

$$y = \left(\frac{\phi}{\phi^*}\right)^{\frac{1}{3}}(1-\psi) \tag{1.11}$$

ϕ and ϕ^* are the packing density of concrete (volume fraction of solids) and the maximum packing density of the concrete mixture, respectively. ψ is a function of the concrete mixture and is defined as follows:

$$\begin{cases} \psi = C_1 \times \dfrac{M_c}{M_w} & \text{Without HRWRA} \\ \psi = C_1 \times \dfrac{M_{HRWRA}}{M_c} \times \dfrac{M_W}{M_c + M_{FineSand+Sand}} & \text{With HRWRA} \end{cases} \tag{1.12}$$

where M_c, M_w, M_{HRWRA}, $M_{FineSand+Sand}$ correspond to the mass of cement, water, high range water reducing admixture (HRWRA), and the total sand, respectively. C_1 is a calibration constant whose value depends on the method of compaction and method of measuring the rheological properties.

Yield Stress

Phenomenological and fundamental yield stress models have been reported in literature. One of the most promising phenomenological models was developed by De Larrard [5]. His empirical model predicts the yield stress of fresh concrete as a function of the partial compaction indices of the mix ingredients, which is a function of the ratio of the packing density to the maximum packing density of the concrete mixture. Chidiac and Mahmoodzadeh [7] followed the same analogy for the plastic viscosity to develop a fundamental yield stress model. The yield stress model is given by:

$$\eta_r \cong \eta_i y^3 \frac{4(1-y^7)}{4(1+y^{10})-25y^3(1+y^4)+42y^5} \quad (1.13)$$

where τ_i is referred to as intrinsic yield stress and is a function of the particle shape. Function `y` is given in equation (1.11) with ψ for yield stress model defined as:

$$\psi = C_1 \frac{M_{CA}}{M_{water}} \quad (1.14)$$

where M_{CA} and M_{water} are the mass of coarse aggregate and water in the concrete mix, respectively.

1.2.4 Compressive Strength

1.2.4.1 Cement Chemistry, Stoichiometry and Hydration

Major Portland cement phases include Tricalcium Silicate (C_3S), Dicalcium Silicate (C_2S), Tricalcium Aluminate (C_3A), Tetracalcium Alumino Ferrite (C_4AF). C_3S and C_2S together form around 75% - 80% of cement [24]. The chemical reaction between cement and water is complex and result in the formation of many hydration products. Hydration products include silicate hydrate gel (C-S-H), calcium hydroxide (CH), calcium aluminate hydrate (C_3AH_6), amorphous hydroxides ($C_2(A,F)H_8$) and other compounds such as ettringite, mono-sulfate and hydrogarnet [24]. Stoichiometry of major hydration reactions are as follows:

$2C_3S+6H \rightarrow C_3S_2H_3 + 3CH$

$2C_2S+4H \rightarrow C_3S_2H_3+CH$

$2C_3A+21H \rightarrow C_4AH_{13}+C_2AH_8 \rightarrow 2C_3AH_6+9H$

$C_4AF+16H \rightarrow 2C_2(A,F)H_8$

Understanding the hydration of individual cement components can be helpful in interpreting the complex hydration reactions between Portland cement and water. The degree of cement hydration, α, has been defined as the ratio between the quantity of

hydrated cement and the original quantity [25]. Research has shown that α, which depends on the cement properties, the water-to-cement ratio, concrete age, temperature and moisture content, is linearly related to the compressive strength of concrete [26]. Based on this and on the understanding of the hydration of different cement compounds, numerous cement hydration models have been proposed. Among these models, Byfors [27], Schindler and Folliard modified Hansen and Pederson [25, 28], and Knudsen [29] models are the most common and account for cement composition and equivalent age maturity function that is based on Arrhenius equation [28]. The two models proposed by Knudsen, i.e. linear and parabolic ones, require a determination of the induction time t_0 and constant k from experiment. These requirements limit its use as a generic model. Bentz models [30] contain fewer constants as compared to the other models and can account for different curing conditions. Bentz models was found to be adequate for comparing the relative hydration rates of one w/c versus another but fail to predict the absolute degrees of hydration especially at early ages. On the other hand, the model proposed by Schindler and Folliard is found to be simpler to apply and the calibration constants τ and β can be computed on the basis of the cementing materials characteristics and proportions. Schindler and Folliard model is as follows:

$$\alpha = \alpha_u . \exp\left(-\left[\frac{\tau}{t_e} \right]^{\beta} \right) \tag{1.15}$$

$$\tau = 66.78 . p_{C3A}{}^{-0.154} p_{C3S}{}^{-0.401} . Blaine^{-0.804} . P_{SO3}{}^{-0.758} \cdot \exp(2.187 . p_{SLAG} + 9.5 . p_{FA} . p_{FA-CaO}) \tag{1.16}$$

$$\beta = 181.4 . p_{C3A}{}^{0.146} . p_{C3S}{}^{0.227} . Blaine^{-0.535} . p_{SO3}{}^{0.558} . \exp(-0.647 . p_{SLAG}) \tag{1.17}$$

$$\alpha_u = \frac{1.031 . w/c}{0.194 + w/c} + 0.50 . p_{FA} + 0.30 . p_{SLAG} \leq 1.0 \tag{1.18}$$

$$t_e = \sum_0^t \exp\left(\frac{E}{R} \left(\frac{1}{293} - \frac{1}{T + 273} \right) \right) . \Delta t \tag{1.19}$$

where w/c is the water-to-cement ratio; t_e and t the equivalent age and age, respectively; α_u the ultimate degree of cement hydration; T the concrete temperature (°C); E the activation energy (33,500 J/mol for T > 20° C), R the universal gas constant (8.3144 J/mol/K); τ, β the hydration time parameter and hydration shape parameter, respectively; p_{C3A}, p_{C3S}, p_{SO3}, p_{FA}, p_{SLAG}, $p_{FA\text{-}CaO}$ the weight ratios in terms of total cement content.

1.2.4.2 Significance and Relation to Mixture

Compressive strength of concrete is a design requirement and a performance measure for engineers to design civil structures and infrastructures. The strength of concrete, which is a porous material, depends on the porosity of hardened concrete and the bond strength of the hydrated cement. Concrete porosity is a function of design variables such as aggregate gradation, mixture proportions, and amount of entrained air, as well as the placement protocols which include mixing, placing and compacting [5]. The bond strength depends on the cement composition, cement degree of hydration, and the aggregates type and shape [5, 31].

In the early nineteen hundreds, Abrams [32] proposed water-to-cement ratio (w/c) as an indicator for the strength of concrete. Since then, it has been shown that there are other factors that contribute to the compressive strength of concrete, namely cement properties, bonding strength / gradation of aggregates, mixture proportions, chemical admixtures and mineral admixtures [5]. Cement's chemical and physical properties contribute greatly to the compressive strength of concrete. The composition and proportions of its major chemical phases (C_3S, C_2S, C_3A, C_4AF) affect the cement hydration reactions and products formed, which in turn affect the strength of the cement paste [24]. Physical properties particularly cement fineness and particle size distributions affect concrete strength [24, 33]. Greater cement fineness increases the surface available for hydration, causing greater early compressive strength and more rapid generation of heat [33].

The aggregate bonding strength is influenced by the aggregate size, shape and surface roughness. Larger aggregate size reduces the specific surface area of the aggregate which

leads to a reduction in bond strength [34]. Crushed rough aggregate tends to provide a higher aggregate to paste bonding strength in comparison to round smooth aggregate [34]. Research has shown that mixtures with aggregate gradation that is uniformly distributed lead to higher packing resulting in concrete with higher density, reduced porosity, and higher compressive strength [34].

Concrete mixture proportions such as cement content, w/c, aggregate volume fraction and the fine-to-coarse aggregate ratio (FA/CA) influence the compressive strength of concrete significantly. An increase in the w/c due to an increase in the water content or due to a reduction in the cement content can dilute the cement paste increasing the volume, reducing the density, increasing the capillary voids, and reducing the compressive strength [34]. The higher the aggregate volume fraction, the longer is the path that a crack needs to follow since it has to move around a greater number of aggregates, which increases the energy absorbed and thus the compressive strength [33]. When the FA/CA is increased, the w/c decreases due to an increased absorption of mix water by sand, which results in an increase in the compressive strength [35].

The use of chemical and mineral admixtures can also influence the compressive strength of concrete. The use of an air entraining agent chemical admixture for durability purposes increases porosity and reduces strength [2]. The addition of fly ash and silica fume, which are mineral admixtures, improve bonding within the concrete and enhances strength [2]. The extreme fineness of the silica fume allows it to fill the microscopic voids between cement, thus also acting as a microfiller.

Research has shown that the aggregate gradation and volume fractions in a concrete mix can be represented by the packing density property which provides an indirect measurement of porosity [5].

1.2.4.3 Experimental Measurement

Testing for compressive strength is done in accordance with ASTM C39-05 [36]. The compressive strength is determined by dividing the load at failure by the average cross

sectional area. A minimum of 3 cylinders should be tested from the same mix at every age and the standard deviation for the specimens tested should not exceed the maximum permitted by ASTM C39-05.

1.2.4.4 Review of Compressive Strength Models

Compressive strength models were developed from a conceptual postulation of how particles and hydrated cement interact and bond. Based on this, the important parameters are later identified in the models. This section presents the evolution of these models, rationale, and limitations.

Feret [37] developed the first compressive strength model. Feret's model is a function of the cement concentration in the paste (cement to paste ratio), which is a physical parameter. Despite its logic, experimentally obtained concrete strengths did not show good enough correlations with this ratio [38]. In addition, the coefficients of proportionality had to be determined by trial mixes, which has limited its use [38]. Bolomey [39] proposed a linear approximation of Feret's formula because calculators were not available in those days. However, the effect of air term has disappeared. Abrams [32] replaced the cement to paste ratio with the water-cement ratio because it gave better correlation with strength when concrete is non-air entrained and due to its simplicity [38]. Unfortunately, the coefficients of proportionality need recalibration when any factor affecting the strength of concrete changes.

Powers [40] postulated that the compressive strength of cement paste is directly related to the gel/space ratio, which is the available space covering the absolute volumes of the gel and the capillary pores. The gel space ratio equals the volume of hydration products divided by the sum of the volume of hydration products and capillary porosity. His approach provides a tool for comparing the strength of cement stone at a certain degree of hydration, made with a given w/c [41]. His model was used for general mixes but the parameters considered were not enough and gave wide range of variation for concrete. Moreover, Powers model fails to account for the aggregates properties, standard cement

strength and assumes that strength starts developing at zero age. Karni [41] studied Powers model and then postulated that the volume of the gel should be related to the total volume of the paste (cement + water) minus dry cement. It was recommended to avoid incorporating the capillary pores fraction which depends on the factors affecting the compressive strength i.e. w/c and α. A revised model was proposed using Bolomey's linear relationship for fitting.

In 1998, Popovics worked on generalizing Abrams model in order to include some of the strength-effecting factors [42]. The proposed mathematical model is based on a cement model, in which the hardening of cement is the sum of two hardening processes of first order reaction. The first hardening component is the C_3S and the second is mostly the C_2S and the mixture of other cement ingredients. Each component is treated to have a different hardening rate in the model. The model also accounts for air empirically but fails to consider aggregate properties and gradation. In a separate attempt, Popovics [43] worked on improving Abrams law by incorporating the cement content parameters. In comparison to Abrams law, Popovics model accounts for air and cement content empirically.

Pann et al. [44] modified Abrams' model by incorporating the cement paste capillary porosity empirically. Hydrated cement paste consists of capillary pores, P_c, and gel pores, in which capillary pores (>10 nm) are the water filled spaces whereas gel pores (>10 nm) are the micro spaces between the hydrated cement grains. Pann stated that P_c depends on the degree of hydration and developed a statistical model to predict α at 28 days, which is a function of w/c. Although Pann claims a superior model to that of Abrams, it consists of many parameters that need calibration. Moreover, the model fails to account for concrete age and the properties and gradation of both cement and aggregates.

For dry packed particles subjected to compression, the coarse particles are subjected to maximum stresses [5]. De Larrard postulated that if cement paste is added then the paste in between two adjacent aggregates will be highly stressed, and that the distance between these aggregates is the maximum paste thickness, *MPT*. A model was presented to calculate the *MPT*, which is a function of the maximum aggregate size, D_{max}, volume

fraction of aggregate, ϕ, and packing density of aggregates, ϕ^*. The effect of aggregates through *MPT* was then incorporated using Feret's model. In addition, Feret's coefficient of proportionality, A, was proposed to be the product of the aggregate bonding strength, K, and the standard cement strength at 28 days, R_{c28}. The effect of age on strength was also considered empirically through fitting of strength versus time data.

de Larrard's model still lacks the effect of cement properties. In addition, the predictive capability of the effect of age on strength is limited by the type and range of experimental data used and so might not be suitable for extrapolation purposes. Although de Larrard's model has its limitations, it is one of the very few models that accounts for packing density. The proposed model is as follows:

$$f'_c = KR_{c28}\left[A\log(t/28)+\left(\frac{V_c}{V_c+V_w+V_a}\right)^B\right]MPT^C \tag{1.20}$$

$$MPT = D_{\max}\left(\sqrt[3]{\frac{\phi^*}{\phi}-1}\right) \tag{1.21}$$

where V_c, V_w, V_a are the volume fractions of cement, water and air in the concrete mix, respectively; A, B, C are calibration coefficients; and t is concrete age.

Mechling et al. [45] modified de Larrard model to account for the effect of cement type on strength by incorporating only the effect of C_3S on strength. The model was developed for cement pastes. The author noted that the model can be used for concrete in a similar fashion to that of de Larrard's model. Many other separate attempts to improve Feret's and Abrams' models were made [46, 47-51]. However, majority of these models are not representative and a common key shortfall is their inability to mathematically account for the effect of the packing density property on strength.

1.2.5 Linking Rheological Properties to Compressive Strength

Linking the mixture design, rheological properties and compressive strength of concrete would provide the industry with a predictive tool for designing the rheology and the compressive strength on the basis of its constituents. Very few experimental attempts [3, 52, 53] have been made to link the rheological properties and compressive strength of concrete to each other. Chidiac et al. [3] worked on correlating the rheological properties to the strength and durability of hardened concrete made with high water to cement ratio. It was observed that the concrete compressive strength increases as the yield stress and plastic viscosity increase up to an optimum value [3]. Laskar and Talukdar [52, 53] worked on correlating the rheological properties to the compressive strength of high performance concrete. It was observed that the compressive strength increases sharply at low values of yield stress and moderately at higher values. For plastic viscosity, it was observed that there exists an optimum value corresponding to maximum compressive strength. These findings illustrate that a link exists between rheology and strength. The previous attempts did not however provide a rationale for linking on the basis of mixture composition.

1.3 Thesis Scope and Objectives

The research conducted in this thesis is concerned with air entrained and non-air entrained normal strength concrete made with Ordinary Portland Cement (OPC). The primary research goal is to investigate the postulation that packing density links the concrete mixture to its rheology to its strength. The research objectives are as follows:

- Develop or adopt a model for predicting the strength of concrete that incorporates packing density as a primary variable.
- Develop or adopt a model for predicting concrete rheological properties from its composition that also employs packing density as a central variable.

- Develop a methodology linking concrete mixture, packing density, rheology and strength, and thus providing a quantitative approach to design concrete mixtures to meet specified strength requirements and rheology.
- Develop an experimental program to evaluate the models as well as the proposed methodology.

1.4 Summary of Papers

Paper I: Compressive Strength Model for Concrete – I: Theory *(To be Submitted)*

This paper presents the development of a concrete compressive strength model that accounts for the type of cement, cement degree of hydration, type and gradation of aggregates, mixture proportions, porosity and age. The theoretical formulation is presented and discussed in details. It is postulated that particles interaction are governed by excess paste theory. An average paste thickness model, *APT*, is proposed to account for concrete mixtures and aggregate gradation through packing density. In addition, the proposed model incorporates a cement hydration model to account for the type of cement and the degree of cement hydration, and parameters to account for the paste to aggregate bond strength, cement strength at 28 days, and amount of water filled and air entrapped and entrained pores.

Paper II: Compressive Strength Model for Concrete - II: Calibration and Validation *(To be Submitted)*

This paper presents the implementation, calibration and validation of the compressive strength model formulated in part I: Theory. To meet these objectives, an experimental program was developed on the basis of fractional factorial statistical design principles. The concrete mixture variables considered for the experiment were water to cement ratio, water content, bulk volume of coarse aggregate, maximum size of coarse aggregate, and air entrainment. A total of 28 mixtures were used to calibrate and validate the model. The evaluation of the proposed model included individual testing of 5 cement hydration

models, and the results revealed that the model is consistent, robust and complete. The proposed model adequately and consistently predicted the strength of the 28 concrete mixtures at 3-day and-28 day. The standard error and the correlation coefficient for the 3-day and the 28-day predictions, respectively, are 2.1 MPa and 1.8 MPa, and 0.95 and 0.96. The proposed model can be used as a tool for designing concrete mixture for a specified strength requirement on the basis of the mixture composition and properties.

Paper III: Assessment of Concrete Compressive Strength Predictions Methods *(To be Submitted)*

Theoretical and phenomenological models for predicting the compressive strength of concrete have been proposed in literature. This paper presents a review of published models, as well as an assessment of their predictive capabilities. The applicability and accuracy of these models in predicting the compressive strength of concrete at 28 days and at different ages was investigated using a large amount of experimental data obtained from literature. This study reveals that the model proposed by Chidiac et al., presented in Paper I, is one of the most representative and accurate models proposed for predicting strength at 28 days and at different ages. It provides the highest predictability with a correlation coefficient of 0.93 and a standard error of 2.2 MPa. It was also revealed that the majority of models give acceptable predications because strength is mostly affected by w/c.

Paper IV: Packing Density Links Concrete Mixture, Rheology and Compressive Strength *(To be Submitted)*

Packing density, which is a function of concrete mixture, influences the rheological properties and the compressive strength of concrete. This study was undertaken to investigate the postulation that packing density provides a link between the concrete mixture, the rheological properties, and the compressive strength. Accordingly, compressive strength model and rheological model that employ packing density as a

primary variable were identified. A model that links all three properties has been developed and evaluated using experimental data. The results have confirmed that packing density links concrete mixture, rheological properties and the compressive strength.

1.5 Conclusions

In the paper 'Compressive Strength Model for Concrete – I: Theory', a new compressive strength model for predicting the strength of concrete has been formulated. The model is characterized by the following features:

1. The hydration process is modelled through the degree of cement hydration.
2. Paste to aggregate bond strength and cement standard strength were modelled following the work of de Larrard [5].
3. Capillary pores and air content were modelled as proposed by Popovics [38].
4. Particles gradation and proportions were modelled using the proposed average paste thickness model.

Compressive Strength Model for Concrete - II: Calibration and Validation, presented in Paper II, revealed the following conclusions:

1. Proposed compressive strength model provides a good fit to the experimental data for all 5 cement hydration models.
2. The model predictions did not contain outliers or discerning pattern.
3. The standard error is found to be less than 2 MPa for both 3-day and 28-day strength predictions when using Schindler and Folliard cement hydration model. The corresponding correlation coefficient is greater than 0.95.
4. The model is capable to consistently and accurately predict the strength of concrete on the basis of its composition at 3-day and 28-day.

5. The model was capable of predicting the same trends reported in the literature due to variations in the concrete composition.
6. The proposed model, in Part I, for predicting the compressive strength of concrete based on the composition of the mixture, is a comprehensive tool for designing concrete mixture for a specific strength requirements.

Assessment of Concrete Compressive Strength Predictions Methods, presented in Paper III, has revealed the followings:

1. A review of published models has revealed that the model proposed by Chidiac et al., presented in paper I, is one of the most representative models because it accounts for the cement properties and strength, concrete age, concrete mixture, aggregate gradation, bonding capability of the aggregates to the paste, air content and voids.
2. An evaluation of published compressive strength models has revealed that the majority of the models predicted well the measured values because strength is mostly affected by w/c. Feret's model [37] which is function of cement to paste ratio resulted in the lowest predictability.
3. The model proposed by Chidiac et al. which mathematically accounts for packing density, aggregate proportions and gradations, resulted in the highest predictability for 28-day strength.
4. Models that employ the effect of age on strength developed to predict the strength at any age were also evaluated and results has revealed that Chidiac et al. model is more accurate than other models giving a correlation coefficient of 0.93 and a standard error of 2.2 MPa.
5. Aggregate proportions and gradation do not greatly influence strength in comparison with the w/c.

The experimental and analytical studies undertaken in Paper IV to investigate the postulation that packing density provides a link between the concrete mixture, the rheological properties and the compressive strength has lead to the following conclusions:

1. The model analogy developed to investigate the desired link was evaluated and has shown to provide good degree of correlation to the experimental data. The correlation factors for yield stress, plastic viscosity, and compressive strength models were 0.74, 0.92, 0.96 for air-entrained concrete and 0.83, 0.95, 0.96 for non air-entrained concrete, respectively.
2. The correlation nomographs demonstrate a continuous link between concrete mixture, rheology, and compressive strength through packing density.
3. The model correlation trends show that an increase in w/c, water content, maximum aggregate size, or air content through entrainment result in a reduction in the yield stress, plastic viscosity, and compressive strength whereas an increase in coarse aggregate volume can result either in a decrease or increase in the same properties, depending on the corresponding maximum packing density of concrete. These trends were found consistent with what has been reported in literature.
4. An analytical methodology which provides a quantitative approach to design concrete mixtures to meet specific strength requirements and rheology was proposed and proven adequate.

1.6 Suggestions for Future Work

- Recognizing that the transport of gas and liquid in concrete is influenced by porosity and that the proposed methodology accounts for porosity through packing density, extension to include mass transport properties is foreseen as a natural progression to the model.
- The compressive strength model needs to be extended to include chemical and mineral admixtures.

- The effect of ITZ on the compressive strength of concrete can be studied. The aggregate to paste bonding constant considered in some compressive strength models can then be expanded as function of ITZ.
- New design procedures can be developed for concrete mixtures that accounts for rheology and strength using packing density.

1.7 References

[1] ACI, 1974. "Proportioning concrete mixes", Publication SP-46, American Concrete Institute, Detroit.

[2] Tattersall G.H. and Banfill P.F.G., 1983. The rheology of fresh concrete. Marshfield, MA: Pitman Publishing.

[3] Chidiac S.E., Maadani O., Razaqpur A.G., Mailvaganam N.P., 2003. "Correlation of rheological properties to durability and strength of hardened concrete", Journal of Materials in civil engineering ASCE, 15(4), 391-399.

[4] Ferraris C.F. and de Larrard F., 1998. "Testing and modelling fresh concrete rheology", NISTIR 6094, Building and Fire Research Laboratory National Institute of Standards and technology, Maryland.

[5] de Larrard F., 1999. Concrete mixture proportioning: a Scientific Approach, Spon Press, London, 320pp.

[6] Wong H. and Kwan A., 2005. "Packing density: a key concept for mix design of high performance concrete", Proceedings of Materials Science and Technology in Engineering Conference (MaSTEC), Hong Kong.

[7] Chidiac S.E. and Mahmoodzadeh F., 2010. "New models for predicting plastic viscosity and yield stress of fresh concrete", Cement and Concrete Composites, To be submitted for publication.

[8] Chidiac S.E. and Mahmoodzadeh F., 2009. "Plastic viscosity of fresh concrete – A critical review of predictions methods", Cement and Concrete Composites, 31(8), 535–544.

[9] Johansen V. and Andersen P.J., 1996. "Particle packing and concrete properties", Materials Science of Concrete II, American Ceramic Society, Westerville, Ohio, 111-147.

[10] Furnas C., 1929. Flow of gases through beds of broken solids, Bureau of Mines Bulletin, Washington, D.C. USA, 164pp.

[11] Aim R.B. and Goff P.L., 1967. "Effet de Paroi dans les Empilements Désor-donnés de Sphe`res et Application a` la Porosité de Mélanges Binaires", Powder Technol. 1, 281–290.

[12] Toufar W., Born M., Klose E., 1976. "Contribution of optimization of components of different density in polydispersed particles systems", Freiberger Booklet A 558, 29-44.

[13] Stovall T., de Larrard F., Buil M., 1986. "Linear packing density model for grain mixtures", Powder Technology, 48(1), 1-12.

[14] Yu A., Zou R., Standish N., 1996. "Modifying the linear packing model for predicting the porosity of nonspherical particle mixtures", Industrial and Engineering Chemistry Research, 35(10), 3730-3741.

[15] Yu A. and Standish N., 1991. "Estimation of the porosity of particle mixtures by a linear-mixture packing model", Industrial and Engineering Chemistry Research, 30(6), 1372–85.

[16] Dewar J.D., 1999. Computer modelling of concrete mixtures, E & FN Spon, London, 238pp.

[17] ASTM C29-97, 1997. "Standard test method for bulk density and voids in aggregate", American Society for Testing of Materials, West Conshohochen, PA, USA.

[18] Koehler E. and Fowler D., 2003. "Measurement of concrete workability: Key principles and current methods", Proceedings of Eleventh Annual International Center for Aggregates Research Symposium, Austin, Texas.

[19] Ferraris C.F., 1999. "Measurement of the rheological properties of high performance concrete: state of the art report", Journal of Research of the National Institute of Standards and Technology, 104(5), 461-478.

[20] ACI Committee 238, 2008. "Report on measurements of workability and rheology of fresh concrete", ACI 238.1R-08, American Concrete Institute, Farmington Hills, MI, USA.

[21] Chidiac S.E. and Habibbeigi F., 2005. "Modelling the rheological behaviour of fresh concrete: an elasto-viscoplastic finite element approach", Computers and Concrete Journal, 2(2), 97-110.

[22] Chidiac S.E., Maadani O., Razaqpur A.G., Mailvaganam N.P., 2000. "Controlling the quality of fresh concrete – a new approach", Magazine of Concrete Research, 52(5), 353-363.

[23] Zholkovskiy E.K., Adeyinka O.B., Masliyah J.H., 2006. "Spherical cell approach for effective viscosity of suspensions", Journal Physics Chemistry B, 110(39), 19726-19734.

[24] Mehta P.K. and Monteiro P., 2006. Concrete: Microstructure, properties, and materials, Third edition, McGraw-Hill, USA.

[25] Schindler A. K. and Folliard K. J., 2005. "Heat of hydration models for cementitious materials", ACI Materials Journal, 102(1), 24–33.

[26] Ye G. and Breugel K., 2002. "Numerical simulated pore structure and its potential application in high performance concrete", In MAN Hendriks & JG Rots (Eds.), Proceedings of the 3rd DIANA world conference Finite elements in civil engineering applications, Tokyo, Japan, 135-140.

[27] Byfors J., 1980. Plain Concrete at Early Ages, Swedish Cement and Concrete Institute, Stockholm, 464pp.

[28] Hansen F. and Pedersen P., 1985. "Curing of concrete structures", Draft DEB-Guide to Durable Concrete Structures, Appendix 1, Comité Euro-International du Béton, Switzerland.

[29] Knudsen T., 1984. "The dispersion model for hydration of Portland cement: I. General concepts", Cement and Concrete Research, 14(5), 622–630.

[30] Bentz D., 2006. "Influence of water-to-cement ratio on hydration kinetics: simple models based on spatial considerations", Cement and Concrete Research, 36(2), 238–244.

[31] de Larrard F. and Belloc A., 1997. "The influence of aggregate on the compressive strength of normal and high-strength concrete", ACI Materials Journal, 94(5), 417–425.

[32] Abrams L. D., 1919, cited by Neville, A. M., Properties of Concrete, 3rd ed., Pitman, 1981.

[33] Kolias S. and Georgiou C., 2005. "The effect of paste volume and of water content on the strength and water absorption of concrete", Cement & Concrete Composites 27(2), 211–216.

[34] Quiroga P, 2003. The effect of the aggregate characteristics on the performance of portland cement concrete, Ph.D. Dissertation, The University of Texas at Austin.

[35] Basheer L., Basheer P.A.M., Long A.E., 2005. "Influence of coarse aggregate on the permeation, durability and the microstructure characteristics of ordinary portland cement concrete", Construction and Building Materials, 19(9), 682–690.

[36] ASTM C 39, 1999. "Standard test method for compressive strength of cylindrical concrete specimens", Philadelphia, PA: American Society for Testing and Materials.

[37] Feret R., 1892. "Sur la compacité des mortiers hydrauliques (On the compactness of hydraulic mortars)", Annales des Ponts et Chaussées, Série 7(4), 5-164.

[38] Popovics S., 1985. "New formulas for the prediction of the effect of porosity on concrete strength", Journal of the American Concrete Institute, 82(2), 136-146.

[39] Bolomey J., 1935. "Granulation et pre´vision de la re´sistance probable des be´tons (Aggregate grading and prediction of probable concrete strength)", Travaux, 19(30), 228–232.

[40] Powers T.C. and Brownyard, T.L., 1960. "Studies of the physical properties of hardened portland cement paste", Journal of American Concrete Institute, 18, 2.

[41] Karni J. 1974. "Prediction of compressive strength of concrete", Materials and Structures Journal., 7(3), 197–200.

[42] Popovics S., 1998. "History of a mathematical model for strength development of Portland cement concrete", ACI Materials Journal, 95(5), 593–600.

[43] Popovics S. and Ujhelyi J., 2008. "Contribution to the concrete strength versus water-cement ratio relationship", Journal Material Civil Engineering, 20(7), 459-463.

[44] Pann K. S., Yen T., Tang C. W., Lin T.D., 2003. "New strength model based on water-cement ratio and capillary porosity", Materials Journal, 100(4), 311-318.

[45] Mechling J.M., Lecomte A., Diliberto C., 2009. "Relation between cement composition and compressive strength of pure pastes", Cement and Concrete Composites, 31(4), 255-262.

[46] Tango C.E.S., 2000. "Time-generalisation of Abrams' model for high performance concrete and practical application examples", Proceedings of the International Symposium on High Performance Concrete, Hong Kong University of Science and Technology. Hong Kong, China.

[47] Yeh I.C., 2006. "Generalization of strength versus water-cementations ratio relationship to age", Cement and Concrete Research, 36(10), 1865-1873.

[48] Tangtermsirikul S., Kaewkhluab T., Jitvutikrai, P., 2004. "A compressive strength model for roller-compacted concrete with fly ash", Magazine of Concrete Research, 56(1), 35-44.

[49] Nipatsat N. and Tangtermsirikul S., 2000. "Compressive strength prediction model for fly ash concrete", Thammasat International Journal of Science and Technology, 5(1), 1–7.

[50] Hwang S.D. Lee K.M., Kim J.K., Kim J.H., 2001. "Microstructure model for estimating early-age concrete strength", First International Structural Engineering and Construction Conference, Honolulu, HI, USA, 493-497.

[51] Namyong J., Sangchun Y., Hongbum C., 2004. "Prediction of compressive strength of in-situ concrete based on mixture proportion", Journal of Asian Architecture and Building Engineering, 3(1), 9-16.

[52] Laskar A.I. and Sudip, T., 2007. "Correlation between compressive strength and rheological parameters of high-performance concrete", Research Letters in Materials Science, 10.1155/2007/45869.

[53] Laskar A.I. and Sudip, T., 2008. "A new mix design method for high performance concrete", Asian Journal of Civil Engineering, 9(1), 15-23.

Chapter 2: Paper I Compressive Strength Model for Concrete - I: Theory

Abstract

A concrete compressive strength model accounting for the type of cement, cement degree of hydration, type and gradation of aggregates, mixture proportions, and porosity was developed to predict the property. This paper presents the formulation, calibration and validation of a new model for predicting the compressive strength of normal concrete at early age and beyond. In Part I of this paper, the theoretical formulation is presented and discussed in details. It is postulated that particles interaction are governed by excess paste theory. An average paste thickness model, *APT*, is proposed to account for concrete mixtures and aggregate gradation through packing density. In addition, the proposed model incorporates a cement hydration model to account for the type of cement and the degree of cement hydration, and parameters to account for the paste to aggregate bond strength, cement strength at 28 days, and amount of water filled, entrapped and entrained pores. Part II of this paper presents the experimental program that was developed for calibrating and validating the model.

Keywords: compressive strength; degree of cement hydration; packing density; excess paste theory, average paste thickness, concrete

2.0 Introduction

Compressive strength of concrete is a performance measure for engineers to design civil structures and infrastructures [1]. Concrete strength depends on the porosity of hardened concrete, the bond strength of the hydrated cement and the strength of aggregate. Concrete porosity is a function of design variables such as aggregate gradation, mixture proportions, and amount of entrapped and entrained air, and of the placement protocols which include mixing, placing and compacting [2]. The bond strength of the hydrated

cement depends on the cement composition, cement degree of hydration, and the aggregate types, sizes and shapes [2, 3]. The aggregate strength depends on the type of aggregate. At present, proportioning concrete mixtures adheres to prescribed guidelines for achieving certain workability and strength requirements [4]. These guidelines were developed using statistical regression models and experimental data. With new advancements in cement and concrete technologies, specifically with the use of chemical and mineral admixtures, these guidelines are becoming statistically biased and therefore flawed due to the limited number of compressive strength test data that accounts for the new concrete. Moreover, concrete placement protocols are changing to accommodate the construction requirements and the workability of new concrete such as self compacting concrete, dry cast concrete, etc. One approach that is proposed to overcome the limitations with the current concrete mixture design is the development of a fundamental model for predicting the concrete compressive strength on the basis of its composition and accounting for the physical and chemical characteristics of the concrete mixture, specifically the packing density, and cement type and degree of hydration. Packing density is singled out because it provides an indirect measurement of porosity and accounts for the aggregate gradation, and proportions of aggregates and cement [3].

Numerous models for predicting the compressive strength of concrete have been proposed in the literature. The first model, proposed in 1892 by Feret [5], noted that compressive strength is a function of cement to paste ratio. Abrams simplified the strength model by replacing the cement to paste ratio with water to cement (w/c) ratio and showed that the revised model yields better correlation with measured data [6]. Powers postulated that the compressive strength of cement paste is directly related to the gel to space ratio, and improved Feret's model by incorporating the degree of cement hydration [7]. Popovics worked on generalizing Abrams model in order to include some of the strength-affecting factors [8]. The model is based on a cement model, in which the hardening of cement is the sum of two hardening processes [8].

Pann modified Abrams' model by incorporating the effects of cement paste capillary porosity on strength by postulating that capillary pores depend on the degree of cement hydration and w/c [9].

de Larrard noted that in a dry packed mixture subjected to compressive forces, the coarse particles will experience the maximum stresses. And by adding cement paste to the mixture, the paste located between the coarse particles will experience the same stress [2]. Based on this analogy, a semi-empirical model was developed to account for the effect of aggregates and their packing density on strength [2]. The model also accounts for the age of concrete using an empirical approach [2]. His proposed model, which is a significant improvement to current models, did not employ a fundamental approach to account for the cement properties and the degree of cement hydration. Mechling et al. [10] incorporated the effect of C_3S into de Larrard's model.

The literature shows that there have been many proposals to improve on Feret's and Abrams' models [11-19]. These models with the exception of de Larrard model, do not account for the aggregate gradation. Moreover, the proposed models are either empirical and/or omit one or more of the following parameters that are deemed important for predicting the compressive strength of concrete; namely, the type of cement, cement degree of hydration, type and gradation of aggregates, mixture proportions and porosity. This study, whose objective is to develop a comprehensive concrete compressive strength model, is presented in two parts. The first part provides a complete mathematical and physical description of the proposed model and the second part presents an experimental program that was developed to calibrate and assess the prediction capabilities of the proposed model.

2.1 Compressive Strength Model

The proposed model for predicting compressive strength of concrete (f'_c) comprises of two fundamental models; cement hydration model that accounts for the type of cement and the degree of cement hydration (α), and average paste thickness (APT) model that

accounts for the concrete mixtures and packing density. Moreover, the proposed model accounts for the paste to aggregate bond strength (K) and for the cement paste strength at 28 days (R_{c28}) [2]. Amount of water filled capillary pores, and entrapped and entrained air pores (EA) are also accounted for through the w/c and EA variables, respectively. Accordingly, the proposed model for f'_c at age t is a function of the following variables:

$$f'_c(t) = F\,(K, R_{c28}, APT, w/c, EA, \alpha(t)) \quad (2.1)$$

2.1.1 Cement Hydration Model

Cement which is a hydraulic material, when mixed with water, hydrates to form two major products, calcium silicate hydrates (CSH) and calcium hydroxide (CH). Cement hydration has been studied and modelled by many researches as it provides the critical link for concrete strength evolution [20]. Studies have shown that α, defined as the ratio between the quantity of hydrated cement to the original quantity, depends on temperature, moisture content, cement composition and fineness, w/c, admixtures and age [21].

Although there are numerous cement hydration models that were proposed in the literature, the ones that are deemed comprehensive and simple to implement are shown in Table 2.1. The two models proposed by Knudsen, i.e. linear and parabolic ones, require a determination of the induction time t_0 and constant k from experiment [22]. These requirements limit its use as a generic model. Bentz model [23] contains fewer constants as compared to the other models and can account for different curing conditions. Bentz model was found to be adequate for comparing the relative hydration rates of one w/c versus another but fails to predict the absolute degrees of hydration especially at early ages. Lam [24] proposed a model that is not a function of time but rather a function of two constants that need to be calibrated for a certain age. On the other hand, Schindler and Folliard model, which is based on modified Hansen and Pederson model [21, 25], is found to be simpler to apply and the calibration constants τ and β can be computed using models that are based on the cementing materials characteristics and proportions. On this basis, Schindler and Folliard model was adopted in this study.

Relation between f'_c and α, represented in Figure 2.1 [26] is found to be bi-linear. The results show that the concrete strength development is slow until the degree of hydration reaches a threshold value referred to as critical degree of hydration, α_{cr}, after which the strength develops at a faster rate as α continues to increase. According to Ramussen et al. [27], for ordinary Portland cement (OPC), α_{cr} is equal to the product of w/c and a constant, k, with k equal to 0.43 [27]. In this study, α_{cr} has been accounted for by proportioning the strength to $(\alpha-\alpha_{cr})$.

2.1.2 Average Paste Thickness Model

Excess paste theory postulates that concrete is a mixture of aggregate and cement paste and that the cement paste in excess of the amount needed to fill up the voids between the aggregate particles disperses the particles and lubricates the concrete mix [28, 7]. The amount of excess paste depends on the amount of voids, which is influenced by the packing density of aggregates. Accordingly, an increase in the packing density of aggregates through improved aggregates gradation and proportions, which leads to reduction in the amount of voids, will yield an increase in the amount of excess paste [28]. In this study, the excess paste theory is extended to incorporate the packing density of aggregate.

A priori, the fine and coarse aggregate particles are assumed to be spherical and mono-sized, thus adhering to the same geometric principles of the excess paste theory. Moreover, to account for the paste surrounding the aggregates, a normalization procedure is implemented, namely, the particle radius, a, is normalized with the summation of the radius and the surrounding excess paste thickness, b, i.e.,

$$y = \frac{a}{b} \tag{2.2a}$$

The same analogy is extended to the sand particles, a_s, and coarse particles, a_{ca}, i.e.,

$$y_s = \frac{a_s}{b_s} \tag{2.2b}$$

$$y_{ca} = \frac{a_{ca}}{b_{ca}} \tag{2.2c}$$

To illustrate the concept proposed for the average paste thickness model, one unit volume of concrete consisting of cement paste, sand and coarse aggregates, shown in Figure 2.2a, is analyzed. By compacting the concrete mixture, one obtains 2 volumes, the squeezed out extra cement paste whose volume is denoted by *P,* as shown in Figure 2.2b, and the compacted concrete mixture which now occupies a volume of *1-P*. The corresponding volume fraction for the sand and coarse aggregates is ϕ_s and ϕ_{ca}, respectively. The same compaction process can also be repeated on a volume that is greater than one, with the requirement that the volume of the compacted concrete mixture is equal to one. In principle, the resulting aggregate volume fraction is the maximum packing density ϕ_{max}, which implicitly accounts for the proportion and gradation of all the particles. Given that the degree of compaction is the same for both cases, i.e. Figure 2.2b and Figure 2.2c, it is postulated that their ratio of the compacted volume to the packing density is the same, i.e.,

$$\frac{1-P}{\phi_s + \phi_{ca}} = \frac{1}{\phi_{\max}} \tag{2.3}$$

Equation 2.3 can be re-arranged to determine the volume fraction that *P* occupies,

$$P = 1 - \frac{\phi_s + \phi_{ca}}{\phi_{\max}} \tag{2.4}$$

The same analogy is extended to determine the volume of the void, between the compacted aggregates, denoted by V_2, as shown in Figure 2.3. Referring to Eq. 2.3, the volume fraction of voids is V_2 for the left side and *1-* ϕ_{max} for the right side of the equation. Accordingly, Eq. 2.3 can be rewritten as:

$$\frac{1-P}{V_2} = \frac{1}{1-\phi_{\max}} \tag{2.5}$$

Re-arranging Eq. 2.5 and substituting for *1-P* using Eq. 2.3, one obtains:

$$V_2 = \frac{\phi_s + \phi_{ca}}{\phi_{\max}}(1 - \phi_{\max}) \tag{2.6}$$

The void volume fraction in the non-compacted concrete mixture, V_1, is greater than that of the compacted mixture, V_2, as illustrated in Figure 2.3. By comparing the two volume fractions, one can determine the volume fraction of the excess paste, P_e,

$$P_e = P - (V_1 - V_2) \tag{2.7}$$

The geometric relation between V_1 and V_2 is derived with the aid of Figure 2.4. For simplicity, the relationship is first developed for 2-D plane and then extended to 3-D. Let A_1 be the area of the triangle that originates from the center of the particle and extend outward at an angle of $\pi/3$ and bounded by the outer perimeter of the particle, as shown in Figure 2.4, and A_2 be the area of the large triangle that encloses all three A_1 and the area between them corresponding to the void, A_3. The particles are mono-sized of radius R. The area corresponding to triangle A_2 can be calculated from:

$$A_2 = \sqrt{3}R^2 \tag{2.8}$$

The area of the void, A_3, can be calculated from:

$$A_3 = A_2 - 3A_1 = \left(\sqrt{3} - \frac{\pi}{2}\right)R^2 = C_2 R^2 \tag{2.9}$$

Extending the analogy to 4 particles instead of 3, the area of the void becomes:

$$A_3' = 2R \times 2R - 4\pi R^2 \frac{\pi/2}{2\pi} = (4 - \pi)R^2 = C_2' R^2 \tag{2.10}$$

where C_2 and C_2' are constants. By expanding to 3-D, the value of the constant will be different and the relation between A_3 and the radius of the particle changes from quadratic to cubic. Applying this concept to the geometric arrangement of Figure 2.3, one derives the following expression:

$$\frac{V_1}{V_2} = \frac{C_3 R_1^{\,3}}{C_3 R_2^{\,3}} = \left(\frac{b}{a}\right)^3 \tag{2.11}$$

where C_3 is a constant that depends on the geometry of the particle.

By substituting Eq. (2.2a) into Eq. 2.11, one can further derive the relation between V_1 and V_2, where:

$$V_1 - V_2 = V_2\left(\frac{1}{y^3} - 1\right) \tag{2.12}$$

Recalling that all the particles are assumed to be spherical, the volume fraction of the sum of sand, monosized of radius a_s, and coarse aggregates, monosized of radius a_{ca}, in the concrete mix becomes:

$$\phi = \phi_s + \phi_{ca} = \frac{4}{3}\pi . a_s{}^3 N_s + \frac{4}{3}\pi . a_{ca}{}^3 N_{ca} \tag{2.13}$$

where N_s and N_{ca} are the number of sand and coarse particles, respectively. From Figure 2.3, the volume fraction of excess paste in the concrete mix can be obtained using the following equation:

$$P_e = \frac{4}{3}\pi\left(b_s{}^3 - a_s{}^3\right)N_s + \frac{4}{3}\pi\left(b_{ca}{}^3 - a_{ca}{}^3\right)N_{ca} \tag{2.14}$$

By combining Eqs (2.7) and (2.14) one obtains:

$$\frac{4}{3}\pi\left(b_s{}^3 - a_s{}^3\right)N_s + \frac{4}{3}\pi\left(b_{ca}{}^3 - a_{ca}{}^3\right)N_{ca} = P - (V_1 - V_2) \tag{2.15}$$

By inserting Eqs (2.2b), (2.2c) and (2.12) into Eq (2.15), the following expression is obtained:

$$\frac{4}{3}\pi a_s{}^3 N_s\left(\frac{1}{y_s{}^3} - 1\right) + \frac{4}{3}\pi a_{ca}{}^3 N_{ca}\left(\frac{1}{y_{ca}{}^3} - 1\right) = P - V_2\left(\frac{1}{y^3} - 1\right) \tag{2.16}$$

Eq. (2.16) can be further simplified using Eq. (2.13), yielding:

$$\phi_s\left(\frac{1}{y_s{}^3} - 1\right) + \phi_{ca}\left(\frac{1}{y_{ca}{}^3} - 1\right) = P - V_2\left(\frac{1}{y^3} - 1\right) \tag{2.17}$$

Inserting Eqs. (2.4) and (2.6) into Eq. (2.17) and re-arranging the terms, one obtains the following expression:

$$\frac{\phi_s}{y_s^3}+\frac{\phi_{ca}}{y_{ca}^3}=1-\frac{\phi}{\phi_{\max}}.\frac{1}{y^3}+\frac{\phi}{y^3} \tag{2.18}$$

The average paste thickness (*APT*) is assumed to depend on the particle shape and size. In this development, it is assumed that the particles are spherical and that APT is the same for all the particle groups, namely sand and coarse aggregate, i.e.;

$$APT_s = APT_{ca} = APT \tag{2.19}$$

With the aid of Figure 2.3, *APT* can be determined according to the following,

$$APT = 2b-2a = 2a\left(\frac{b}{a}-1\right) = D\left(\frac{1}{y}-1\right) \tag{2.20}$$

Similarly, APT_s and APT_{ca} are obtained:

$$APT_s = D_s\left(\frac{1}{y_s}-1\right) \tag{2.21}$$

$$APT_{ca} = D_{ca}\left(\frac{1}{y_{ca}}-1\right) \tag{2.22}$$

Rearranging the following equations to solve for y, y_s, and y_{ca}, one obtains:

$$y=\frac{1}{\left(\frac{APT}{D}+1\right)};\qquad y_s=\frac{1}{\left(\frac{APT_s}{D_s}+1\right)};\qquad y_{ca}=\frac{1}{\left(\frac{APT_{ca}}{D_{ca}}+1\right)} \tag{2.23}$$

Substituting (2.23) into (2.18), yields:

$$\phi_s\left(\frac{APT_s}{D_s}+1\right)^3+\phi_{ca}\left(\frac{APT_{ca}}{D_{ca}}+1\right)^3=1-\frac{\phi}{\phi_{\max}}.\left(\frac{APT}{D}+1\right)^3+\phi\left(\frac{APT}{D}+1\right)^3 \tag{2.24}$$

By invoking the assumption that $APT_s = APT_{ca} = APT$, Eq. (2.24) is further simplified yielding the following relation for *APT*,

$$\frac{\phi_s}{D_s^3}(APT + D_s)^3 + \frac{\phi_{ca}}{D_{ca}^3}(APT + D_{ca})^3 - \left(\frac{\phi - \frac{\phi}{\phi_{\max}}}{D^3}\right)(APT + D)^3 - 1 = 0 \quad (2.25)$$

By expanding Eq. (2.25) and assuming that the cubic terms are negligible, a simplified equation for *APT* is derived.

$$APT \approx -\frac{1}{2}\left(D_s + \frac{\phi_{ca} D_s^2}{\phi_s D_{ca}} + \frac{\phi D_s^2 (1 - \phi_{\max})}{\phi_s \phi_{\max} D}\right) + \frac{1}{2}\sqrt{\left(D_s + \frac{\phi_{ca} D_s^2}{\phi_s D_{ca}} + \frac{\phi D_s^2 (1 - \phi_{\max})}{\phi_s \phi_{\max} D}\right)^2 + \frac{4}{3}\frac{(\phi_{\max} - \phi)}{\phi_{\max}}\frac{D_s^2}{\phi_s}} \quad (2.26)$$

The maximum packing density, ϕ_{max}, can be predicted using the compressible packing model, CPM [2]. Using statistical analysis, the proposed *APT* model was found to follow a power relation with strength, i.e.,

$$f'_c \propto \left(\frac{APT}{D}\right)^A \quad (2.27)$$

where A is a calibration constant that depends on the shape of the sand and coarse particles. APT was divided by D to make the term dimensionless.

2.1.3 Capillary Pores, Air Pores, Bond Strength and Cement Standard Strength

Capillary pores, whose sizes vary from 0.01 to 5 μ-m, are the spaces around the cement grains not filled by cement gel [20]. The capillary pores are controlled by the w/c i.e. an increase in w/c results in an increase in the amount of capillary pores which has a negative effect on strength. In addition, the amount of air pores, whether entrapped or entrained, also have a negative effect on strength. These effects were accounted for by adopting the model proposed by Popovics [6]; i.e.,

$$f'_c \propto B^{\frac{W+EA}{C}} \tag{2.28}$$

where B is a constant that depends on specimen shape and test conditions. The effect of air is considered in practice as an extra volume of water [6, 12]. This additional water content due to the presence of air results in an increase in the w/c which is referred to as the equivalent w/c [12]. This ratio is considered by weight after accounting for air as an extra volume of water.

In de Larrard's model, the effect of aggregate type on the paste to aggregate bond strength was accounted for by means of a bonding constant, K [2]. Moreover, de Larrard's model accounts for the cement type by including the standard cement strength at 28 days, R_{c28} [2]. In this study, de Larrard's logic is adopted, and accordingly, both K and R_{c28} are incorporated into the model.

2.1.4 Concrete Compressive Strength Model

The proposed model for predicting the compressive strength of concrete accounts for the type of cement, cement degree of hydration, type and gradation of aggregates, mixture proportions and porosity. The combination of Eq. (2.27), Eq. (2.28), K, R_{c28}, and the (α-α_{cr}) relation to strength, yields the following final expression:

$$f'_c(t) = KR_{c28}\left(\frac{APT}{D}\right)^A B^{\frac{W+EA}{C}}\left(\alpha(t)-\alpha_{cr}\right) \tag{2.29}$$

where:

$$APT \approx -\frac{1}{2}\left(D_s + \frac{\phi_{ca}D_s^{\,2}}{\phi_s D_{ca}} + \frac{\phi D_s^{\,2}(1-\phi_{\max})}{\phi_s\phi_{\max}D}\right)$$
$$+\frac{1}{2}\sqrt{\left(D_s + \frac{\phi_{ca}D_s^{\,2}}{\phi_s D_{ca}} + \frac{\phi D_s^{\,2}(1-\phi_{\max})}{\phi_s\phi_{\max}D}\right)^2 + \frac{4}{3}\frac{(\phi_{\max}-\phi)}{\phi_{\max}}\frac{D_s^{\,2}}{\phi_s}} \tag{2.30}$$

$$\alpha_{cr} = k \times w/c \tag{2.31}$$

$$\alpha = \alpha_u . \exp\left(-\left[\frac{\tau}{t_e} \right]^{\beta} \right) \tag{2.32}$$

$$\tau = 66.78 . p_{C3A}{}^{-0.154} p_{C3S}{}^{-0.401} . Blaine^{-0.804} . P_{SO3}{}^{-0.758} . \exp(2.187 . p_{SLAG} + 9.5 . p_{FA} . p_{FA-CaO}) \tag{2.33}$$

$$\beta = 181.4 . p_{C3A}{}^{0.146} . p_{C3S}{}^{0.227} . Blaine^{-0.535} . p_{SO3}{}^{0.558} . \exp(-0.647 . p_{SLAG}) \tag{2.34}$$

$$\alpha_u = \frac{1.031 . w/c}{0.194 + w/c} + 0.50 . p_{FA} + 0.30 . p_{SLAG} \leq 1.0 \tag{2.35}$$

$$t_e = \sum_0^t \exp\left(\frac{E}{R} \left(\frac{1}{293} - \frac{1}{T + 273} \right) \right) . \Delta t \tag{2.36}$$

2.2 Closing Remarks

In this study a new compressive strength model for predicting the strength of concrete has been formulated. The model is characterized by the following features:

1. The hydration process is modelled through the degree of cement hydration [21, 22, 23, 24, 25, 26] and accounts for the critical degree of hydration.
2. Paste to aggregate bond strength and cement standard strength were modelled following the work of de Larrard [2].
3. Capillary pores and air pores were modelled as proposed by Popovics [6].
4. Particles gradation and proportions were modelled using the proposed average paste thickness model.

The model developed in this study requires implementation, then calibration and validation using experimental data. This task is pursued in Part II of this study.

Acknowledgments

The authors would like to thank NSERC and McMaster University's Center for Effective Design of Structures, for the financial support, and Lafarge Canada and BASF for donating the material.

Notation

f'_c	Compressive strength of concrete;
α, α_{cr}, α_u	Degree of cement hydration, critical degree of cement hydration, and ultimate degree of cement hydration, respectively;
APT, APT_s, APT_{ca}	Average paste thickness of aggregates, of fine aggregate, and of coarse aggregates, respectively;
K	Paste to aggregate bond strength constant;
R_{c28}	Standard cement strength at 28 days;
w/c	Water-to-cement ratio;
a, a_s, a_{ca}	Radius of particles, fine aggregates, and coarse aggregates, respectively;
b, b_s, b_{ca}	Summation of radius and surrounding excess paste thickness for fine aggregates and coarse aggregates, respectively;
y, y_s, y_{ca}	Ratio of particle radius to the summation radius and surrounding excess paste thickness for fine aggregates and coarse aggregates, respectively;
P	Volume fraction of extra paste;
P_e	Volume fraction of excess paste;
ϕ, ϕ_s, ϕ_{ca}	Volume fraction of aggregates, fine aggregates, and coarse aggregates, respectively;
ϕ_{max}	Maximum packing density of aggregates;
$Void_1$	Volume fraction of voids in normal concrete mixture;
$Void_2$	Volume fraction of voids in a squeezed concrete mixture;
C_2, C_2'	stnatsnoC;
N_s, N_{ca}	Number of fine aggregates and coarse aggregates in a concrete mix, respectively;
D, D_s, D_{ca}	Mean diameters of the total particles gradation, fine aggregate gradation, and coarse aggregate gradation, respectively;
t_e, t, t_o	Equivalent age, age, and induction time, respectively;
T	Concrete temperature;
E	Activation energy (33,500 J/mol for T> 20° C);
R	Universal gas constant (8.3144 J/mol/K);
τ, β	Hydration time parameter and hydration shape parameter, respectively;
ρ_{cem}	Specific gravity of cement;
f_{exp}	Volumetric expansion coefficient for the solid cement hydration products relative to the cement reacted;
CS	Chemical shrinkage per gram of cement;
p_{C3A}, p_{C3S}, p_{SO3}	Weight ratios in terms of total cement content;
p_{FA}, p_{SLAG}, $p_{FA\text{-}CaO}$	Weight ratios of mineral admixtures proportions in terms of total cement content;
a, b, a_c, b_c, c_c, k, k_1, k_2	Constants.

References

[1] CSA, 2002. "Design of concrete structures", Standard CAN/CSA A23.3-04, Canadian Standards Association (CSA), Rexdale, Ont.

[2] de Larrard F., 1999. Concrete mixture proportioning: a Scientific Approach, Spon Press, London, 320pp.

[3] de Larrard F. and Belloc A., 1997. "The influence of aggregate on the compressive strength of normal and high-strength concrete", ACI Materials Journal, 94(5), 417–425.

[4] ACI, 1974. "Proportioning concrete mixes", Publication SP-46, American Concrete Institute, Detroit.

[5] Feret R., 1892. "Sur la compacité des mortiers hydrauliques (On the compactness of hydraulic mortars)", Annales des Ponts et Chaussées, Série 7(4), 5-164.

[6] Popovics S., 1985. "New formulas for the prediction of the effect of porosity on concrete strength", Journal of the American Concrete Institute, 82(2), 136-146.

[7] Powers T.C. and Brownyard, T.L., 1960. "Studies of the physical properties of hardened portland cement paste", Journal of American Concrete Institute, 18, 2.

[8] Popovics S., 1998. "History of a mathematical model for strength development of Portland cement concrete", ACI Materials Journal, 95 (5), 593–600.

[9] Pann K. S., Yen T., Tang C. W., Lin T.D., 2003. "New strength model based on water-cement ratio and capillary porosity", Materials Journal, 100(4), 311-318.

[10] Mechling J.M., Lecomte A., Diliberto C., 2009. "Relation between cement composition and compressive strength of pure pastes", Cement and Concrete Composites, 31(4), 255-262.

[11] Bolomey J., 1935. "Granulation et pre´vision de la re´sistance probable des be´tons (Aggregate grading and prediction of probable concrete strength)", Travaux, 19(30), 228–232.

[12] Karni J. 1974. "Prediction of compressive strength of concrete", Materials and Structures Journal., 7(3), 197–200.

[13] Popovics, S., 1990. "Analysis of concrete strength vs. water-cement ratio relationship", ACI Materials Journal, 87(5), 517-528.

[14] Tango C.E.S., 2000. "Time-generalisation of Abrams' model for high performance concrete and practical application examples", Proceedings of the International Symposium on High Performance Concrete, Hong Kong University of Science and Technology. Hong Kong, China.

[15] Yeh I.C., 2006. "Generalization of strength versus water-cementations ratio relationship to age", Cement and Concrete Research, 36(10), 1865-1873.

[16] Tangtermsirikul S., Kaewkhluab T., Jitvutikrai, P., 2004. "A compressive strength model for roller-compacted concrete with fly ash", Magazine of Concrete Research, 56(1), 35-44.

[17] Nipatsat N. and Tangtermsirikul S., 2000. "Compressive strength prediction model for fly ash concrete", Thammasat International Journal of Science and Technology, 5(1), 1–7.

[18] Hwang S.D. Lee K.M., Kim J.K., Kim J.H., 2001. "Microstructure model for estimating early-age concrete strength", First International Structural Engineering and Construction Conference, Honolulu, HI, USA, 493-497.

[19] Namyong J., Sangchun Y., Hongbum C., 2004. "Prediction of compressive strength of in-situ concrete based on mixture proportion", Journal of Asian Architecture and Building Engineering, 3(1), 9-16.

[20] Mehta P.K. and Monteiro P., 2006. Concrete: microstructure, properties, and materials, 3rd edition, McGraw-Hill, USA.

[21] Schindler A. K. and Folliard K. J., 2005. "Heat of hydration models for cementitious materials", ACI Materials Journal, 102(1), 24–33.

[22] Knudsen T., 1984. "The dispersion model for hydration of Portland cement: I. General concepts", Cement and Concrete Research, 14(5), 622–630.

[23] Bentz D., 2006. "Influence of water-to-cement ratio on hydration kinetics: simple models based on spatial considerations", Cement and Concrete Research, 36(2), 238–244.

[24] Lam L., Wong Y.L., Poon C.S., 2000. "Degree of hydration and gel/space ratio of high-volume fly ash/cement systems", Cement and Concrete Research, 30(5), 747-756.

[25] Hansen F. and Pedersen P., 1985. "Curing of concrete structures", Draft DEB-Guide to Durable Concrete Structures, Appendix 1, Comité Euro-International du Béton, Switzerland.

[26] Beek A., Breugel K., Hilhorst M.A., 1999. "Monitoring system for hardening concrete based on dielectric properties", Proceedings of the International Conference Utilizing ready mix concrete and mortar, University of Dundee, Scotland, 303-312.

[27] Rasmussen R.O., Ruiz J.M., Rozycki D.K., McCullough B.F., 2002. "Constructing high-performance concrete pavements with FHWA HIPERPAV systems analysis software", Transportation Research Record 1813, Transportation Research Board, Washington, DC, 11-20.

[28] Wong H.H.C. and Kwan A.K.H., 2008. "Packing density of cementitious materials: measurement and modelling", Magazine of Concrete Research, 60(3) 165–175.

Table 2.1 Cement hydration models

Model	Equation	
Schindler and Folliard [21]	$\alpha = \alpha_u.\exp\left(-\left[\frac{\tau}{t_e}\right]^{\beta}\right)$	(1)
	$\tau = 66.78.p_{C3A}{}^{-0.154}p_{C3S}{}^{-0.401}.Blaine^{-0.804}.P_{SO3}{}^{-0.758}$ $.\exp(2.187.p_{SLAG} + 9.5.p_{FA}.p_{FA-CaO})$	
	$\beta = 181.4.p_{C3A}{}^{0.146}.p_{C3S}{}^{0.227}.Blaine^{-0.535}.p_{SO3}{}^{0.558}$ $.\exp(-0.647.p_{SLAG})$	
	$\alpha_u = \frac{1.031.w/c}{0.194 + w/c} + 0.50.p_{FA} + 0.30.p_{SLAG} \le 1.0$	
	$t_e = \sum_0^t \exp\left(\frac{E}{R}\left(\frac{1}{293} - \frac{1}{T+273}\right)\right).\Delta t$	
Bentz [30]	$\alpha_2 = \frac{p\{\exp[R(1-p)t]-1\}}{\{\exp[R(1-p)t]-p\}}$;	(2)
	$p = \frac{\rho_{cem}(w/c)}{(f_{\exp} + \rho_{cem}CS)}$; $R = \frac{k_2(f_{\exp} + \rho_{cem}CS)}{[1+\rho_{cem}(w/c)]^2}$	
Knudsen [24]	Linear Model: $\alpha_1 = \alpha_u \frac{k(t-t_0)}{1+k(t-t_0)}$	(3)
Knudsen [24]	Parabolic Model: $\alpha_2 = \alpha_u \frac{k\sqrt{(t-t_0)}}{1+k\sqrt{(t-t_0)}}$	(4)
Lam et al. [31]	$\alpha = ae^{\left[-\frac{b}{w/c}\right]}$	(5)

w/c = water-to-cement ratio; t_e, t, t_0 = equivalent age, age, and induction time, respectively; α_u = ultimate degree of cement hydration; T = concrete temperature (°C); E = activation energy (33,500 J/mol for T > 20° C), R = universal gas constant (8.3144 J/mol/K); τ, β = hydration time parameter and hydration shape parameter, respectively; ρ_{cem} = specific gravity of cement; f_{exp} = volumetric expansion coefficient for the solid cement hydration products relative to the cement reacted; CS = chemical shrinkage per gram of cement; p_{C3A}, p_{C3S}, p_{SO3}, p_{FA}, p_{SLAG}, p_{FA-CaO} = weight ratios in terms of total cement content; and a, b, a_c, b_c, c_c, k, k_1, k_2 = constants.

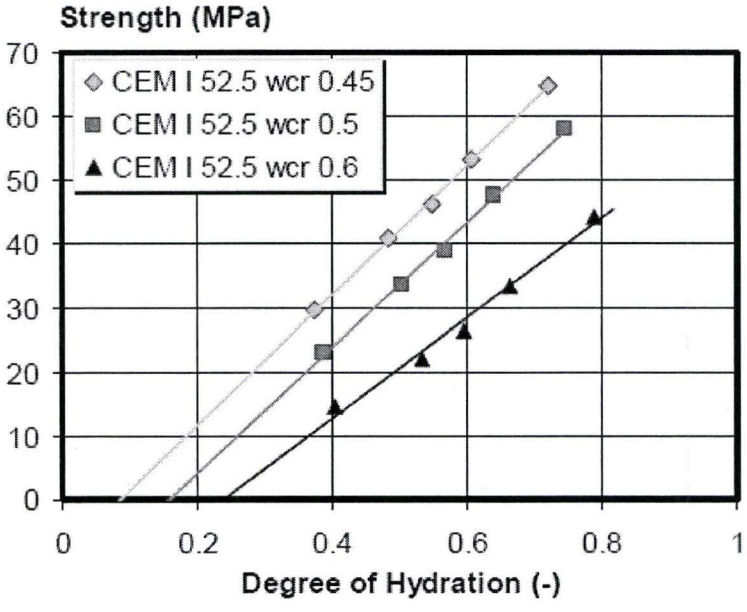

Figure 2.1 Strength versus degree of hydration for different w/c [26]

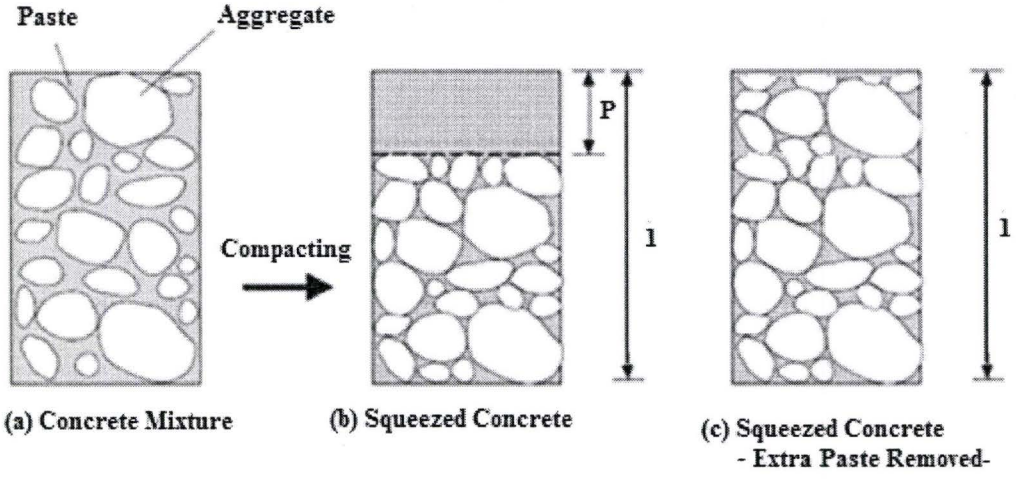

Figure 2.2 Particles illustration for average paste thickness derivation

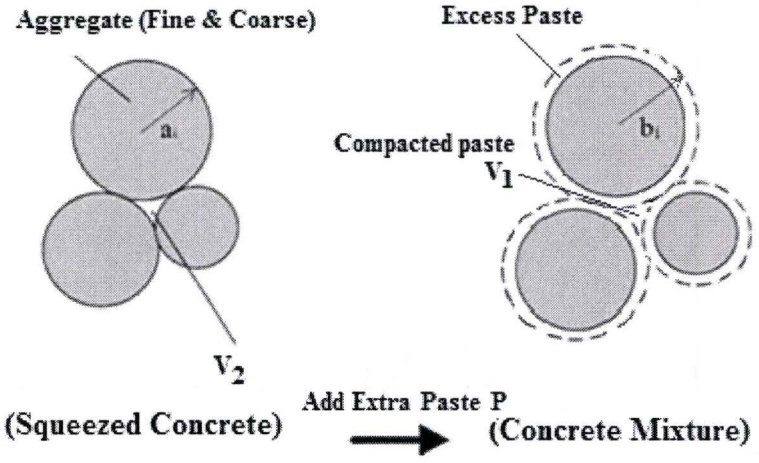

Figure 2.3 Particles without and with surrounding excess paste

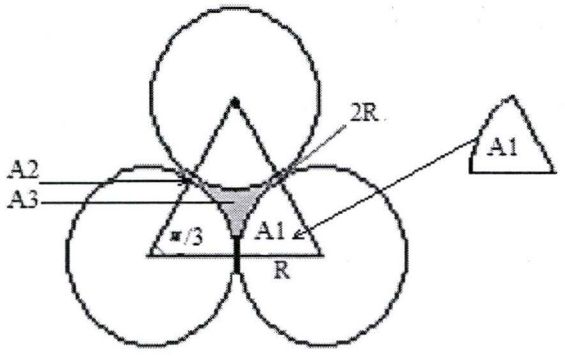

Figure 2.4 Geometric illustration of 3 mono-sized spherical particles of radius R

Chapter 3: Paper II Compressive Strength Model for Concrete - II: Calibration and Validation

Abstract

This paper presents the implementation, calibration and validation of the compressive strength model formulated in part I: Theory. To meet this, an experimental program was developed on the basis of fractional factorial statistical design principles. The concrete mixture variables considered for the experiment were water to cement ratio, water content, bulk volume of coarse aggregate, maximum size of coarse aggregate, and air entrainment. A total of 28 mixtures were used to calibrate and validate the model. The evaluation of the proposed model included individual testing of 5 cement hydration models, and the results revealed that the model is consistent, robust and complete. The proposed model adequately and consistently predicted the strength of the 28 concrete mixtures at 3-day and-28 day. The standard error and the correlation coefficient for the 3-day and the 28-day predictions, respectively is 2.1 MPa and 1.8 MPa, and 0.95 and 0.96.

Keywords: compressive strength; degree of hydration; packing density; excess paste theory

3.0 Introduction

In the companion paper, Part I of this study, a new model was proposed for predicting the compressive strength of concrete on the basis of its constituents. This model accounts for the cement properties and strength, concrete maturity, concrete mixture, cement to aggregate bond strength, air content and voids. The model is described by [1]:

$$f'_c(t) = KR_{c28}\left(\frac{APT}{D}\right)^A B^{\frac{W+EA}{C}}\left(\alpha(t)-\alpha_{cr}\right) \tag{3.1}$$

where f'_c is the compressive strength of concrete, α the degree of cement hydration, α_{cr} the critical degree of hydration after which concrete starts developing strength at a fast rate, K the aggregate to paste bond constant, R_{c28} the standard cement strength at 28 days, APT the average paste thickness, D the mean diameter of all the aggregate sizes in the mix, $(W+EA)/C$ is the ratio by weight of water plus entrapped and entrained air to cement, and A and B are calibration constants. Constant A depends on the shape of the fine and coarse aggregate particles while constant B depends on specimen shape and test conditions. The effect of air is considered in practice as an extra volume of water.

APT, which is derived mathematically following the concept of excess paste theory [2], accounts for aggregate gradation, aggregate mean size, aggregate volume fractions, and method of compaction. It takes the following form:

$$APT \approx -\frac{1}{2}\left(D_s + \frac{\phi_{ca} D_s^{\,2}}{\phi_s D_{ca}} + \frac{\phi D_s^{\,2}(1-\phi_{\max})}{\phi_s \phi_{\max} D}\right) + \frac{1}{2}\sqrt{\left(D_s + \frac{\phi_{ca} D_s^{\,2}}{\phi_s D_{ca}} + \frac{\phi D_s^{\,2}(1-\phi_{\max})}{\phi_s \phi_{\max} D}\right)^2 + \frac{4}{3}\frac{(\phi_{\max}-\phi)}{\phi_{\max}}\frac{D_s^{\,2}}{\phi_s}} \tag{3.2}$$

where D_s and D_{ca} are the mean diameter of sand particles gradation and mean diameter of coarse aggregate particles gradation, respectively (mm). ϕ, ϕ_s, and ϕ_{ca} are the volume fraction of aggregates, of sand particles, and coarse particles, respectively. ϕ_{max} is the maximum packing density of aggregates and can be calculated using any packing model such as the compressible packing model [3].

The degree of cement hydration, α, can be obtained using any cement hydration model such as the one proposed by Schindler and Folliard [2] and adopted in this study. The critical degree of hydration, α_{cr}, can be predicted according to Rasmussen et al. [18]. The adopted models are as follows:

$$\alpha_{cr} = k \times w/c \tag{3.3}$$

$$\alpha = \alpha_u . \exp\left(-\left[\frac{\tau}{t_e}\right]^{\beta}\right) \tag{3.4}$$

$$\tau = 66.78.p_{C3A}{}^{-0.154} p_{C3S}{}^{-0.401}.Blaine^{-0.804}.P_{SO3}{}^{-0.758} \\ .\exp(2.187.p_{SLAG} + 9.5.p_{FA}.p_{FA-CaO}) \quad (3.5)$$

$$\beta = 181.4.p_{C3A}{}^{0.146}.p_{C3S}{}^{0.227}.Blaine^{-0.535}.p_{SO3}{}^{0.558}.\exp(-0.647.p_{SLAG}) \quad (3.6)$$

$$\alpha_u = \frac{1.031.w/c}{0.194 + w/c} + 0.50.p_{FA} + 0.30.p_{SLAG} \leq 1.0 \quad (3.7)$$

$$t_e = \sum_0^t \exp\left(\frac{E}{R}\left(\frac{1}{293} - \frac{1}{T+273}\right)\right).\Delta t \quad (3.8)$$

where t_e is the equivalent age (hrs); α_u the ultimate degree of cement hydration; T the concrete temperature (°C); E the activation energy (33,500 J/mol for T > 20° C); R the universal gas constant (8.3144 J/mol/K); τ, β the hydration time parameter and hydration shape parameter, respectively; p_{C3A}, p_{C3S}, p_{SO3}, p_{FA}, p_{SLAG}, $p_{FA\text{-}CaO}$ the weight ratios in terms of total cement content; and k a calibration constant (0.43 for OPC concrete).

Although the model is developed using complex mathematical arguments, it was simplified so that it can be implemented using a spreadsheet type software [4]. The decision also included the rationale for the selection of the cement hydration model. This paper, which forms the second part, presents the experimental program that was developed to calibrate and validate the proposed model for predicting the compressive strength of concrete.

3.1 Experimental Program

The experimental program was developed on the basis of factorial design principle to measure the compressive strength of concrete mixtures [5]. For the air entrained mixes, fractional factorial design of resolution four (2^{4-1}) was adopted to study the effects of the main variables and the interaction effects of two variables [5]. Accordingly, a set of 8 mixtures are required. To account for the nonlinearities on the measured response, a new set referred to as star points was added to assess the influence of the variable in four levels instead of two levels [5]. The variables included in the study are water to cement ratio (w/c), water content, bulk volume of coarse aggregate (CA), maximum size of CA, and air entrainment.

3.1.1 Concrete Mix Design

The concrete mixture was proportioned following the statistical fractional factorial design method and the ranges recommended by the Cement Association of Canada (CAC) for designing and proportioning normal concrete mixtures [6]. The range selected for w/c was from 0.4 to 0.7. The water content values ranged from 175 to 228 kg/m^3, covering the full range of slump for non-air entrained and air entrained concrete. The cement content ranged from 250 to 570 kg/m^3. The bulk volume of CA per unit volume of concrete ranged from 0.45 to 0.69. The CA maximum sizes were 20 mm and 14 mm. For the air-entrained concrete mixtures, an air entraining agent was used to achieve 5% air content. The total number of concrete mixtures was 28 and the corresponding proportions are given in Table 3.1. Of the 28 concrete mixtures, 20 were air entrained and 8 were non-air entrained.

Details of the factorial design for the air entrained mixes are given in Table 3.2 which shows the variables and the corresponding coded values that are needed to account for both the linear and non linear anticipated interactions among variables and the response. The table shows the main points which vary between -1 and +1 coded values and the star points with different levels of each variable in order to assess the influence of the variable in at least 4 levels instead of 2. The main points are mixtures 1 to 8 in Table 3.1 whereas the star points are mixtures 9 to 20.

3.1.2 Materials

The concrete was prepared using a mixture of crushed limestone, siliceous sand, Ordinary Portland Cement (OPC), AEA and water. Hydraulic cement type GU-type 10 used in this study was obtained from Lafarge North America. The chemical and physical properties are summarized in Table 3.3. Crushed limestone CA with 20 mm and 14 mm nominal maximum aggregate sizes were used. The aggregates were obtained from Lafarge, North America's Dundas quarry located in Dundas, Ontario, Canada. The specific gravities,

absorption values, and bulk density for the 20 mm CA are 2.75, 0.92%, and 1636 kg/m^3, and for the 14 mm CA are 2.74, 0.88%, and 1576 kg/m^3, respectively. The sand was obtained from Lafarge North America's West Paris plant. The fineness modulus, specific gravities, absorption values, and bulk density for the sand are 2.72, 2.71, 1.58%, and 1812 kg/m^3, respectively. The bulk density, specific gravity, and absorption for CA and sand were obtained following ASTM C127-04 [7] and ASTM C128-04 [8], respectively. The particle size distribution test was carried out in accordance with CSA A23.2a [9] and the results for CA and sand are shown in Figure 3.1. Micro Air, which is manufactured by BASF construction chemicals and which meets the requirements of ASTM C260-06, was used to entrain air [10].

3.1.3 Packing Density

The maximum packing density of aggregates, ϕ_{max}, for each concrete mixture was computed using the compressible packing model (CPM) [3]. Knowing the followings; volume fractions of the fine aggregate and coarse aggregate particles from the mixture, their characteristic diameters, and their measured maximum packing densities (oven dried) according to ASTM C29-97 [11] with rodding the method of compaction; the CPM can be employed to calculate ϕ_{max}. Experimental measurement of the maximum packing densities was carried out using 3 specimens and both the mean value and the standard deviation are reported. The mean maximum packing densities of sand, 14mm max CA size, and 20mm max CA size were measured to be 0.669, 0.575, and 0.595, respectively, and the corresponding standard deviation is 0.016, 0.011, and 0.012. The mean characteristic diameters corresponding to 63.2% passing, as recommended by Goltermann et al [12], were measured for sand, 14 mm max aggregate size, and 20 mm max aggregate size and found to be 1.1 mm, 10.4 mm, and 14.3 mm, respectively. The corresponding standard deviations are 0.05 mm, 1.48 mm and 1.22 mm, respectively. The mean values of the mean diameters, corresponding to 50% passing, needed for the proposed *APT* model, were determined to be 0.74 mm, 9.1 mm, and 12 mm for sand, 14mm max CA

size, and 20mm max CA size, respectively. The corresponding standard deviations are 0.06 mm, 0.48 mm and 1.55 mm, respectively.

3.1.4 Experimental Procedure

The experimental procedure implemented for this study was consistent for all of the concrete mixtures which included the mixing, placing, consolidating, curing and test methods. The proportions of the concrete mixtures were first obtained as per the design given in Table 3.1. The concrete was mixed in a pan mixer following these steps:

1- Mix water and AEA for 30 s.
2- Place CA, sand, cement, 1/3 of the mixed water and AEA into the pan mixer.
3- Mix the content for 2 min.
4- Add the remaining quantity of water while the mixer is still running.
5- Mix the content for 2 min.
6- Stop the mixer for 1 min.
7- Mix the content for 1 min.
8- Measure concrete slump according to CSA test method A23.2-5C [13].
9- Measure air content for two samples according to CSA test method A23.3-4C [14].

For every mixture, six standard cylinders, 100 mm in diameter and 200 mm high, were cast, consolidated by rodding and finished in accordance with ASTM C192-02 [15]. The cylinders were sealed for 24 h then placed in a moist curing room, where the relative humidity was in excess of 95% and the temperature was 24° C. The concrete compressive strength was evaluated in accordance with ASTM C39-05 [16]. The specimens were tested for every mixture after 3 days and 28 days to a total of 168 concrete cylinders.

3.2 Calibration and Validation Procedure

The proposed concrete compressive strength model comprises of measurable material properties and calibration constants. The calibration constants, namely A, B and K, are

included to account for physical and chemical attributes of the materials that are either random, non-uniform, and/or very difficult to quantify. This task was achieved using statistics and the method of least squares [5]. Accordingly, calibration constants were determined by minimizing the model standard error (σ), between the model predictions and measured experimental data. The model standard error, which provides a global assessment of the model predictions, is obtained as follows [5]:

$$\sigma = \sqrt{\frac{\sum_i \left(f'_{c\,model_i} - f'_{c\,exp_i}\right)^2}{n-p}} \tag{3.9}$$

where $f'_{c\ model\_i}$ and $f'_{c\ exp\_i}$ are the model and experimental compressive strengths corresponding to mix i, respectively. n is the number of test points and p is the number of model constants. The corresponding correlation coefficient (R^2), which provides a measure of the proportion of variability that is accounted for by the model, was also calculated.

Model calibration analysis considers different cement hydration models, namely those mentioned in part I of this paper and are listed in Table 3.4, to study their effect on the model calibration constants K, A, and B. Sensitivity of the calibration constants was assessed via the cement hydration models. The results can be interpreted as an indication of the robustness of the model and the degree of dependency of the model predictive capabilities on the calibration constants. Five cement hydration models, namely those of Schindler and Folliard [2], Bentz [17], Lam et al. [18], and Knudsen's linear and parabolic models [19], were incorporated into the proposed compressive strength model.

Three types of evaluation were carried out to assess the adequacy and predictability of the proposed model. Global assessment of the model was first carried out using a statistical evaluation of the predicted values in comparison with the measured ones. This evaluation includes the soundness and good fit of the model. The second type of evaluation includes the assessment of the model capabilities for predicting the trends reported in the literature.

The model ability to predict concrete strength properties at early age, specifically at 3 days, was evaluated.

3.3 Results

Following the proposed calibration procedure, the model constants were determined for the five cement hydration models and are listed in Table 3.4. These results reveal that the model adequately and consistently accounts for the factors that influence the strength of concrete for the following reasons: 1) For all models except Bentz's model, values of the calibration constants, A and B, are found to have negligible dependencies on the cement hydration model; 2) calibration factor K, as expected, is found to have some dependency on the cement hydration model; 3) the standard error, σ, is consistent for all five cement hydration models and its value is 1.8 MPa; and 4) the correlation coefficient, R^2, indicates a very good fit for all five models.

Schindler and Folliard cement hydration model was adopted in this study because its parameters can be computed without calibration. The corresponding 28-day compressive strength values are given in Table 3.5 along with the experimental data. Calculated values for ϕ_s, ϕ_{ca}, ϕ_{max}, α_{28d} and APT are also given for each concrete mixture. The errors as a percent difference between predicted and measured values are also given in Table 3.5. The values for the percent difference are found to range from 0% to 15% and the coefficient of variance from the experiment ranges from 0.6% to 8.5%. This indicates the model predictions are within plus or minus one standard deviation of the measured values.

Figure 3.2 shows the goodness of fit of the proposed model in comparison to the measured experimental data. The soundness of the model was also evaluated by comparing the predicted values to the residual values as shown in Figure 3.3. The results indicate that there are no visible patterns or outliers, thus indicating the good fitness of the model [20]. Moreover, the statistical evaluation revealed that the model parameters are all statistically significant beyond the 95% confidence level and that the proposed model is

very significant in predicting the outcome. The model p-value is found to be less than 0.00001.

Model's ability to predict known trends for concrete compressive strength was evaluated and the results are shown in Figures 3.4 and 3.5. Results of Figure 3.4 display the effects of air content, maximum CA size and w/c on the compressive strength of concrete. For the air content, it was assumed 5% for AE concrete and 1.5% entrapped air for non AE concrete, which are approximate mean values obtained from experiment. The results, which indicate a difference of 7 to 10 MPa in strength between AE and non AE concrete mixture, are consistent with the results reported in the literature [6]. Moreover, the results display the common trend where an increase in the w/c yields a decrease in the strength. The results also reveal that the maximum size of CA has minor effect on the strength of concrete. These results are consistent with the literature [21] and design guidelines [6].

The effect of the remaining variables on strength i.e. the water content, and bulk volume fractions and size of the aggregates are accounted for through APT. Figure 3.5 presents the relationship between APT and the 28-day compressive strength obtained using the proposed model for a fixed w/c of 0.4, 14 mm maximum size CA and 5% air. The figure displays a somewhat linear and inversely proportional relation between APT and strength of concrete. For a given mixture, an increase in the thickness of the paste between aggregate particles either due to an increase in the water content for fixed w/c or a reduction in the volume fraction of the aggregates, would result in a less compact mix. Consequently, the shorter is the path that a crack needs to follow since it has to move around a fewer number of aggregates. This reduces the energy absorbed and so the compressive strength [22]. Moreover, APT is found to have a smaller effect on strength in comparison to w/c and porosity.

The compressive strength of the concrete mixtures was also tested at 3 days and the results in the form of mean value and one standard deviation are given in Table 3.6. The model, which was calibrated for the 28-day strength using least squares analysis, was used to predict the strength at 3 day and the results are given in Table 3.6 and shown in Figure 3.6. Statistical evaluation of the predicted results reveals that the model predictions

are very good and consistent, where R^2 is found equal to 0.95 and σ equal to 2.1 MPa. The goodness of fit was also evaluated and the results reveal neither outliers nor a discerning pattern. Moreover, results of Figure 3.6 demonstrate the good fit of the model for the full range of concrete strength. The exception is observed for four mixtures, in which the corresponding errors in percent differences are 20%, 12%, 12%, and 13%. Again, with the exception of two mixtures, the percent error between measured and predicted is within the COV of the measured compressive strength values.

3.4 Summary and Conclusions

An experimental program consisting of 28 concrete mixtures was developed using fractional factorial statistical principles to calibrate and evaluate the proposed compressive strength model. The variables considered in the experimental program are w/c, water content, max CA size, bulk volume of CA, and air content. Five cement hydration models reported in the literature were also tested as part of the proposed model. Following the calibration procedure part formulated in this study, it was revealed that the model is consistent and robust for all cement hydration models. Evaluation of the proposed model has revealed the following conclusions:

1. Proposed compressive strength model provides a good fit to the experimental data for all 5 cement hydration models, namely those proposed by Schindler and Folliard [2], Knudsen's models [22], Bentz [23], and Lam et al. [24].
2. The model predictions did not contain outliers or discerning pattern.
3. The standard error is found to be less than 2 MPa for both 3-day and 28-day strength predictions when using Schindler and Folliard cement hydration model. The corresponding correlation coefficient is greater than 0.95.
4. The model is capable to consistently and accurately predict the strength of concrete on the basis of its composition at 3-day and 28-day.

5. The model was capable of predicting the same trends reported in the literature due to variations in the concrete composition.

6. The proposed model, in Part I, for predicting the compressive strength of concrete based on the composition of the mixture, which is given by the following expression $f'_c(t) = KR_{c28}\left(\frac{APT}{D}\right)^A B^{\frac{W+EA}{C}}(\alpha(t)-\alpha_{cr})$, is a comprehensive tool for designing concrete mixture for a specific strength requirements.

Acknowledgments

The authors would like to acknowledge the financial contribution of the National Science and Engineering Research Council of Canada, McMaster University's Centre for Effective Design of Structures; Lafarge North America and BASF for donating the materials needed to conduct the experiments.

References

[1] Chidiac S.E., Moutassem F., and Mahmoodzadeh F., 2010. "Compressive strength model for concrete – I: Theory", Cement and Concrete Composites, To be submitted for publication.

[2] Schindler A. K. and Folliard K. J., 2005. "Heat of hydration models for cementitious materials", ACI Materials Journal, 102(1), 24–33.

[3] de Larrard F., 1999. Concrete mixture proportioning: a Scientific Approach, Spon Press, London, 320pp.

[4] Microsoft Excel 2007. http://office.microsoft.com/en-us/excel/default.aspx

[5] Montgomery D.C. and Runger G.C., 2003. Applied statistics and probability for engineers, Third edition, NewYork: John Wiley and Sons Inc.

[6] Kosmatka S.H., Kerkhoff B., Panarese W.C., 2002. Design and control of concrete mixtures, Seventh Canadian Edition, Cement Association of Canada.

[7] ASTM C127-04, 2004. "Standard test method for specific gravity and absorption of coarse aggregate", American Society for Testing of Materials, West Conshohochen, PA, USA.

[8] ASTM C128-04, 2004 "Standard test method for specific gravity and absorption of fine aggregate", American Society for Testing of Materials, West Conshohochen, PA, USA.

[9] CSA A23.2-2A, 2000. "Sieve analysis of Fine and Coarse Aggegate", Concrete Materials and Methods of Concrete Construction/Methods of Tests for Concrete, Rexdale, ON., Canada.

[10] ASTM C260-04, 2004. "Air-entraining admixtures for concrete", American Society for Testing of Materials, West Conshohochen, PA, USA.

[11] ASTM C29-97, 1997. "Standard test method for bulk density and voids in aggregate", American Society for Testing of Materials, West Conshohochen, PA, USA.

[12] Goltermann P., Johansen V., Palbol L., 1997. "Packing of aggregates: an alternative tool to determine the optimal aggregate mix", ACI Material journal, 94 (5), 435-443.

[13] CSA A23.2-5C, 2000. "Slump of concrete", Concrete Materials and Methods of Concrete Construction/Methods of Tests for Concrete, Rexdale, ON., Canada..

[14] CSA A23.2-4C, 2000. "Air content of plastic concrete by the pressure method", Concrete Materials and Methods of Concrete Construction/Methods of Tests for Concrete, Rexdale, ON., Canada.

[15] ASTM C192-02, 2002. "Making and curing concrete specimens in the laboratory", American Society for Testing of Materials, West Conshohochen, PA, USA.

[16] ASTM C39-05, 2005. "Standard test method for compressive strength of cylindrical specimens", American Society for Testing of Materials, West Conshohochen, PA, USA.

[17] Powers T.C. and Brownyard, T.L., 1960. "Studies of the physical properties of hardened portland cement paste", Journal of American Concrete Institute, 18, 2.

[18] Rasmussen R.O., Ruiz J.M., Rozycki D.K., McCullough B.F., 2002. "Constructing high-performance concrete pavements with FHWA HIPERPAV systems analysis software", Transportation Research Record 1813, Transportation Research Board, Washington, DC, 11-20.

[19] Moutassem F. and Chidiac S.E., 2008. "Evaluation of Packing Density Models for Concrete Applications", 2nd Canadian Conference on Effective Design of Structures, McMaster University, Hamilton, Ontario, Canada.

[20] SPSS for Windows, Rel. 10.0.0. 1999. Chicago: SPSS Inc.

[21] Quiroga P, 2003. The effect of the aggregate characteristics on the performance of portland cement concrete, Ph.D. Dissertation, The University of Texas at Austin.

[22] Kolias S. and Georgiou C., 2005. "The effect of paste volume and of water content on the strength and water absorption of concrete", Cement & Concrete Composites 27(2), 211–216.

[22] Knudsen T., 1984. "The dispersion model for hydration of Portland cement: I. General concepts", Cement and Concrete Research, 14(5), 622–630.

[23] Bentz D., 2006. "Influence of water-to-cement ratio on hydration kinetics: simple models based on spatial considerations", Cement and Concrete Research, 36(2), 238–244.

[24] Lam L., Wong Y.L., Poon C.S., 2000. "Degree of hydration and gel/space ratio of high-volume fly ash/cement systems", Cement and Concrete Research, 30(5), 747-756.

Table 3.1 Concrete mixture design composition

Mixture #	w/c	Size	Water (kg/m^3)	Cement (kg/m^3)	Coarse aggregate (bulk volume)	Coarse aggregate (kg/m^3)	Sand (kg/m^3)	%Air
1	0.40	14	193	483	0.50	794	851	5.9
2	0.60	14	193	322	0.62	971	815	5.3
3	0.40	14	205	513	0.62	971	618	4.8
4	0.60	14	205	342	0.50	794	939	5.1
5	0.40	20	184	460	0.69	1134	563	4.6
6	0.60	20	184	307	0.57	928	898	5.6
7	0.40	20	197	493	0.57	928	703	4.8
8	0.60	20	197	328	0.69	1134	641	3.1
9	0.50	14	193	386	0.504	794	934	5.7
10	0.70	14	175	250	0.504	794	1100	8.8
11	0.50	14	205	410	0.504	794	881	5.1
12	0.70	14	193	276	0.504	794	1029	7.5
13	0.50	14	193	386	0.616	971	759	5.1
14	0.70	14	175	250	0.616	971	925	8.7
15	0.50	14	205	410	0.616	971	706	4.8
16	0.70	14	193	276	0.616	971	854	5.6
17	0.50	14	199	398	0.560	883	820	5.0
18	0.50	14	199	398	0.448	706	994	7.8
19	0.50	14	199	398	0.672	1059	645	6.7
20	0.50	14	199	398	0.560	883	820	5.8
21	0.40	14	216	540	0.50	794	807	2.1
22	0.60	14	216	360	0.62	971	787	1.0
23	0.40	14	228	570	0.62	971	574	1.8
24	0.60	14	228	380	0.50	794	912	1.2
25	0.40	20	205	513	0.69	1134	542	1.6
26	0.60	20	205	342	0.57	928	892	1.5
27	0.40	20	216	540	0.57	928	692	1.4
28	0.60	20	216	360	0.69	1134	643	1.5

Table 3.2 Factorial design

Variables \ Codes	CA Size	Star pt.	-1	0	+1	Star pt.
w/c		-	0.4	0.5	0.6	0.7
Water content (Kg/m^3)	14 mm	175	193	199	205	-
	20 mm	-	184	-	197	-
CA size (mm)		-	14	-	20	-
Bulk volume of CA	14 mm	0.49	0.50	0.56	0.62	0.67
	20 mm	-	0.57	-	0.69	-

Table 3.3 Chemical and physical properties of hydraulic cement GU-type 10

SiO_2 (%)	19.7
Al_2O_3 (%)	4.9
Fe_2O_3 (%)	2.4
CaO (%)	62.2
MgO (%)	3.1
SO_3 (%)	3.4
Na_2O (%)	1.3
Loss on Ignition (%)	2.9
Equivalent Alkalies (%)	0.75
Specific Surface Area (Blaine) (cm^2/g)	4280
% Passing 325 (45um) Mesh (%)	90.7
Time of Setting-Initial (min)	115
Compressive Strength – 28 Days (MPa)	41.9

Table 3.4 Calibration of proposed model for all degree of hydration models

Model	K	A	B	σ (MPa)	R^2
Schindler and Folliard (2005)	4.05	-0.016	0.19	1.8	0.96
Lam et al. (2000)	3.79	-0.013	0.19	1.8	0.96
Knudsen (1984) $_{\text{model 2}}$	4.05	-0.016	0.19	1.8	0.96
Knudsen (1984) $_{\text{model 1}}$	3.96	-0.013	0.19	1.8	0.96
Bentz (2005)	2.85	-0.070	0.24	1.8	0.95

Table 3.5 Experimental and predicted concrete compressive strength at 28 day

Mixture #	ϕ_s	ϕ_{ca}	ϕ_{max}	D (mm)	APT (mm)	α_{28d}	$f'c_{28d}$ (MPa)	$f'c_{model\_28d}$ (MPa)	Error (%)
1	0.311	0.287	0.808	7.1	0.154	0.65	37.8±2.3	36.5	3
2	0.300	0.353	0.814	7.4	0.124	0.73	23.1±1.2	24.3	5
3	0.228	0.355	0.815	7.7	0.209	0.65	36.4±1.0	38.1	5
4	0.346	0.289	0.805	7.0	0.118	0.73	27.2±1.1	24.9	9
5	0.209	0.414	0.828	10.5	0.203	0.65	35.7±1.8	37.9	6
6	0.329	0.335	0.821	9.6	0.114	0.73	23.9±2.0	23.7	1
7	0.260	0.338	0.829	9.9	0.192	0.65	38.4±1.4	38.0	1
8	0.241	0.420	0.831	10.3	0.154	0.73	23.8±2.3	27.3	15
9	0.342	0.288	0.805	7.0	0.122	0.69	30.4±0.8	30.0	1
10	0.391	0.279	0.799	6.8	0.084	0.75	14.9±0.8	14.7	2
11	0.325	0.290	0.807	7.1	0.138	0.69	32.9±1.0	31.1	5
12	0.370	0.283	0.802	6.9	0.099	0.75	18.4±0.7	16.7	9
13	0.280	0.354	0.815	7.5	0.145	0.69	30.7±2.6	30.6	0
14	0.329	0.342	0.811	7.3	0.102	0.75	13.6±0.6	14.8	9
15	0.261	0.355	0.816	7.6	0.166	0.69	32.5±0.2	31.4	3
16	0.313	0.352	0.813	7.4	0.111	0.75	18.6±2.0	18.7	0
17	0.303	0.322	0.812	7.3	0.142	0.69	31.9±0.6	31.0	3
18	0.357	0.251	0.799	6.8	0.129	0.69	26.3±1.0	27.7	5
19	0.234	0.380	0.814	7.8	0.180	0.69	25.5±1.3	28.9	13
20	0.300	0.320	0.812	7.3	0.146	0.69	33.1±2.2	30.0	9
21	0.299	0.291	0.809	7.2	0.166	0.65	42.6±1.5	41.7	2
22	0.295	0.360	0.815	7.5	0.125	0.73	31.0±0.3	30.3	2
23	0.213	0.357	0.813	7.8	0.229	0.65	43.8±3.5	42.1	4
24	0.341	0.294	0.806	7.0	0.120	0.73	29.7±0.3	30.2	2
25	0.201	0.414	0.826	10.5	0.215	0.65	40.5±2.4	42.4	5
26	0.331	0.339	0.821	9.6	0.110	0.73	31.9±2.3	29.8	7
27	0.257	0.340	0.829	9.9	0.195	0.65	43.3±1.4	42.9	1
28	0.239	0.415	0.831	10.3	0.162	0.73	27.3±0.7	29.8	9

Table 3.6 Experimental and predicted concrete compressive strength at 3 day

Mixture #	ϕ_s	ϕ_{ca}	ϕ_{max}	D (mm)	APT (mm)	α_{3d}	$f'c_{3d}$ (MPa)	$f'c_{model\_3d}$ (MPa)	Error (%)
1	0.311	0.287	0.808	7.1	0.154	0.51	32.7±0.8	26.2	20
2	0.300	0.353	0.814	7.4	0.124	0.58	16.3±0.2	16.5	1
3	0.228	0.355	0.815	7.7	0.209	0.54	29.1±2.0	29.5	1
4	0.346	0.289	0.805	7.0	0.118	0.58	18.1±0.7	16.8	7
5	0.209	0.414	0.828	10.5	0.203	0.51	30.7±0.9	27.1	12
6	0.329	0.335	0.821	9.6	0.114	0.61	18.5±0.4	17.6	5
7	0.260	0.338	0.829	9.9	0.192	0.54	32.1±1.1	29.5	8
8	0.241	0.420	0.831	10.3	0.154	0.58	16.5±1.3	18.5	12
9	0.342	0.288	0.805	7.0	0.122	0.58	23.3±0.6	22.8	2
10	0.391	0.279	0.799	6.8	0.084	0.63	11.8±0.2	10.6	10
11	0.325	0.290	0.807	7.1	0.138	0.58	24.5±0.7	23.6	4
12	0.370	0.283	0.802	6.9	0.099	0.60	10.9±0.3	10.9	0
13	0.280	0.354	0.815	7.5	0.145	0.58	23.2±1.4	23.3	0
14	0.329	0.342	0.811	7.3	0.102	0.54	8.5±0.2	7.9	7
15	0.261	0.355	0.816	7.6	0.166	0.60	25.8±0.2	25.2	2
16	0.313	0.352	0.813	7.4	0.111	0.60	11.6±0.4	12.2	5
17	0.303	0.322	0.812	7.3	0.142	0.58	23.6±1.2	23.5	0
18	0.357	0.251	0.799	6.8	0.129	0.58	20.8±0.3	21.0	1
19	0.234	0.380	0.814	7.8	0.180	0.58	20.8±0.6	21.9	5
20	0.300	0.320	0.812	7.3	0.146	0.55	22.0±3.7	20.9	5
21	0.299	0.291	0.809	7.2	0.166	-	-	-	-
22	0.295	0.360	0.815	7.5	0.125	-	-	-	-
23	0.213	0.357	0.813	7.8	0.229	0.51	31.0±0.6	30.2	3
24	0.341	0.294	0.806	7.0	0.120	0.61	22.5±0.7	22.5	0
25	0.201	0.414	0.826	10.5	0.215	0.51	31.1±0.7	30.4	2
26	0.331	0.339	0.821	9.6	0.110	0.61	24.4±0.2	22.2	9
27	0.257	0.340	0.829	9.9	0.195	0.51	35.1±0.9	30.7	13
28	0.239	0.415	0.831	10.3	0.162	0.61	21.5±0.5	22.1	3

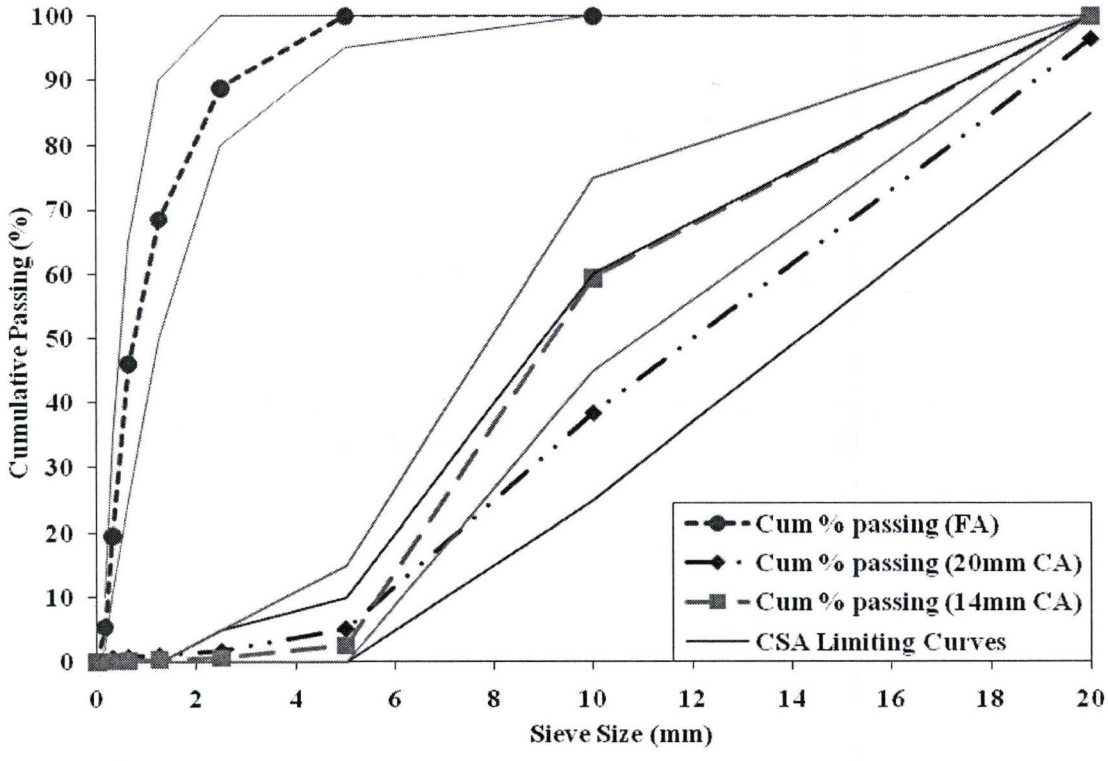

Figure 3.1 Particles size distribution for fine and coarse aggregates

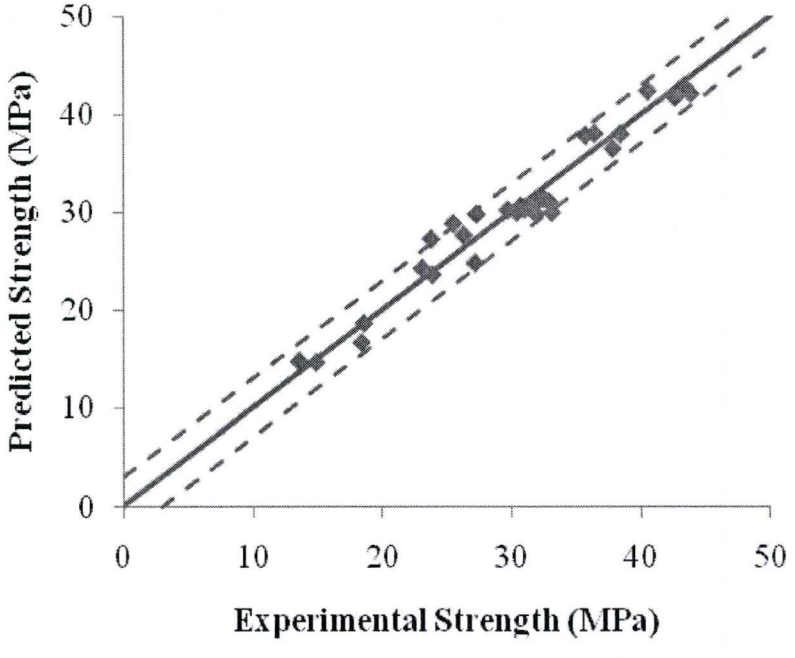

Figure 3.2 Compressive strength model predictions versus measured values

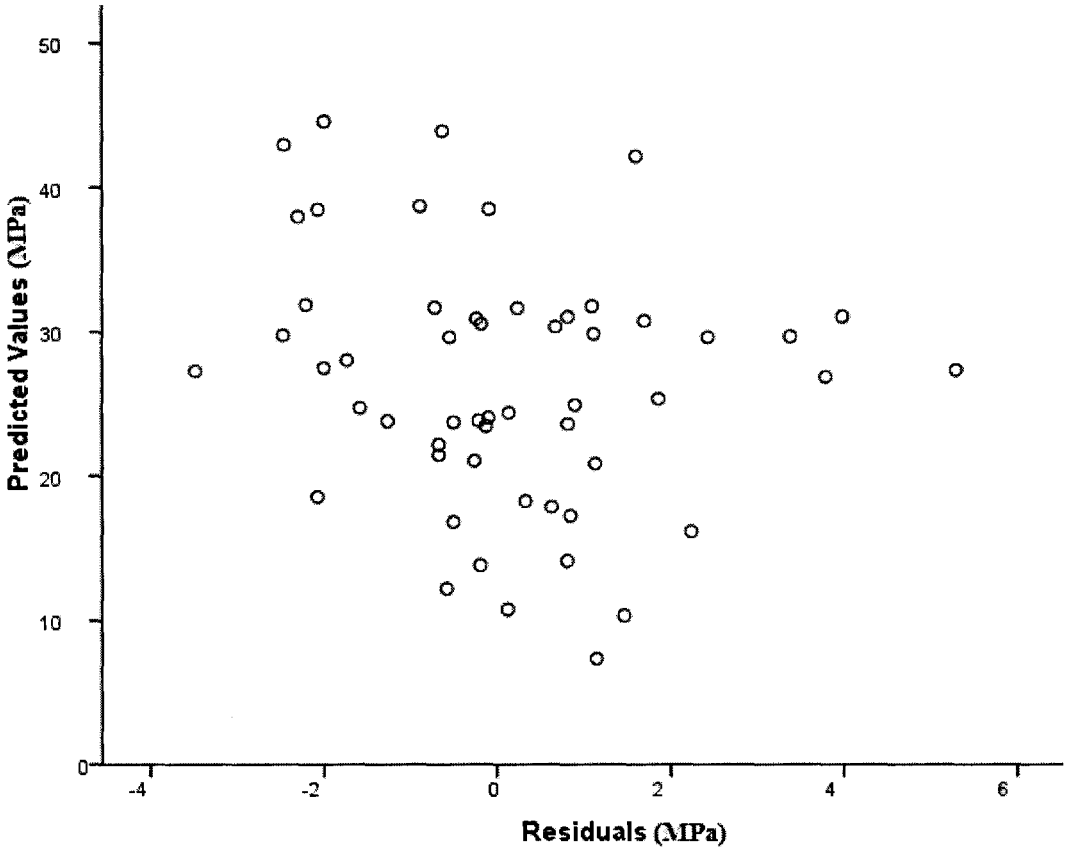

Figure 3.3 Model assessment - residuals plot

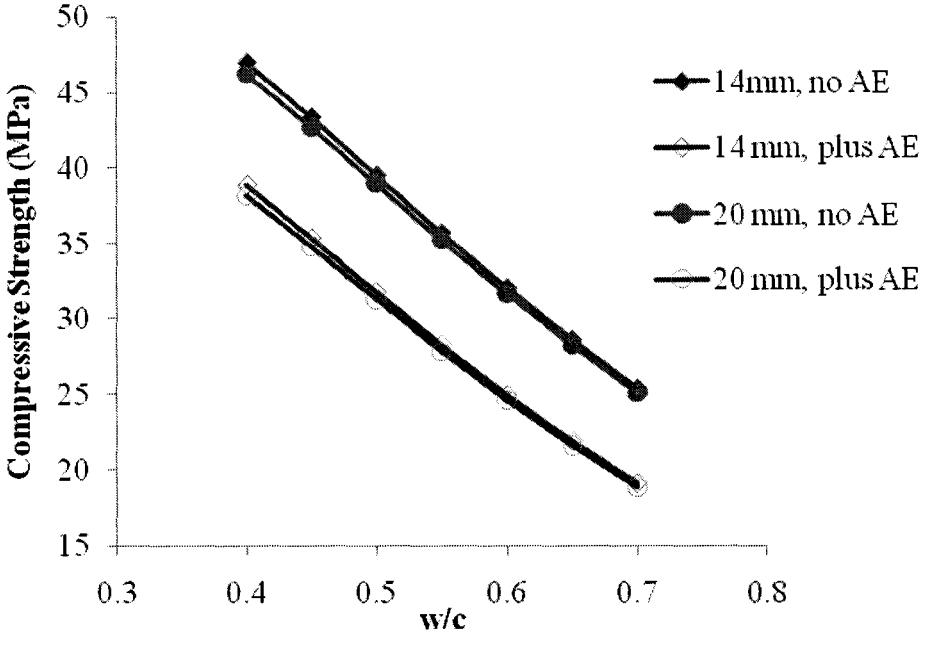

Figure 3.4 Compressive strength vs. w/c – Effect of air and maximum aggregate size

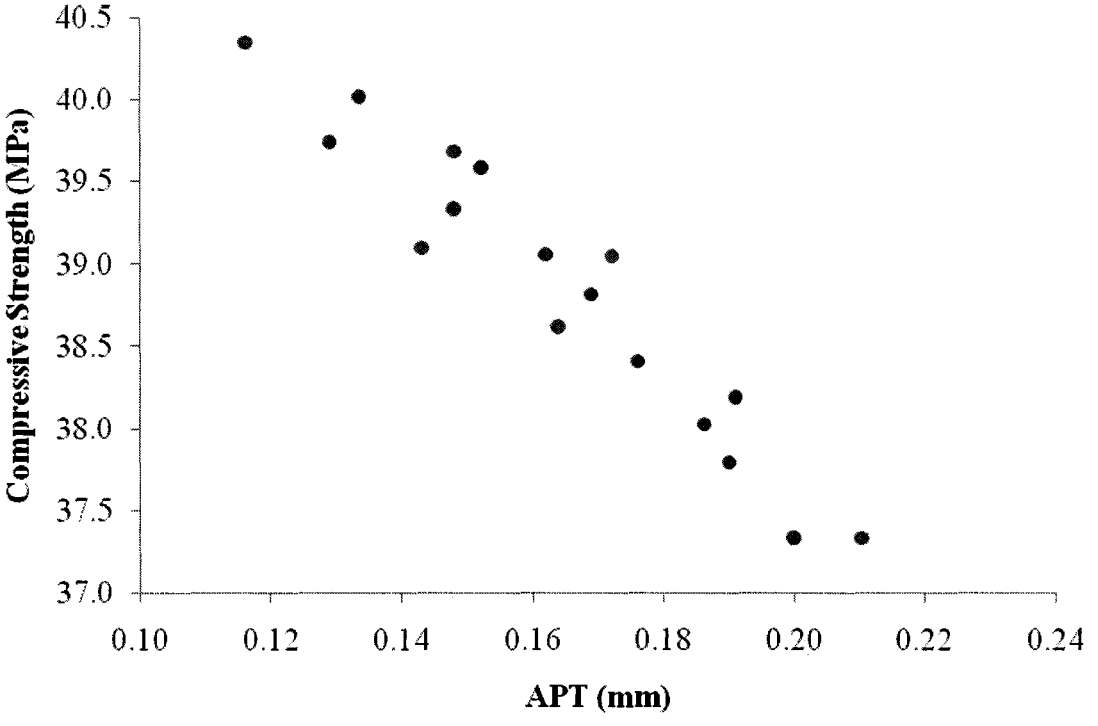

Figure 3.5 Relationship between APT and compressive strength of concrete – Varying water and coarse aggregate contents

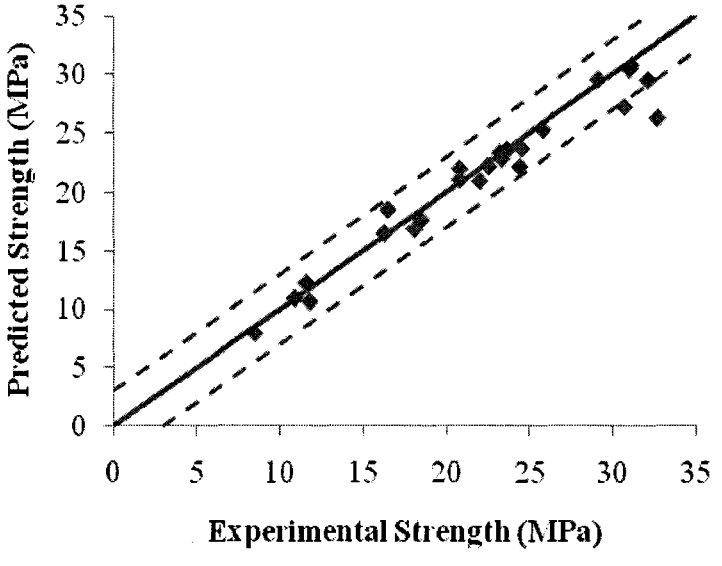

Figure 3.6 Extrapolation for 3-day compressive strength predictions

Chapter 4: Paper III Assessment of Concrete Compressive Strength Predictions Methods

Abstract

Theoretical and phenomenological models for predicting the compressive strength of concrete have been proposed in literature. This paper presents a review of published models, as well as an assessment of their predictive capabilities. The applicability and accuracy of these models in predicting the compressive strength of concrete at 28 days and at different ages were investigated using a large amount of experimental data obtained from literature. This study reveals that the model proposed by Chidiac et al. [1] is a representative model for predicting strength at 28 days and at different ages. It provides the highest predictability with a correlation coefficient of 0.92 and a standard error of 2.3 MPa. It was also revealed that the majority of models give acceptable predications because strength is mostly affected by w/c.

Keywords: compressive strength; strength models, water-cement ratio.

4.0 Introduction

Abrams [2] was one of the pioneers to recognize the significance of concrete compressive strength and proposed to use water-to-cement ratio (w/c) to quantify its value. Since then, it has been shown that there are other parameters that contribute to the compressive strength of concrete, namely cement properties, bonding strength / gradation of aggregates, mixture proportions, chemical admixtures and mineral admixtures [3].

Cement chemical and physical properties contribute greatly to the compressive strength of concrete. The composition and proportions of its major chemical phases (C_3S, C_2S, C_3A, C_4AF) affect the cement hydration reactions and products formed, which in turn affect the strength of the cement paste [4]. Physical properties particularly cement

fineness and particle size distributions affect concrete strength [4, 5]. Greater cement fineness increases the surface available for hydration, causing greater early compressive strength and more rapid generation of heat [5]. Research has also shown that the particle size distribution of cement is of equal importance.

The aggregate bonding strength is influenced by the size, shape and surface roughness of aggregates. Larger aggregates reduce the specific surface area of the aggregates which leads to a reduction in bond strength [6]. Crushed and rough aggregates provide a higher aggregate to paste bonding strength in comparison to round and smooth aggregates [6]. Research has shown that mixtures with aggregate gradation that is uniformly distributed lead to higher packing which results in concrete with higher density, reduced porosity, and higher compressive strength [6].

Research has shown that concrete mixture proportions such as cement content, w/c, aggregate volume fraction and fine-to-coarse aggregate ratio (FA/CA) influence the compressive strength of concrete [5, 7]. An increase in the w/c due to an increase in the water content or due to a reduction in the cement content can dilute the cement paste increasing the volume and thus reducing the compressive strength [5]. The higher the aggregate volume fraction, the longer is the crack path, which results in an increase in the absorbed energy and thus an increase in the compressive strength [5]. An increase in the FA/CA results in a reduction in w/c due to an increased absorption of mix water by sand, which results in an increase in the compressive strength [7].

Research has also shown that chemical and mineral admixtures influence the compressive strength of concrete. The use of an air entraining agent chemical admixture results in an increase in porosity and a reduction in strength [8]. The addition of mineral admixtures such as fly ash, blast furnace slag and silica fume, have been shown to enhance strength due to their pozzolanic properties [8].

Because compressive strength of concrete is a design requirement, various models have been proposed in the literature to predict strength using the concrete mixtures [3]. The majority of these models are phenomenological models and follow either Feret's

postulation [9] or Abram's [2]. This paper presents a brief review of published models, as well as an assessment of their predictive capabilities. Experimental data reported in the literature was used for the assessment.

4.1 Concrete Compressive Strength Models

Compressive strength models were developed from a conceptual postulation of how particles and hydrated cement interact and bond. Accordingly, controlling parameters were identified in the development of these models. This section presents the evolution of these models in brief. Notations are listed at the end of the paper.

Feret's Model

Feret was the first to propose a model for predicting concrete compressive strength and is given by the following equation:

$$f'_c = A\left(\frac{V_c}{V_c + V_w + V_a}\right)^B \tag{4.1}$$

It postulates that strength is a function of the ratio of cement to paste and air [9]. Experimental data have shown poor agreement with this ratio [10]. In addition, the coefficients of proportionality, A and B, need to be determined by trial mixes, which has limited its use [10].

Abrams' Model

Abrams [2] proposed a replacement of the ratio of cement to paste and air with water to cement ratio because it is simpler and it gave better correlation with strength data for non-air entrained concrete [10]. Abrams's model for non-air entrained concrete is as follows:

$$f'_c = \frac{A}{B^{w/c}} \tag{4.2}$$

However, the model is not complete because different A and B values are needed whenever any factor affecting the strength of concrete changes. A and B parameters

depend on cement type and strength, aggregate gradations and proportions, admixtures, curing conditions, testing conditions, and age of concrete.

Powers' Model

Powers postulated that the compressive strength of cement paste is directly related to the gel to space ratio, denoted by X, which is the ratio of the gel volume to the volume of capillary porosity [11]. The gel space ratio equals the volume of hydration products divided by the sum of the volume of hydration products and capillary porosity. The final form of the model after fitting using Feret's power relationship is as follows:

$$f'_c = A(X)^B = A\left(\frac{0.66\alpha}{\frac{w+a}{c}+0.32\alpha}\right)^B \tag{4.3}$$

The effect of air is considered in practice as an extra volume of mixing water [12]. Powers was the first to introduce degree of hydration to the strength model. The model fails to account for important factors such as aggregates properties, standard cement strength and assumes strength starts developing at zero age.

Karni's Model

Karni [12] studied Powers model and then postulated that the volume of the gel should be related to the total volume of the paste (cement + water) minus cement. This was recommended to avoid incorporating the capillary pores fraction which depends on the factors affecting the compressive strength i.e. w/c and α. The following model was developed after using Bolomey's linear relationship for fitting:

$$f'_c = A\left[\frac{\alpha\times 100}{1.53\left(\frac{w+a}{c}\right)+\frac{\alpha}{2.06}}-B\right] \tag{4.4}$$

Popovics' Models

In 1985, Popovics modified Bolomey's model by incorporating the effect of air empirically as follows [10]:

$$f'_c = A\frac{c}{w} + B\times 10^{-0.038\alpha} \tag{4.5}$$

In 1998, Popovics worked on generalizing Abrams model in order to include some of the strength-effecting factors [13]. The mathematical model is based on a cement model, in which the hardening of cement is the sum of two hardening processes of first order reaction. The first hardening component is the C_3S and the second is mostly the C_2S and the mixture of other cement ingredients. Each component has a different hardening rate accounted for in the model. The model also accounts for air content empirically but fails to consider aggregate properties and gradations. The proposed model is as follows [13]:

$$f'_c = \frac{A}{B^{w/c}}\sqrt{\frac{S_s}{S_0}}\cdot\frac{100-C_3e^{-b_1t}-(100-C_3)e^{-b_2t}}{100-C_3e^{-90b_1}-(100-C_3)e^{-90b_2}}\times 10^{-0.038\alpha} \tag{4.6}$$

In 2008, Popovics attempted to improve Abrams model by incorporating the cement content parameters after noting that if two comparable concretes have the same *w/c*, the one with more cement has a lower strength [14]. In comparison to Abrams model, the revised model accounts for air and cement content empirically as follows [14]:

$$f'_c = \frac{A}{B^{\left(\frac{w}{c}+Ec\right)}}\times 10^{-0.038\alpha} \tag{4.7}$$

Pann et al. Model

Pann et al. modified Abrams' model by incorporating the cement paste capillary porosity empirically [15]. Hydrated cement paste consists of capillary pores, P_c, and gel pores, in which capillary pores (>10 nm) reflect the water filled spaces whereas gel pores (>10 nm) reflect the micro spaces between the hydrated cement grains. Pann stated that P_c depends on the degree of hydration and developed a statistical model to predict α at 28 days, which is a function of w/c. The proposed model is as follows:

$$f'_c = \frac{A}{B^{w/c}} + \frac{C}{D^{P_c}}$$
$$P_c = E\ln(\alpha) + \frac{F}{G^{w/c}} + H \tag{4.8}$$

Pann claims that the proposed model is superior to that of Abram's because it accounts for the capillary porosity term. Unfortunately, the model consists of many parameters that need re-calibration when other factors not accounted for by the model are changed. These factors include the properties and gradation of both cement and aggregates.

de Larrard's Model

In a dry packing of particles subjected to compression, the coarse particles are subjected to maximum stress [16]. de Larrard postulated that if cement paste is added then this paste in between two adjoint aggregates will be highly stressed [3] and that the distance between these aggregates is the maximum paste thickness. A model is then presented to calculate the *MPT*, which is a function of the maximum aggregate size, D_{max}, volume fraction of aggregate, ϕ, and maximum packing density of aggregates, ϕ^*:

$$MPT = D_{\max}\left(\sqrt[3]{\frac{\phi^*}{\phi}} - 1\right) \tag{4.9}$$

The effect of aggregates through MPT was then incorporated into Feret's model. In addition, Feret's A coefficient was proposed to be the product of the aggregate bonding strength, K, and the standard cement strength at 28 days, R_{c28}. The effect of age on strength was also considered empirically through fitting of strength versus time data. The proposed model takes the following form:

$$f'_c = KR_{c28}\left[A\log(t/28) + \left(\frac{V_c}{V_c + V_w + V_a}\right)^B\right] MPT^C \tag{4.10}$$

de Larrard's model, which is a significant improvement to current models, did not employ a fundamental approach to account for the chemical properties of cement and the degree of cement hydration. In addition, the predictive capability of the effect of age on strength is limited by the type and range of experimental data used since it is an empirical relationship and so might not be suitable for extrapolation purposes. It should be noted that another form of the model was also presented which considers the type of aggregates through two coefficients p, q that need calibration for any given type of aggregate:

$$f'_c = \frac{p.fc_m}{q.fc_m + 1} \tag{4.11}$$

$$fc_m = 13.4R_{c28}\left[A\log(t/28) + \left(\frac{V_c}{V_c + V_w + V_a}\right)^B\right]MPT^C \tag{4.12}$$

Mechling et al. Model

The K and B parameters in de Larrard's model do not account for the chemical properties of the clinker. Mechling et al. conducted a study to check if the chemical nature of the clinker had an influence on the compressive strength of pastes [17]. It was determined that it is possible to connect K to the C_3S content which is linked to the strength of hydrated cement paste. The author mentioned that the model can also be used for concrete in a similar fashion to that of de Larrard's model as follows:

$$f'_c = KR_{c28}(0.2.[C_3S] - 1.65)\left[A\log(t/28) + \left(\frac{V_c}{V_c + V_w + V_a}\right)^B\right]MPT^C \tag{4.13}$$

Tango Model

Power's law requires knowing the value of α. Tango worked on simplifying Powers law by substituting for α. Function of transformed time, $t^{-0.5}$, is proposed to account for initial hydration and derivative of initial hydration [18]. The final formulation is as follows:

$$f'_c = \frac{A}{B^{\left(\frac{w}{c}\right)}E^{\left(\frac{w}{c}\right)t^{-0.5}}D^{t^{-0.5}}} \tag{4.14}$$

Although the model is simpler to apply, two calibration parameters E and D were added thus limiting the application of the model. In addition, the model lacks to account for cement and aggregate properties.

Chidiac, Moutassem, and Mahmoodzadeh Model

Chidiac et al. [1] postulated that particles interact according to excess paste theory, which states that concrete may be considered a mixture of aggregate and cement paste and that the cement paste in excess of the amount needed to fill up the voids between the

aggregate particles disperses the particles and lubricates the concrete mixture [19]. A mathematical model for the average paste thickness, *APT*, was developed and was found to account for concrete mixtures and aggregate gradation through packing density. The proposed model consists of two fundamental models; cement hydration model and the *APT* model. Moreover, the proposed model accounts for the paste to aggregate bond strength (*K*) and for the cement strength at 28 days (R_{c28}) [3]. Amount of water filled capillary pores, entrapped and entrained air are also accounted for through the w/c and EA variables, respectively. Accordingly, the proposed model is as follows:

$$f'_c(t) = KR_{c28}\left(\frac{APT}{D}\right)^A B^{\frac{W+EA}{C}}\left(\alpha(t)-\alpha_{cr}\right) \tag{4.15}$$

where:

$$APT \approx -\frac{1}{2}\left(D_s + \frac{\phi_{ca}D_s^{\,2}}{\phi_s D_{ca}} + \frac{\phi D_s^{\,2}(1-\phi_{\max})}{\phi_s\phi_{\max}D}\right) + \frac{1}{2}\sqrt{\left(D_s + \frac{\phi_{ca}D_s^{\,2}}{\phi_s D_{ca}} + \frac{\phi D_s^{\,2}(1-\phi_{\max})}{\phi_s\phi_{\max}D}\right)^2 + \frac{4}{3}\frac{(\phi_{\max}-\phi)}{\phi_{\max}}\frac{D_s^{\,2}}{\phi_s}} \tag{4.16}$$

Chidiac et al. model accounts for the cement properties, aggregate properties and its gradation, mixture proportions, porosity, and age.

The degree of cement hydration, α, can be obtained using a cement hydration model such as the one proposed by Schindler and Folliard [20] which is adopted in this study. The critical degree of hydration, α_{cr}, can be predicted according to Rasmussen et al. [21]. The adopted models are as follows:

$$\alpha_{cr} = k \times w/c \tag{4.17}$$

$$\alpha = \alpha_u.\exp\left(-\left[\frac{\tau}{t_e}\right]^{\beta}\right) \tag{4.18}$$

$$\tau = 66.78.p_{C3A}{}^{-0.154}p_{C3S}{}^{-0.401}.Blaine^{-0.804}.P_{SO3}{}^{-0.758}.\exp(2.187.p_{SLAG} + 9.5.p_{FA}.p_{FA-CaO}) \tag{4.19}$$

$$\beta = 181.4.p_{C3A}{}^{0.146}.p_{C3S}{}^{0.227}.Blaine^{-0.535}.p_{SO3}{}^{0.558}.\exp(-0.647.p_{SLAG}) \tag{4.20}$$

$$\alpha_u = \frac{1.031.w/c}{0.194 + w/c} + 0.50.p_{FA} + 0.30.p_{SLAG} \leq 1.0 \tag{4.21}$$

$$t_e = \sum_0^t \exp\left(\frac{E}{R}\left(\frac{1}{293} - \frac{1}{T+273}\right)\right).\Delta t \tag{4.22}$$

Other Empirical and Statistical Models

Many other models that are purely empirical or statistical have been reported in the literature. Cheng Yeh [22] modified Abrams law by including the effect of age on strength empirically. Models such Nipatsat and Tangtermsirikul [23], Hwang et al. [24], and Namyong at al. [25] are examples of statistical models that are only functions of the mixture composition and do not account for cement properties, aggregate properties, their gradations and concrete age.

4.2 Procedure for Calibration and Evaluation

Using experimental data reported in the literature, the strength models were first calibrated using 12 data points, and then evaluated using the remaining points. For the formulas that require the use of cement hydration model, Schindler and Folliard hydration model [20] was adopted. Calibration of the compressive strength models was done by minimizing the standard error using least squares analysis. Standard error (σ), which provides a global assessment of the model prediction, is defined by [26]:

$$\sigma = \sqrt{\frac{\sum_i \left(f'_{c\,model_i} - f'_{c\,\exp_i}\right)^2}{n-p}} \tag{4.23}$$

In addition, the correlation coefficient (R^2) of a model, which measures the degree of correlation between model and experiment, was also calculated [26].

Since the aggregate type is different for the different sources from literature, the aggregate bonding constant K and constant A in models were calibrated for each source. Since many models were developed to predict the 28-day strength only, all models were first evaluated at 28 days then extended to all ages using the models accounting for age. It

should be noted that in order to allow some models such as Pann and Tango to account for air, the *w/c* term was replaced with *(w+a)/c* as recommended by Popovics [14].

4.3 Experimental Data

Over 250 reported concrete strength values with concrete age ranging from 3 days to 191 days were used to assess the strength models. Each strength value is an average of a minimum of three measured values. Concrete was mixed, cast, consolidated, finished, and cured in accordance with ASTM C192-02 [27], and tested in accordance with ASTM C39-05 [28].

Chidiac, Moutassem, and Mahmoodzadeh [29]:

Ordinary Portland cement OPC (Hydraulic cement type GU-type 10) obtained from Lafarge Canada was used. Crushed limestone coarse aggregate (CA) with 20 mm and 14 mm nominal maximum aggregate sizes were used. The fine aggregate was siliceous sand with a fineness modulus of 2.71. The range selected for w/c was from 0.4 to 0.7 with 0.1 increments. The water content values ranged from 175 to 228 kg/m^3, which covers the full range of slump for non-air entrained and air entrained concretes. The cement content ranged from 250 to 570 kg/m^3. The bulk volume of CA per unit volume of concrete ranged from 0.45 to 0.69. The specific gravities and bulk densities for the 20 mm CA are 2.75 and 1636 kg/m^3, for the 14 mm CA are 2.74, and 1576 kg/m^3, and for sand are 2.71 and 1812 kg/m^3, respectively. The characteristic diameters and mean diameters for the 20 mm CA are 14.3 and 12 mm, for 14 mm CA are 10.4 and 9.1 mm, and for sand are 1.1 and 0.74 mm, respectively. The Blaine of cement and weight ratios in terms of total cement content for the C_3A, C_3S and SO_3 compounds are 428 cm^2/g, 0.09, 0.58 and 0.034, respectively. Twenty mixes were air entrained and 8 were non-air entrained. Concrete was tested for compressive strength at 3 days and 28 days. Concrete mixture proportions and strength data are given in Table 4.1.

Bloem and Walker [30]:

Ordinary Portland cement (ASTM Type I) was used. The CA was hard, subangular, quartzile gravel with nominal maximum aggregate sizes of 9.5 mm, 19 mm, 38 mm and 63 mm. The fine aggregate was siliceous sand with a fineness modulus of 2.70. The w/c ranged from 0.37 to 0.89. The water content values ranged from 167 to 197 kg/m^3. The cement content ranged from 219 to 453 kg/m^3. The bulk volume of CA per unit volume of concrete ranged from 0.59 to 0.68. The specific gravities for CA and sand are 2.64 and 2.64, respectively. The bulk densities for the 9.5, 19, 38 and 63 mm CA are 1647, 1721, 1742 and 1828 kg/m^3, respectively. The characteristic diameters and mean diameters were assumed to be 7.5 and 6.3 mm for 9.5 mm CA, 15 and 12.6 mm for 19 mm CA, 30 and 25.1 mm for 38 mm CA, and 50 and 41.9 mm for 63.5 mm CA, respectively. The assumed values for the Blaine of cement and weight ratios in terms of total cement content for the C_3A, C_3S and SO_3 compounds are 428 cm^2/g, 0.09, 0.58 and 0.034, respectively. Mixes 13 to 24 were air entrained. Concrete was tested for compressive strength at the ages of 7, 28, and 91 days. Concrete mixture proportions and strength data are given in Table 4.2.

Kim, Moon, and Eo [31]:

Ordinary Portland cement (ASTM Type I) was used. The CA was angular crushed stone with nominal maximum aggregate size of 25 mm. The fine aggregate was river sand with a fineness modulus of 2.64. The w/c were 0.35 and 0.55. The water contents values were 175 and 185 kg/m^3. The cement content were 335 and 495 kg/m^3. The bulk volume of CA per unit volume of concrete were 0.61 and 0.62. The specific gravities and bulk densities for the 25 mm CA are 2.66 and 1537 kg/m^3 and for sand are 2.65 and 1469 kg/m^3, respectively. The assumed characteristic diameters and mean diameters for the 25 mm CA are 19.7 and 16.5 mm and for sand are 1.1 and 0.74 mm, respectively. The assumed values for the Blaine of cement and weight ratios in terms of total cement content for the C_3A, C_3S and SO_3 compounds are 428 cm^2/g, 0.09, 0.58 and 0.034, respectively. The mixes were air entrained to achieve around 5% air. Concrete was tested for compressive

strength at the ages of 3, 7, 14, and 28 days. The mixture proportions and corresponding strength data are given in Table 4.3.

Gardner [32]:

Ordinary Portland cement (CSA Type 10) was used. The CA was crushed stone with nominal maximum aggregate size of 20 mm. The w/c were 0.34 and 0.55. The water content were 138 and 169 kg/m^3. The cement content were 305 and 409 kg/m^3. The bulk volume of CA per unit volume of concrete was 0.66. The specific gravities and assumed bulk densities for the 20 mm CA are 2.66 and 1576 kg/m^3 and for sand are 2.65 and 1812 kg/m^3, respectively. The assumed characteristic diameters and mean diameters for the 25 mm CA are 15.8 and 13.2 mm and for sand are 1.1 and 0.74 mm, respectively. The given cement Blaine and the assumed weight ratios in terms of total cement content for the C_3A, C_3S and SO_3 compounds are 375 cm^2/g, 0.09, 0.58 and 0.034, respectively. Concrete was tested for compressive strength at the ages of 3, 7, 14, 28, 56, and 112 days. The mixture proportions and corresponding strength data up to 28 days are given in Table 4.3. The strength values at 56 and 112 days for w/c of 0.34 are 49.4 and 54.3 MPa and for w/c of 0.55 are 38.9 and 42.6 MPa, respectively.

Zain and Abd [33]:

Ordinary Portland cement (ASTM type I) was used. The CA was crushed granite stone with nominal maximum aggregate size of 20 mm. The fine aggregate was mining sand with a fineness modulus of 3.01. The w/c, water content, cement content and bulk volume of CA were 0.50, 200 kg/m^3, 400 kg/m^3, and 0.67, respectively. The specific gravities and assumed bulk densities for the 20 mm CA are 2.62 and 1576 kg/m^3 and for sand are 2.62 and 1812 kg/m^3, respectively. The assumed characteristic diameters and mean diameters for the 20 mm CA are 15.8 and 13.2 mm and for sand are 1.1 and 0.74 mm, respectively. The assumed values for the cement Blaine and the weight ratios in terms of total cement content for the C_3A, C_3S and SO_3 compounds are 428 cm^2/g, 0.09, 0.58 and 0.034, respectively. The concrete was air entrained to achieve 6% air. Concrete was tested for

compressive strength at the ages of 3, 7, 14, 28, and 91 days. The mixture proportions and corresponding strength data up to 28 days are given in Table 4.3. The 91 day strength is 32.3 MPa.

Gallo and Popovics [34]:

Ordinary Portland cement (ASTM Type I) was used. The CA was crushed limestone with nominal maximum aggregate size of 25 mm. The fine aggregate was well graded sand. The w/c ranged from 0.40 to 0.52. The water contents values ranged from 164 kg/m^3 to 187 kg/m^3. The cement content ranged from 344 to 423 kg/m^3. The bulk volume of CA per unit volume of concrete was 0.72. The assumed specific gravities and bulk densities for the 20 mm CA are 2.62 and 1576 kg/m^3 and for sand are 2.62 and 1812 kg/m^3, respectively. The assumed characteristic diameters and mean diameters for the 25 mm CA are 19.7 and 16.5 mm and for sand are 1.1 and 0.74 mm, respectively. The assumed values for the cement Blaine and the weight ratios in terms of total cement content for the C_3A, C_3S and SO_3 compounds are 428 cm^2/g, 0.09, 0.58 and 0.034, respectively. Mixes 1 to 4 were air entrained. Concrete was tested for compressive strength at the ages of 7, 14, and 28 days. Concrete mixture proportions and strength data are given in Table 4.4.

Namyong, Sangchun, and Hongbum [25]:

Ordinary Portland cement was used (ASTM Type I). The CA was angular crushed stone with nominal maximum aggregate size of 25 mm. The fine aggregate was sea sand and crushed sand with their fineness modulus ranging from 2.70 – 3.0. The w/c ranged from 0.39 to 0.62. The water content ranged from 164 to 196 kg/m^3. The cement contents ranged from 289 to 463 kg/m^3. The bulk volume of CA per unit volume of concrete were 0.55 and 0.72. The specific gravities and assumed bulk densities for the 25 mm CA are 2.63 and 1576 kg/m^3 and for sand are 2.60 and 1812 kg/m^3, respectively. The assumed characteristic diameters and mean diameters for the 25 mm CA are 19.7 and 16.5 mm and for sand are 1.1 and 0.74 mm, respectively. The assumed values for the cement Blaine and the weight ratios in terms of total cement content for the C_3A, C_3S and SO_3

compounds are 428 cm^2/g, 0.09, 0.58 and 0.034, respectively. Concrete was tested for compressive strength at the ages of 7 and 28 days. Mixture proportions and strength data are given in Table 4.5.

4.4 Results and Discussion

The results of the evaluation of the models at 28 days in terms of the number of calibration constants (p), σ, and R^2 are given in Table 4.6. Results show that the model proposed by Chidiac et al. [1], which mathematically accounts for packing density through APT, gave better prediction of strength in comparison to other models. The effect of *APT*, which accounts for aggregate proportions and gradations through packing density, on strength was studied using experimental data and was shown to affect the strength values [29].

Table 4.6 shows that all models give good results. Looking at the form of the models, one can observe that most models are function of w/c. It is well established in the literature that w/c is the most significant factor affecting the compressive strength of concrete [2, 8, 14]. Figure 4.1 demonstrates the effect of w/c on the 28-day strength for non air entrained concrete mixes. The results display the common trend where an increase in w/c yields a decrease in strength, which is consistent with the design guidelines [35]. The results also reveal the degree of significance of w/c on strength in which an increase in w/c from 0.30 to 0.90 resulted in a reduction in strength from 47 to 16 MPa. The scatter in the plot is due to the influence of other variables that need be accounted for such as aggregate mixture proportions, sizes, gradation, bonding capability, etc.

Table 4.6 also shows that Feret's model [9], which is function of the cement to paste ratio, is the least accurate model. This coincides with Popovics' claim that experimental data were shown not to have a very good agreement with this ratio [10]. Models that employ the effect of age on strength developed to predict the strength at any age were also evaluated. The same 17 points were used for calibration and the remaining points were used for evaluation. Results of the evaluation of these models are shown in Table

4.7. Results reveal that Chidiac et al. model, which accounts for age through α, is more accurate than other models. Although Powers [11] and Karni [12] models also account for α, they still fail to account for aggregate properties and gradation, standard cement strength, and α_{cr}. Although Mechling and de Larrard models, which account for packing density, have resulted in high accuracy for predicting the strength at 28 days, their accuracy is diminished for other ages because of the empirical relationship between age and strength. The predictive capability of the models that account for age empirically are limited by the type and range of experimental data used and thus might require recalibration for a new set of data. Nevertheless, these models are still acceptable.

The result of this evaluation is also shown in Figure 4.2, which provide a visual comparison of models predictions versus experimental data. These graphs demonstrate that the model proposed by Chidiac et al. provides a higher degree of correlation to the experimental data in comparison to other models.

4.5 Conclusions

The results of this study can be summarized as follows:

1. A review of published models has revealed that the model proposed by Chidiac et al. [1] is one of the most representative models because it accounts for the cement properties and strength, concrete age, concrete mixture, aggregate gradation, bonding capability of the aggregates to the paste, air content and voids.

2. An evaluation of published compressive strength models has revealed that the majority of the models predicted well the measured values because strength is mostly affected by w/c. Feret's model which is function of cement to paste ratio resulted in the lowest predictability.

3. The model proposed by Chidiac et al. [1] which mathematically accounts for packing density, aggregate proportions and gradations, resulted in the highest predictability for 28-day strength.

4. Models that employ the effect of age on strength developed to predict the strength at any age were also evaluated and results has revealed that Chidiac et al. model is more accurate than other models giving a correlation coefficient of 0.93 and a standard error of 2.2 MPa.
5. Aggregate proportions and gradation do not greatly influence strength in comparison with the w/c.

Acknowledgments

This study forms a part of ongoing research at McMaster University's Centre for Effective Design of Structures funded through the Ontario Research and Development Challenge Fund. The authors would like to thank Natural Science and Engineering Research Council of Canada and McMaster University for their support and funding.

Notation

f'_c	Compressive strength of concrete;
f'_{cm}	Compressive strength of the matrix;
v_c, v_w, v_a	volumes of cement, water, and air, respectively;
w/c	water-to-cement ratio;
a	volume fraction of air;
S_s, S_o	specific surface of the cement and that of a typical ASTM Type 1 cement, respectively;
C_3	C_3S content of cement;
t	testing age;
R_{c28}	cement standard strength at 28 days;
MPT	maximum paste thickness;
c, s, g	quantities of cement, sand, and aggregate, respectively;
α_{cr}	critical degree of cement hydration;
α_u	ultimate degree of cement hydration;
APT	Average paste thickness;
D, D_s, and D_{ca}	the mean diameters of the full aggregate gradation, of sand particles gradation, and of coarse aggregate particles gradation, respectively;
ϕ, ϕ_s, and ϕ_{ca}	volume fraction of aggregates, of sand particles, and of coarse particles, respectively;
ϕ^*	maximum packing density of aggregate;
$f'_{c\ model\_i}, f'_{c\ exp\_i}$	the model and experimental compressive strengths corresponding to mix i, respectively.
n	the number of test points;
p	the number of model constants;
t_e	equivalent age;
T	concrete temperature;
E	activation energy;
τ	hydration time parameter;
β	hydration shape parameter;
$p_{C3A}, p_{C3S}, p_{SO3}, p_{FA}, p_{SLAG}, p_{FA\text{-}CaO}$	weight ratios in terms of total cement content
$A, B, C, D, E, F, H, K, b_1, b_2, p, q, k$	calibration constants.

References

[1] Chidiac S.E., Moutassem F., and Mahmoodzadeh F., 2010. "Compressive strength model for concrete – I: Theory", Cement and Concrete Composites, To be submitted for publication.

[2] Abrams L. D., 1919, cited by Neville, A. M., Properties of Concrete, 3rd ed., Pitman, 1981.

[3] de Larrard F., 1999. Concrete mixture proportioning: a Scientific Approach, Spon Press, London, 320pp.

[4] Mehta P.K. and Monteiro P., 2006. Concrete: Microstructure, properties, and materials, Third edition, McGraw-Hill, USA.

[5] Kolias S. and Georgiou C., 2005. "The effect of paste volume and of water content on the strength and water absorption of concrete", Cement & Concrete Composites 27(2), 211–216.

[6] Quiroga P, 2003. The effect of the aggregate characteristics on the performance of portland cement concrete, Ph.D. Dissertation, The University of Texas at Austin.

[7] Basheer L., Basheer P.A.M., Long A.E., 2005. "Influence of coarse aggregate on the permeation, durability and the microstructure characteristics of ordinary portland cement concrete", Construction and Building Materials, 19(9), 682–690.

[8] Neville A.M., 1981. Properties of concrete, 3rd Edition, Pitman Publishing Ltd., London.

[9] Feret R., 1892. "Sur la compacité des mortiers hydrauliques (On the compactness of hydraulic mortars)", Annales des Ponts et Chaussées, Série 7(4), 5-164.

[10] Popovics S., 1985. "New formulas for the prediction of the effect of porosity on concrete strength", Journal of the American Concrete Institute, 82(2), 136-146.

[11] Powers T.C. and Brownyard, T.L., 1960. "Studies of the physical properties of hardened portland cement paste", Journal of American Concrete Institute, 18, 2.

[12] Karni J. 1974. "Prediction of compressive strength of concrete", Materials and Structures Journal., 7(3), 197–200.

[13] Popovics S., 1998. "History of a mathematical model for strength development of Portland cement concrete", ACI Materials Journal, 95(5), 593–600.

[14] Popovics S. and Ujhelyi J., 2008. "Contribution to the concrete strength versus water-cement ratio relationship", Journal Material Civil Engineering, 20(7), 459-463.

[15] Pann K. S., Yen T., Tang C. W., Lin T.D., 2003. "New strength model based on water-cement ratio and capillary porosity", Materials Journal, 100(4), 311-318.

[16] de Larrard F. and Belloc A., 1997. "The influence of aggregate on the compressive strength of normal and high-strength concrete", ACI Materials Journal, 94(5), 417–425.

[17] Mechling J.M., Lecomte A., Diliberto C., 2009. "Relation between cement composition and compressive strength of pure pastes", Cement and Concrete Composites, 31(4), 255-262.

[18] Tango C.E.S., 2000. "Time-generalisation of Abrams' model for high performance concrete and practical application examples", Proceedings of the International Symposium on High Performance Concrete, Hong Kong University of Science and Technology. Hong Kong, China.

[19] Wong H.H.C. and Kwan A.K H., 2008. "Packing density of cementitious materials: measurement and modelling", Magazine of Concrete Research, 60(3), 165–175.

[20] Schindler A. K. and Folliard K. J., 2005. "Heat of hydration models for cementitious materials", ACI Materials Journal, 102(1), 24–33.

[21] Rasmussen R.O., Ruiz J.M., Rozycki D.K., McCullough B.F., 2002. "Constructing high-performance concrete pavements with FHWA HIPERPAV systems analysis software", Transportation Research Record 1813, Transportation Research Board, Washington, DC, 11-20.

[22] Yeh I.C., 2006. "Generalization of strength versus water-cementations ratio relationship to age", Cement and Concrete Research, 36(10), 1865-1873.

[23] Nipatsat N. and Tangtermsirikul S., 2000. "Compressive strength prediction model for fly ash concrete", Thammasat International Journal of Science and Technology, 5(1), 1–7.

[24] Hwang S.D. Lee K.M., Kim J.K., Kim J.H., 2001. "Microstructure model for estimating early-age concrete strength", First International Structural Engineering and Construction Conference, Honolulu, HI, USA, 493-497.

[25] Namyong J., Sangchun Y., Hongbum C., 2004. "Prediction of compressive strength of in-situ concrete based on mixture proportion", Journal of Asian Architecture and Building Engineering, 3(1), 9-16.

[26] Montgomery D.C. and Runger G.C., 2003. Applied statistics and probability for engineers, Third edition, NewYork: John Wiley and Sons Inc.

[27] ASTM C192-02, 2002. "Making and curing concrete specimens in the laboratory", American Society for Testing of Materials, West Conshohochen, PA, USA.

[28] ASTM C39-05, 2005. "Standard test method for compressive strength of cylindrical specimens", American Society for Testing of Materials, West Conshohochen, PA, USA.

[29] Chidiac S.E., Moutassem F., and Mahmoodzadeh F., 2010. "Compressive strength model for concrete - II: calibration and validation", Cement and Concrete Composites, To be submitted for publication.

[30] Bloem D. L, and Walker S., 1960. "Effects of aggregate size on properties of concrete", ACI Materials Journal, 57(13), 283–297.

[31] Kim J.K., Moon J.H., Eo S.H., 1998. "Compressive strength development of concrete with different curing time and temperature", Cement and Concrete Research, 28(12), 1761–1773.

[32] Gardner N.J., 1990. "Effect of temperature on the early-age properties of type I, type III, and type I/fly ash concrete". ACI Materials Journal, 87(1), 68–78.

[33] Zain M.F.M. and Abd S.M., 2009. "Multiple regression model for compressive strength prediction of high performance concrete", Journal of Applied Sciences, 9 (1), 155-160.

[34] Gallo G.E. and Popovics J.S., 2005. "The use of surface waves to estimate in-place strength of concrete", Journal of Advanced Concrete Technology, 3(3) 355-362.

[35] Kosmatka S.H., Kerkhoff B., Panarese W.C., 2002. Design and control of concrete mixtures, Seventh Canadian Edition, Cement Association of Canada.

Table 4.1 Concrete mixture proportions and strength data [29]

Mixture #	w/c	Size	Water (kg/m^3)	Cement (kg/m^3)	Coarse aggregate (kg/m^3)	Sand (kg/m^3)	Air (%)	$f'_{c\ 3\ days}$ (MPa)	$f'_{c\ 28\ days}$ (MPa)
1	0.40	14	193	483	794	851	5.9	32.7	37.8
2	0.60	14	193	322	971	815	5.3	16.3	23.1
3	0.40	14	205	513	971	618	4.8	29.1	36.4
4	0.60	14	205	342	794	939	5.1	18.1	27.2
5	0.40	20	184	460	1134	563	4.6	30.7	35.7
6	0.60	20	184	307	928	898	5.6	18.5	23.9
7	0.40	20	197	493	928	703	4.8	32.1	38.4
8	0.60	20	197	328	1134	641	3.1	16.5	23.8
9	0.50	14	193	386	794	934	5.7	23.3	30.4
10	0.70	14	175	250	794	1100	8.8	11.8	14.9
11	0.50	14	205	410	794	881	5.1	24.5	32.9
12	0.70	14	193	276	794	1029	7.5	10.9	18.4
13	0.50	14	193	386	971	759	5.1	23.2	30.7
14	0.70	14	175	250	971	925	8.7	8.5	13.6
15	0.50	14	205	410	971	706	4.8	25.8	32.5
16	0.70	14	193	276	971	854	5.6	11.6	18.6
17	0.50	14	199	398	883	820	5.0	23.6	31.9
18	0.50	14	199	398	706	994	7.8	20.8	26.3
19	0.50	14	199	398	1059	645	6.7	20.8	25.5
20	0.50	14	199	398	883	820	5.8	22.0	33.1
21	0.40	14	216	540	794	807	2.1	-	42.6
22	0.60	14	216	360	971	787	1.0	-	31.0
23	0.40	14	228	570	971	574	1.8	31.0	43.8
24	0.60	14	228	380	794	912	1.2	22.5	29.7
25	0.40	20	205	513	1134	542	1.6	31.1	40.5
26	0.60	20	205	342	928	892	1.5	24.4	31.9
27	0.40	20	216	540	928	692	1.4	35.1	43.3
28	0.60	20	216	360	1134	643	1.5	21.5	27.3

Table 4.2 Concrete mixture proportions and strength data [30]

Mix #	w/c	Size	Water (kg/m^3)	Cement (kg/m^3)	Coarse aggregate (kg/m^3)	Sand (kg/m^3)	Air (%)	$f'_{c\ 7\ days}$ (MPa)	$f'_{c\ 28\ days}$ (MPa)	$f'_{c\ 191\ days}$ (MPa)
1	0.89	9.5	197	222	977	945	0.5	10.7	16.0	16.8
2	0.80	19.1	179	223	1137	795	1.8	12.9	19.2	20.7
3	0.74	38.1	165	223	1163	795	2.2	13.7	20.1	22.8
4	0.73	63.5	162	223	1159	808	2.2	13.9	20.1	20.8
5	0.56	9.5	187	335	985	821	2.3	26.2	34.7	37.0
6	0.51	19.1	172	336	1143	722	1.5	27.8	35.1	39.6
7	0.50	38.1	165	334	1163	721	1.5	27.2	33.9	36.4
8	0.48	63.5	162	335	1161	734	1.4	25.7	32.2	35.8
9	0.44	9.5	194	445	982	721	2.0	32.7	41.0	45.8
10	0.41	19.1	180	442	1129	616	1.9	32.3	39.1	44.5
11	0.39	38.1	174	442	1158	622	1.1	31.5	38.2	42.1
12	0.39	63.5	172	441	1148	632	1.4	30.0	35.2	41.2
13	0.86	9.5	188	219	963	879	4.5	10.5	16.3	17.7
14	0.75	19.1	166	221	1125	768	4.7	14.7	20.8	22.8
15	0.70	38.1	155	221	1151	771	4.7	15.1	21.4	22.8
16	0.70	63.5	155	220	1145	789	4.3	14.8	20.4	21.6
17	0.53	9.5	178	337	990	778	4.5	27.0	35.3	38.3
18	0.48	19.1	160	337	1146	661	4.8	25.6	32.2	36.1
19	0.46	38.1	156	337	1174	649	4.6	25.2	32.3	34.9
20	0.45	63.5	152	338	1170	664	4.6	25.6	30.8	31.4
21	0.41	9.5	185	451	995	654	4.7	32.5	39.3	44.6
22	0.39	19.1	172	444	1132	550	5.0	28.3	34.2	38.6
23	0.38	38.1	171	451	1177	521	4.2	26.4	32.4	36.2
24	0.37	63.5	167	453	1174	537	4.1	26.5	31.8	34.3

Table 4.3 Concrete mixture proportions and strength data [31, 32, 33]

Mix #	w/c	Size	Water (kg/m^3)	Cement (kg/m^3)	Coarse aggregate (kg/m^3)	Sand (kg/m^3)	Air (%)	f'_c (MPa)			
								3d	7d	14d	28d
1	0.35	25	175	495	940	759	4.3	30.9	39.6	45.5	49.6
2	0.55	25	185	335	959	835	5.4	16.4	25.1	31.7	35.9
3	0.55	20	169	305	1040	830	-	20.0	27.7	31.0	35.2
4	0.34	20	138	409	1040	820	-	29.3	39.1	42.8	46.6
5	0.50	19	200	400	1055	707	6.0	18.0	24.7	26.9	31.0

Table 4.4 Concrete mixture proportions and strength data [34]

Mix #	w/c	Size	Water (kg/m^3)	Cement (kg/m^3)	Coarse aggregate (kg/m^3)	Sand (kg/m^3)	Air (%)	$f'_{c\ 28\ days}$ (MPa)
1	0.40	25	167	418	1129	585	3.3	39.2
2	0.44	25	164	372	1128	636	4.4	31.0
3	0.48	25	165	344	1136	654	6.3	25.8
4	0.52	25	166	319	1140	675	5.1	23.8
5	0.40	25	185	463	1124	578	1.2	45.7
6	0.44	25	186	423	1129	613	1.5	40.2
7	0.48	25	186	388	1134	641	1.5	33.8
8	0.52	25	187	360	1139	663	2.7	34.7

Table 4.5 Concrete mixture proportions and strength data [25]

Mix #	w/c	Size	Water (kg/m^3)	Cement (kg/m^3)	Coarse aggregate (kg/m^3)	Sand (kg/m^3)	Air (%)	$f'_{c\ 7\ days}$ (MPa)	$f'_{c\ 28\ days}$ (MPa)
1	0.60	25	174	244	900	933	-	15.5	21.1
2	0.60	25	184	254	860	927	-	17.5	24.2
3	0.61	25	183	253	860	926	-	16.3	23.0
4	0.58	25	173	236	863	961	-	21.5	26.2
5	0.60	25	190	256	862	904	-	18.6	24.0
6	0.62	25	190	255	859	911	-	17.4	22.5
7	0.60	25	184	260	975	821	-	15.8	22.6
8	0.50	25	164	252	942	886	-	23.2	31.2
9	0.48	25	176	298	988	805	-	19.1	26.9
10	0.49	25	178	276	914	858	-	23.3	30.7
11	0.52	25	178	263	931	839	-	22.6	28.8
12	0.45	25	165	294	1000	810	-	20.7	27.6
13	0.45	25	164	298	940	847	-	18.9	28.5
14	0.49	25	169	264	902	882	-	24.0	32.0
15	0.49	25	181	284	887	866	-	23.3	30.5
16	0.50	25	171	263	913	885	-	23.0	31.6
17	0.50	25	181	286	874	865	-	21.6	31.7
18	0.45	25	179	312	894	835	-	22.0	30.2
19	0.45	25	180	308	939	790	-	22.4	30.2
20	0.47	25	183	313	981	759	-	20.4	29.7
21	0.50	25	175	294	955	804	-	16.0	29.8
22	0.47	25	183	312	962	778	-	19.8	26.7
23	0.47	25	184	319	962	778	-	18.1	25.3
24	0.48	25	184	306	924	810	-	20.1	27.8
25	0.48	25	183	295	902	807	-	22.0	29.1
26	0.48	25	183	292	924	818	-	22.8	29.2
27	0.48	25	184	303	922	812	-	21.2	27.6
28	0.46	25	175	247	905	846	-	22.8	28.9

29	0.47	25	173	291	878	889	-	21.3	27.3
30	0.47	25	179	302	862	879	-	21.2	27.6
31	0.44	25	168	300	903	868	-	21.1	29.1
32	0.48	25	182	305	956	812	-	20.0	26.2
33	0.45	25	172	299	940	815	-	21.5	28.3
34	0.48	25	183	300	923	807	-	20.7	27.5
35	0.46	25	184	306	978	754	-	23.7	31.3
36	0.49	25	185	297	946	800	-	21.9	28.7
37	0.46	25	175	304	888	863	-	20.6	28.2
38	0.48	25	172	284	965	794	-	21.0	27.2
39	0.46	25	189	309	947	730	-	25.0	30.9
40	0.46	25	189	326	951	732	-	20.7	30.7
41	0.43	25	180	325	927	784	-	22.7	30.0
42	0.41	25	184	348	977	713	-	22.6	30.7
43	0.41	25	184	346	983	704	-	23.6	31.0
44	0.42	25	183	336	889	804	-	22.8	29.8
45	0.44	25	187	329	882	812	-	22.4	30.2
46	0.44	25	183	324	920	785	-	22.8	30.7
47	0.44	25	183	314	921	780	-	23.9	30.1
48	0.44	25	183	316	923	791	-	23.6	30.9
49	0.41	25	168	317	936	811	-	22.6	33.3
50	0.43	25	180	327	891	813	-	22.9	30.8
51	0.44	25	183	327	956	783	-	20.8	29.3
52	0.48	25	196	314	879	786	-	22.4	30.7
53	0.45	25	187	319	883	818	-	22.8	29.5
54	0.44	25	183	306	900	780	-	25.9	34.3
55	0.44	25	183	312	914	783	-	24.5	32.4
56	0.40	25	176	336	970	760	-	24.7	29.4
57	0.49	25	182	318	954	771	-	23.4	30.8
58	0.42	25	175	322	937	782	-	23.7	31.5
59	0.44	25	171	293	969	768	-	24.9	30.6

Table 4.6 Evaluation of compressive strength models at 28 days

Model	p (#)	σ (MPa)	R^2
Chidiac et al. (2010)	3	1.9	0.93
Mechling et al. (2009)	4	2.2	0.91
De Larrard (1999)	4	2.2	0.91
Tango (2000)	4	2.2	0.90
Pann et al. (2003)	4	2.3	0.89
Popovics (1998)	4	2.3	0.89
Karni (1974)	2	2.4	0.89
Popovics (2008)	4	2.5	0.89
Powers (1960)	2	2.5	0.88
Popovics (1985)	3	2.5	0.87
Feret (1892)	2	3.3	0.86

Table 4.7 Evaluation of compressive strength models for all ages

Model	p (#)	σ (MPa)	R^2
Chidiac et al. (2010)	3	2.2	0.93
Tango (2000)	4	2.3	0.90
Karni (1974)	2	2.7	0.86
Powers (1960)	2	2.8	0.86
Mechling et al. (2009)	4	2.9	0.86
De Larrard (1999)	4	2.9	0.86
Popovics (1998)	4	4.9	0.68

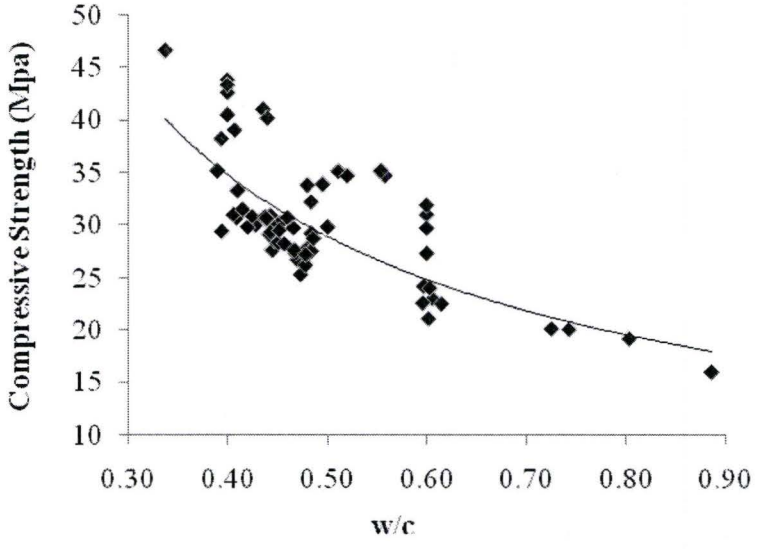

Figure 4.1 Compressive strength vs. w/c – Non air entrained concrete

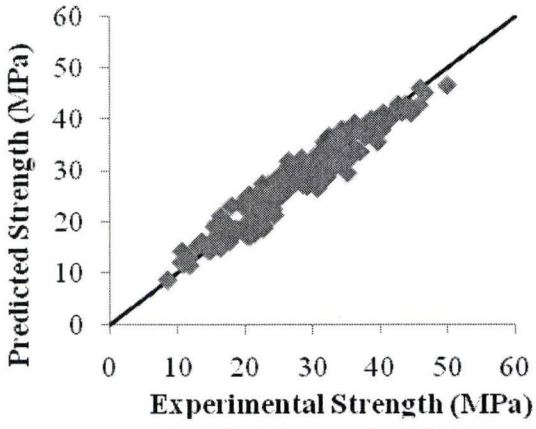

(a) Chidiac et al. (2010)

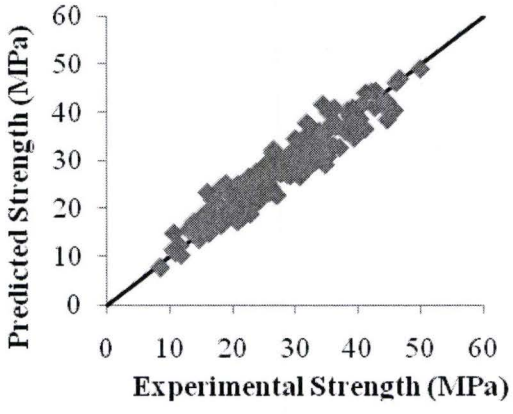

(b) Tango (2000)

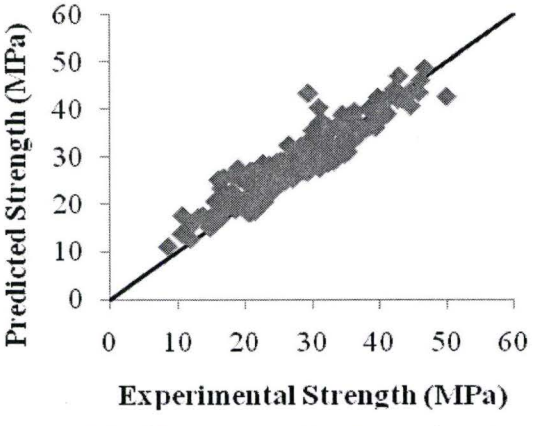

(c) Mechling et al. (2009) and De Larrard (1999)

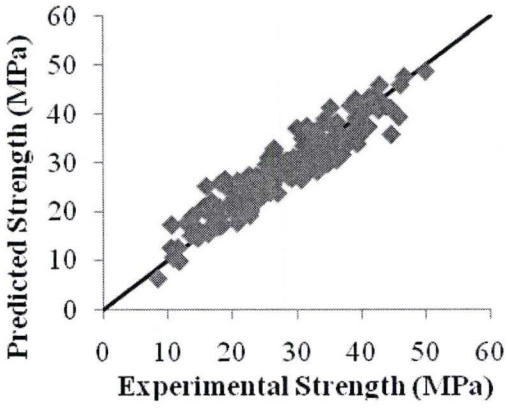

(d) Karni (1974)

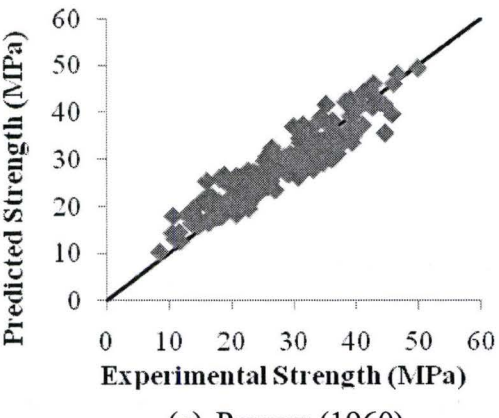

(e) Powers (1960)

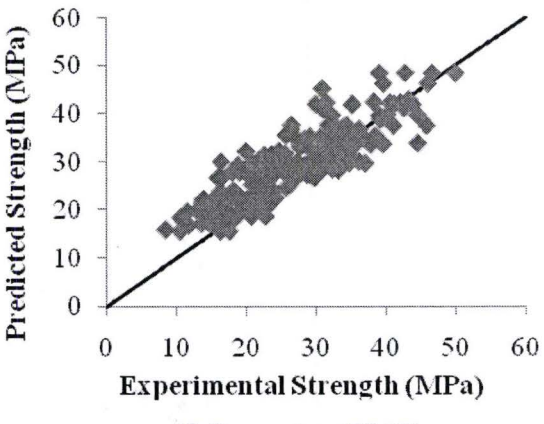

(f) Popovics (1998)

Figure 4.2 Visual comparison of the results obtained in the evaluation of compressive strength models for all ages

Chapter 5: Paper IV Packing density links concrete mixture, rheology, and compressive strength

Abstract

Packing density, which is a function of concrete mixture, influences the rheological properties and the compressive strength of concrete. This study was undertaken to investigate the postulation that packing density provides a link between the concrete mixture, the rheological properties, and the compressive strength. Accordingly, compressive strength model and rheological model that employ packing density as a primary variable were identified. A model analogy that links all three properties has been developed and evaluated using experimental data. The assessment of the postulated link and the successful generation of correlation nomographs have revealed a continuous link that is adequate. On this basis, a methodology was proposed to integrate packing density and rheology into the design of concrete mixture.

Keywords: compressive strength; rheological properties; plastic viscosity; yield stress; packing density; concrete.

5.0 Introduction

Traditionally, concrete mixture design aims to meet workability and compressive strength requirements [1]. Workability is defined as "the property of freshly mixed concrete or mortar which determines the ease and homogeneity, with which it can be mixed, placed, consolidated and finished" [2]. Research has shown that workability of fresh concrete can be quantified using Bingham's rheological properties, namely the yield stress and plastic viscosity [3, 4, 5]. The main variables that affect these properties include the size, shape, and volume fraction of the solid particles, and method of compaction [5]. Experimentally, different apparatuses were developed to estimate the rheological properties. ACI has grouped them into 4 subgroups. These are confined flow tests, free flow tests, vibration

tests, and rotational rheometers. Concrete rheometers provide a measure of shear stress and shear strain rate, which are fitted using the Bingham model to estimate the rheological properties [6, 7]. Given that there are no standard test method for quantifying the concrete rheological properties, the reported measurements are therefore specific to the apparatus. Analytically, fundamental and phenomenological rheology models have been proposed in literature. Chidiac and Mahmoodzadeh reviewed the predictive capabilities of the rheological models and concluded that the fundamental models they developed which are based on excess paste theory and the cell method provide good and consistent predictions [8, 9]. Both the plastic viscosity and yield stress models employ packing density of fresh concrete as a central variable.

The strength of hardened concrete depends on its porosity and the bond strength of the hydrated cement. Concrete's porosity is a function of design variables such as aggregate gradation, mixture proportions, and amount of entrained air, as well as the placement protocols which include mixing, placing and compacting. The bond strength depends on the cement composition, cement degree of hydration, and the aggregate types and shapes [5]. Experimentally, compressive strength is evaluated in accordance with ASTM C39-05 [10]. Moutassem and Chidiac [11] reviewed the predictive capabilities of the compressive strength models proposed in literature and concluded that most models provide good estimate of the measured values and that the one developed by Chidiac et al. provide the highest degree of correlation to experiemental data [12, 13]. Chidiac el al. model accounts for the cement properties, aggregate properties and its gradation, mixture proportions, porosity, and age [13].

Research has shown that the optimum packing density of aggregates and concrete yield optimum rheology and strength by reducing concrete porosity [14, 15, 16, 17]. Studies have revealed the following; rheology is a function of concrete packing density [5, 8, 9], compressive strength is a function of aggregates packing density [5, 13], and aggregates packing density and concrete packing density correlate [5]. Accordingly, packing density is a common variable that relates the mixture composition to these properties. Packing density which is defined as the ratio of the volume of the solid particles to the bulk

volume occupied by these particles [5] is a function of the size, shape, and volume fraction of the solid particles, and method of compaction [15]. Packing density is measured experimentally in accordance with ASTM C29 [18]. Moutassem and Chidiac evaluated the suitability of the packing density models proposed in the literature for concrete applications and concluded that the compressible packing model, CPM, provide the highest predictability [19].

Some researchers have attempted to establish a link between the rheological properties and compressive strength using experimental means [20, 21, 22]. Chidiac et al. worked on correlating the rheological properties to the strength and durability of hardened concrete made with mixture composed of high water to cement ratio. It was observed that concrete compressive strength increases as the yield stress and plastic viscosity increase up to an optimum value [20]. Laskar and Talukdar worked on correlating the rheological properties to the compressive strength of high performance concrete. It was observed that the compressive strength increases with yield stress and that the increase is rapid at low values of yield stress. For the plastic viscosity, it was observed that there exists an optimum value corresponding to maximum compressive strength [21, 22]. These findings strongly suggest that a link exists between rheology and strength. However, they do not provide explanations nor do they identify the common variables that permit linking these properties.

This paper presents an experimental program as well as an analytical methodology to demonstrate whether a link can be established between the concrete mixture, rheological properties and compressive strength with packing density identified as the common variable.

5.1 Experimental program

5.1.1 Materials

The concrete was prepared using a mixture of crushed limestone, siliceous sand, Ordinary Portland Cement (OPC), AEA and water. Hydraulic cement type GU-type 10 used in this

study was obtained from Lafarge North America. The chemical and physical properties are summarized in Table 5.1. Crushed limestone CA with 20 mm and 14 mm nominal maximum aggregate sizes were used. The aggregates were obtained from Lafarge, North America's Dundas quarry located in Dundas, Ontario, Canada. The specific gravities, absorption values, and bulk density for the 20 mm CA are 2.75, 0.92%, and 1636 kg/m^3, and for the 14 mm CA are 2.74, 0.88%, and 1576 kg/m^3, respectively. The sand was obtained from Lafarge North America's West Paris plant. The fineness modulus, specific gravities, absorption values, and bulk density for the sand are 2.72, 2.71, 1.58%, and 1812 kg/m^3, respectively. The bulk density, specific gravity, and absorption for CA and sand were obtained following ASTM C127-04 [23] and ASTM C128-04 [24], respectively. The particle size distribution test was carried out in accordance with CSA A23.2a [25] and was found to conform to the specification requirements. Micro Air, which is manufactured by BASF construction chemicals and which meets the requirements of ASTM C260-06, was used to entrain air [26].

5.1.2 Concrete Mixture Design

The concrete mixture was proportioned following the statistical fractional factorial design method and the ranges recommended by the cement association of Canada (CAC) for designing and proportioning normal concrete mixtures [27]. The range selected for w/c was from 0.4 to 0.7. The water content values ranged from 175 to 228 kg/m^3, covering the full range of slump for non-air entrained and air entrained concrete. The cement content ranged from 250 to 570 kg/m^3. The bulk volume of CA per unit volume of concrete, V_{CA}, ranged from 0.45 to 0.69. The CA maximum sizes were 20 mm and 14 mm. For the air-entrained concrete mixtures, an air entraining agent was used to achieve 5% air content. The concrete materials were mixed using a pan mixer according to the following procedure:

1- Mix water and AEA for 30 s.
2- Place CA, sand, cement, 1/3 of the mixed water and AEA into the pan mixer.

3- Mix the content for 2 min.
4- Add the remaining quantity of water while the mixer is still running.
5- Mix the content for 2 min.
6- Stop the mixer for 1 min.
7- Mix the content for 1 min.
8- Measure the fresh properties of concrete.

The total number of concrete mixtures was 28 and the corresponding proportions are given in Table 5.2. Of the 28 concrete mixtures, 20 were air entrained and 8 were non-air entrained.

5.1.3 Air Content

The air content of the mixtures was measured in accordance with CSA test method A23.3-4C [28]. The test was repeated two times and the average is reported.

5.1.4 Packing Density

The maximum packing density, ϕ^*, for each mixture was computed using the compressible packing model [5], which requires the dry packing densities, volume fractions and the characteristic diameters of the particles as an input. The dry packing density of sand and CA (oven dried) were measured in accordance with ASTM C29-97 [18] with rodding as the method of compaction. The test was carried out using 3 specimens and both the mean value and the standard deviation are reported. The mean packing densities of sand, 14mm max CA size, and 20mm max CA size were measured to be 0.669, 0.575, and 0.595, respectively, and the corresponding standard deviation is 0.016, 0.011, and 0.012. The mean characteristic diameters corresponding to 63.2% passing, as recommended by Goltermann et al [29], were measured for sand, 14 mm max aggregate size, and 20 mm max aggregate size and found to be 1.1 mm, 10.4 mm, and 14.3 mm, respectively. The corresponding standard deviations are 0.05 mm, 1.48 mm and 1.22 mm, respectively. The mean values of the mean diameters, corresponding to 50%

passing, needed for the proposed *APT* model, were determined to be 0.74 mm, 9.1 mm, and 12 mm for sand, 14mm max CA size, and 20mm max CA size, respectively. The corresponding standard deviations are 0.06 mm, 0.48 mm and 1.55 mm, respectively.

5.1.5 Rheological Properties

Bingham material properties, namely the yield stress and plastic viscosity, were estimated using the slump rate machine II (SLRM II) [7]. Once the mixing procedure is completed, the slump was measured in accordance to CSA test method A23.2-5C [30] and the SLRM II is used to measure the concrete slump as a function of time, the slump flow, S_f, the slump, S_l, and the time of slump, t_{slump}. Subsequently, the rheological properties are determined:

$$\tau_o = \frac{4gV\rho}{\sqrt{3}\pi S_f^{\,2}} = 0.0397\left(\frac{\rho}{S_f^{\,2}}\right) \tag{5.1}$$

$$\eta = \frac{\rho g H V}{150\pi S_l S_f^{\,2}} t_{slump} \tag{5.2}$$

where ρ is the concrete density, H the height of the slump cone, V the volume of slump cone, and g the gravitational acceleration.

5.1.6 Compressive Strength

For every mixture, six standard cylinders, 100 mm in diameter and 200 mm high, were cast, consolidated by rodding and finished in accordance with ASTM C192-02 [31]. The cylinders were sealed for 24 h then placed in a moist curing room, where the relative humidity was in excess of 95% and the temperature was 24° C. The concrete compressive strength was evaluated in accordance with ASTM C39-05 [10] at 28 days. Three specimens were tested for each mix.

5.2 Analytical Models

5.2.1 Packing Density

Moutassem and Chidiac reviewed the literature and evaluated the adequacy of many models proposed for predicting the maximum packing density of aggregates [19]. Of the nine packing density models investigated, only the Compressible packing model (CPM), modified Toufar model (MTM), and theory of particle mixtures model (TPM) were found to correctly predict the maximum packing density of aggregate used in concrete [19]. In this study, the maximum packing density of aggregates, ϕ^*_{agg}, and concrete, ϕ^*_{conc}, are predicted using the CPM [5], where:

$$\Pi = \sum_{i=1}^{n} \frac{\frac{\theta_i}{\beta_i}}{\frac{1}{\phi^*} - \frac{1}{\gamma_i}} \tag{5.3}$$

where Π is the partial compaction index that depends on the method of compaction; θ_i the volume fraction of particle i; β_i the residual packing density of particle i at infinite amount of packing energy, which is approximated from $\beta_i = \phi_i^*/\Pi + \phi_i^*$; γ_i the virtual packing density of component i in the mixture. γ_i is defined as the maximum value of ϕ^*, which is attainable by placing the grains one by one, without altering their shape. The virtual packing density is the maximum packing density attainable with the material considered with an infinite amount of packing energy and is expressed as follows [5]:

$$\gamma = \gamma_i = \frac{\beta_i}{1 - \sum_{j=1}^{i-1} \theta_j \left(1 - \beta_i + b_{i,j}\beta_i \left(1 - \frac{1}{\beta_j}\right)\right) - \sum_{j=i+1}^{n} \theta_j \left(1 - a_{i,j}\frac{\beta_i}{\beta_j}\right)} \tag{5.4}$$

$$a_{i.j} = \sqrt{1 - \left(1 - \frac{d_j}{d_i}\right)^{1.02}} \tag{5.5}$$

$$b_{i.j} = 1 - \left(1 - \frac{d_i}{d_j}\right)^{1.5} \tag{5.6}$$

Where d_i, d_j are the diameters of the monosized grains i and j, respectively; $a_{i,j}$ describes the loosening effect exerted by the finer particles i.e. class j on the class i (if $d_i > d_j$); $b_{i,j}$ describes the wall effect exerted by the coarser grains i.e. class j on the class i (if $d_j > d_i$).

In order to account for the different sizes of fine aggregate, coarse aggregate and cement particles, a characteristic diameter concept corresponding to 63.2% passing was introduced [29]. Given the method of compaction and knowing the followings; volume fractions of cement, fine aggregate and coarse aggregate, their characteristic diameters, and their maximum packing densities; the CPM model can be employed to calculate ϕ^*_{agg} and ϕ^*_{conc}.

5.2.2 Rheology

Chidiac and Mahmoodzadeh carried out a review of the models reported in the literature for predicting the plastic viscosity and yield stress of fresh concrete [8, 9]. They revealed that there are different types of models reported in the literature and that there are few models that are capable of predicting the properties. However, closer examination of the results revealed that the model proposed by Chidiac and Mahmoodzadeh, which is a fundamental model, yielded both good and consistent predictions.

Plastic Viscosity

Mahmoodzadeh and Chidiac [32] developed the following model for determining the plastic viscosity of fresh concrete based on the composition of the mixture:

$$\eta_r \cong \eta_i y^3 \frac{4(1-y^7)}{4(1+y^{10})-25y^3(1+y^4)+42y^5} \tag{5.7}$$

where η_i is the dynamic intrinsic viscosity and is a function of the particle shape, and y the ratio of the radius of the cell to the radius of the particle and is given by [33]:

$$y = \left(\frac{\phi}{\phi^*}\right)^{\frac{1}{3}}(1-\psi) \tag{5.8}$$

ϕ and ϕ^* are the packing density of concrete (volume fraction of solids) and the maximum packing density of the concrete mixture, respectively. ψ is a function of the concrete mixture and is defined as follows:

$$\begin{cases} \psi = C_1 \times \dfrac{M_c}{M_w} & \text{Without HRWRA} \\ \psi = C_1 \times \dfrac{M_{HRWRA}}{M_c} \times \dfrac{M_W}{M_c + M_{FineSand+Sand}} & \text{With HRWRA} \end{cases} \tag{5.9}$$

where M_c, M_w, M_{HRWRA}, $M_{FineSand+Sand}$ correspond to the mass of cement, water, high range water reducing admixture, and the total sand, respectively. C_1 is a calibration constant whose value depends on the method of compaction and method of measuring the rheological properties.

Yield Stress

Mahmoodzadeh and Chidiac [32] followed the same analogy to develop a fundamental model for yield stress and is given by:

$$\tau_o \cong \tau_i y^3 \frac{4(1-y^7)}{4(1+y^{10})-25y^3(1+y^4)+42y^5} \tag{5.10}$$

where τ_i is referred to as intrinsic yield stress and is a function of the particle shape. Function `y` is given in Eq. (5.8) with ψ for yield stress model defined as:

$$\psi = C_1 \frac{M_{CA}}{M_{water}} \tag{5.11}$$

where M_{CA} and M_{water} are the mass of coarse aggregate and water in the concrete mix, respectively.

5.2.3 Compressive Strength

Moutassem and Chidiac reviewed the literature and evaluated the adequacy of many models proposed for predicting the compressive strength of concrete [11]. Although most models provide good estimates, the one proposed by Chidiac et al. [13] is adopted

because it provides a high degree of correlation to the experimental data and mathematically accounts for packing density [12]. The model is given by:

$$f'_c(t) = KR_{c28}\left(\frac{APT}{D}\right)^A B^{\frac{W+EA}{C}}(\alpha(t)-\alpha_{cr}) \tag{5.12}$$

where f'_c is the compressive strength of concrete, α the degree of cement hydration at age t, α_{cr} the critical degree of hydration, K the aggregate to paste bond constant, R_{c28} the standard cement strength at 28 days, APT the average paste thickness, D is the mean diameter of all aggregate particles in the mix, $(W+EA)/C$ is the ratio of the volume fractions of water + Entrapped and Entrained air to cement, and A and B are calibration constants. Constant A depends on the shape of the fine and coarse aggregate particles while constant B depends on specimen shape and test conditions. APT which is a function of aggregate gradations, mean sizes, volume fractions, and method of compaction, can be obtained by solving the following equation:

$$\frac{\phi_s}{D_s^3}(APT+D_s)^3+\frac{\phi_{ca}}{D_{ca}^3}(APT+D_{ca})^3 - \left(\frac{\phi-\frac{\phi}{\phi^*}}{D^3}\right)(APT+D)^3-1=0$$

Or, APT can be approximated using the modified equation:

$$APT \approx -\frac{1}{2}\left(D_s+\frac{\phi_{ca}D_s^2}{\phi_s D_{ca}}+\frac{\phi D_s^2(1-\phi^*)}{\phi_s\phi^* D}\right) + \frac{1}{2}\sqrt{\left(D_s+\frac{\phi_{ca}D_s^2}{\phi_s D_{ca}}+\frac{\phi D_s^2(1-\phi^*)}{\phi_s\phi^* D}\right)^2+\frac{4}{3}\frac{(\phi^*-\phi)}{\phi^*}\frac{D_s^2}{\phi_s}} \tag{5.13}$$

where D_s and D_{ca} are the mean diameter of sand particles and mean diameter of coarse aggregate particles, respectively. ϕ, ϕ_s, ϕ_{ca} are the volume fraction of the aggregates, volume fraction of sand particles, and of volume fraction of coarse particles, respectively.

The degree of cement hydration, α, can be obtained using a cement hydration model such as the one proposed by Schindler and Folliard [34] and adopted in this study. The critical degree of hydration, α_{cr}, was predicted according to Rasmussen et al. [35]. The adopted models are as follows:

$$\alpha_{cr} = k \times w/c \tag{5.14}$$

$$\alpha = \alpha_u . \exp\left(-\left[\frac{\tau}{t_e} \right]^{\beta} \right) \tag{5.15}$$

$$\tau = 66.78 . p_{C3A}{}^{-0.154} p_{C3S}{}^{-0.401} . Blaine^{-0.804} . P_{SO3}{}^{-0.758} \cdot \exp(2.187 . p_{SLAG} + 9.5 . p_{FA} \cdot p_{FA-CaO}) \tag{5.16}$$

$$\beta = 181.4 . p_{C3A}{}^{0.146} . p_{C3S}{}^{0.227} . Blaine^{-0.535} . p_{SO3}{}^{0.558} . \exp(-0.647 . p_{SLAG}) \tag{5.17}$$

$$\alpha_u = \frac{1.031 . w/c}{0.194 + w/c} + 0.50 . p_{FA} + 0.30 . p_{SLAG} \leq 1.0 \tag{5.18}$$

$$t_e = \sum_0^t \exp\left(\frac{E}{R} \left(\frac{1}{293} - \frac{1}{T + 273} \right) \right) . \Delta t \tag{5.19}$$

where t_e is the equivalent age (hrs); α_u the ultimate degree of cement hydration; T the concrete temperature (°C); E the activation energy (33,500 J/mol for T > 20° C); R the universal gas constant (8.3144 J/mol/K); τ, β the hydration time parameter and hydration shape parameter, respectively; p_{C3A}, p_{C3S}, p_{SO3}, p_{FA}, p_{SLAG}, $p_{FA\text{-}CaO}$ the weight ratios in terms of total cement content; and k a calibration constant (0.43 for OPC concrete).

5.3 Models Calibration and Prediction

5.3.1 Calibration Procedure

The experimental test results are used to calibrate the parameters η_i, τ_i, and C_1 in the plastic viscosity and yield stress models and the parameters K, A and B in the compressive strength model. Since the yield stress and plastic viscosity models do not account for air content, two models were calibrated, one for the concrete mixture containing entrained air and the second one for the mixtures that do not contain entrained air.

Model calibration was achieved using least squares analysis. The values of the constants were selected such that the minimum possible standard error of the model is obtained. The model standard error (σ), which provides a global assessment of the model prediction, is calculated as follows [36]:

$$\sigma = \sqrt{\frac{\sum_i (Model_i - Experiment_i)^2}{n - p}} \tag{5.20}$$

where $Model_i$ and $Experiment_i$ are the model and experiment values corresponding to mix i, respectively. n is the number of test points and p is the number of model constants. In addition, the correlation coefficient (R^2), which measures the degree of correlation between model and experiment, was also calculated.

5.3.2 Models Prediction

The properties of the concrete mixture listed in Table 5.2 were evaluated. Table 5.3 shows the experimental values and the predicted values for yield stress, plastic viscosity and compressive strength. Errors as a percent difference between experiment and model predicted values are also presented. Table 5.4 presents the calibrated values for these constants for non-air entrained and air entrained concretes in addition to σ and R^2. These results reveal a higher uncertainty with the rheological properties in comparison with the compressive strength but the results are acceptable and provide a reasonable degree of correlation to the experimental data. Figure 5.1 illustrates graphically the goodness of fit of the rheological properties and compressive strength prediction models for air entrained and non-air entrained mixes. Since the compressive strength model accounts for air, the corresponding graph consists of both.

5.4 Correlation between Mixture Design, Rheological Properties, and Compressive Strength

5.4.1 Potential Use of Correlation Nomographs

Equations 5.3, 5.7, 5.10, and 5.12 were used to produce correlation nomographs and investigate the postulation that packing density provides a continuous link between concrete mixture, rheology, and strength. The input properties to develop the nomograph are w/c, water content, air content, V_{CA}, and max CA size. For illustration, nomograph corresponding to the concrete mixtures listed in Table 5.3 are presented in Figures 5.2 to 5.21. Each Figure contains 3 charts. The dashed lines in chart 1 correspond to the yield stress versus ϕ/ϕ^*_{conc}, whereas the solid lines correspond to the water content versus ϕ/ϕ^*_{conc}. Chart 2 is similar to chart 1 except that the rheological property is the plastic viscosity instead of the yield stress. The dashed lines in chart 3 correspond to ϕ/ϕ^*_{conc} vs. ϕ/ϕ^*_{agg}, whereas the solid lines correspond to ϕ/ϕ^*_{agg} versus compressive strength.

Once the mixture design is known then charts 1 and 2 can be used to determine ϕ/ϕ^*_{conc} and then determine the corresponding yield stress and plastic viscosity values. Knowing ϕ/ϕ^*_{conc} from charts 1 or 2, the ϕ/ϕ^*_{agg} can be determined using the dashed lines shown in chart 3. With ϕ/ϕ^*_{agg} determined, the solid lines in chart 3 can be used to determine the corresponding compressive strength of concrete. These nomographs demonstrate a continuous link between concrete mixture, rheology, and compressive strength through packing density.

5.4.2 Correlations Trend

The effect of w/c, water content, V_{CA}, maximum aggregate size and air content on the properties, were investigated to ensure their consistence with what has been reported in literature. The Figures reveal that an increase in w/c due to an increase in water content or a reduction in the cement content result in a decrease in yield stress, plastic viscosity and compressive strength, which is consistent with literature [37]. The volume fraction of solids, ϕ_{conc}, can be determined from $1-V_{air}-V_{water}$. An increase in water content (or a

reduction in cement content) reduces ϕ_{conc} significantly relative to its effect on ϕ^*_{conc}, which depends on the mixture gradation. This results in a reduction in ϕ/ϕ^*_{conc} and hence a reduction in the yield stress and plastic viscosity according to equations (5.7) and (5.10). In addition, an increase in w/c results in a reduction in strength mainly due to an increase in the water filled capillary porosity and in accordance with equation (5.12).

These Figures also reveal that an increase in the water content for fixed w/c results in a reduction in yield stress, plastic viscosity and strength, which is consistent with literature [37]. The reduction in yield stress and plastic viscosity is due to the presence of a larger volume of excess paste beyond what is required to fill the voids between the particles which results in further lubrication. A larger volume of excess paste results in a less compact mix. Consequently, the shorter is the path that a crack needs to follow since it has to move around a fewer number of aggregates. This reduces the energy absorbed and so the compressive strength [38].

An increase in V_{CA} for fixed w/c and water content (i.e. fixed ϕ_{agg}) influences the sand-to aggregate ratio (S/A) which can result in either a decrease or an increase in ϕ^*_{agg} depending on the total aggregates gradation. Research has shown that there is an optimum S/A which equals the maximum binary packing of these elements. This optimum S/A corresponds to minimum porosity and thus maximum workability and strength [14, 37]. Comparing the Figures with 14 mm maximum aggregate size to the figures with 20 mm maximum aggregate size, it is revealed that an increase in the maximum aggregate size results in an increase in workability and a slight reduction in compressive strength, which is consistent with literature [1, 5, 37]. The larger the maximum aggregate size the smaller is the surface area of the particles, the less the water demand, and the higher is the workability [37]. Also, a reduction in the surface area of the aggregate leads to a reduction in bond strength and hence a reduction in the compressive strength [37].

The Figures also reveal, such as comparing Figure 5.1 to Figure 5.12, that an increase in the air content through air entrainment for fixed mix constituents results in a reduction in yield stress, plastic viscosity, and compressive strength which is consistent with literature [2]. In the context of packing density, an increase in the amount of air results in smaller

ϕ_{conc} but has no influence on ϕ^*_{conc}. Therefore, ϕ/ϕ^*_{conc} would decrease and hence lower yield stress and plastic viscosity according to equations (5.7) and (5.10). An increase in air content would increase the porosity and hence a reduction in the compressive strength of concrete [1].

5.5 Methodology for Design of Concrete Mixture

Current design practice is based on meeting workability and strength requirements [1]. The slump test which has been the standard test for workability is not sufficient and the two rheological properties parameters, namely yield stress and plastic viscosity are needed to quantify workability [2, 3, 20]. For the compressive strength, current design targets the cement content and water-to-cement ratio (w/c) [1]. However, research has shown that other factors can be considered for a better prediction [5]. In addition, the current mix design approach is not fundamental but is rather statistical and does not provide a link between the mixture proportions, slump, and compressive strength, which is needed to provide control over the design.

Recognizing that packing density is a statistically significant variable for both strength and slump (rheology), and it is a mixture property, it was postulated and then confirmed that packing density is a central variable providing a continuous link between concrete mixture, rheology, and compressive strength. On this basis, the following methodology is proposed to integrate packing density and rheology in the design of concrete mixture:

Proposed Methodology:

- Design Requirements: f'_c, τ_o, μ.
- From $f'_{c\ required}$ and according to CA guidelines [27] → Estimate w/c
- From $\tau_{o\ required}$ compute slump using model [4, 7] and from CA guideline → Estimate water content
- From w/c and water content → Determine cement content.
- Determine V_{CA}/V_{agg} via optimization of ϕ^*_{agg} using the CPM.

- From $V_{agg}=1-V_w-V_c-V_{air}$ and from known V_{CA}/V_{agg} → Find V_{CA}
- Determine V_s remaining and mixture proportions in Kg/m^3
- From mixture, aggregate mean sizes, and ϕ^*_{agg} → Compute APT
- Predict f'_c using model or using the nomographs and Check f'_c > required f'_c
- Determine $\phi_{concrete}$ from mixture and compute $\phi^*_{concrete}$ using CPM
- Using models or nomographs → Predict τ_o, μ and check if OK
- If $f'_{c\ predicted} < f'_{c\ required}$ → adjust w/c and iterate.
- If predicted τ_o or μ are not as desired → adjust water content and iterate

The following design example demonstrates the applicability and adequacy of the proposed methodology:

Given: $f'_{c\ required} > 35$MPa, $\tau_{o\ required} < 1000$ Pa, $\mu_{\ required} < 30$ Pa-s, 14 mm max agg size, air entrained concrete, materials properties and gradations.

- From CA guideline → w/c = 0.39
- For τ_o=1000 Pa → Slump=200 mm. From CA guide → W=205 Kg/m^3 → C=526 Kg/m^3.
-Using CPM → V_{CA}= 0.58 and ϕ^*_{agg}=0.816 → CA=914 Kg/m^3 and FA=663 Kg/m^3
-Using APT model: APT = 0.208 mm
- Using f'_c model: f'_c = 37.8 MPa > 35 → OK
- Using rheology models: μ =29.8 Pa-s < 30 Pa-s → OK

  τ_o =1201 Pa > 1000 Pa → NO → Increase water content
- Assume W=220 Kg/m^3 → C= 564 Kg/m^3
- From the CPM → V_{CA}= 0.56 and ϕ^*_{agg}=0.816 → CA=883 Kg/m^3 and FA=620 Kg/m^3
- Using APT model: APT = 0.240 mm
- Using f'_c model: f'_c = 36.3 MPa > 35 → OK
- And: μ =20.9 Pa-s < 30 Pa-s → OK

  τ_o =975 Pa< 1000 Pa → OK

5.6 Conclusions

The experimental and an analytical study undertaken to investigate the postulation that packing density provides a link between the concrete mixture, the rheological properties and the compressive strength has revealed the following:

1. The model analogy developed to investigate the desired link was evaluated and has shown to provide good degree of correlation to the experimental data. The correlation factors for yield stress, plastic viscosity, and compressive strength models were 0.74, 0.92, 0.96 for air-entrained concrete and 0.83, 0.95, 0.96 for non air-entrained concrete, respectively.
2. The correlation nomographs demonstrate a continuous link between concrete mixture, rheology, and compressive strength through packing density.
3. The model correlation trends show that an increase in w/c, water content, maximum aggregate size, or air content through entrainment result in a reduction in the yield stress, plastic viscosity, and compressive strength whereas an increase in coarse aggregate volume can result in either in a decrease or increase in the properties, depending on the corresponding maximum packing density of concrete. These trends were found consistent with what has been reported in literature.
4. An analytical methodology which provides a quantitative approach to design concrete mixtures to meet specific strength requirements and rheology was proposed and proven adequate.

Acknowledgments

This study forms a part of ongoing research at McMaster University's Centre for Effective Design of Structures funded through the Ontario Research and Development Challenge Fund. The authors would like to thank Natural Science and Engineering Research Council of Canada and McMaster University for their support and funding.

References

[1] ACI Committee 318, 2005. Building code requirements for structural concrete and commentary, American Concrete Institute, USA.

[2] Tattersall G.H. and Banfill P.F.G., 1983. The rheology of fresh concrete. Marshfield, MA: Pitman Publishing.

[3] Ferraris C.F. and de Larrard F., 1998. "Testing and modelling fresh concrete rheology", NISTIR 6094, Building and Fire Research Laboratory National Institute of Standards and technology, Maryland.

[4] Chidiac S.E., Maadani O., Razaqpur A.G., Mailvaganam N.P., 2000. "Controlling the quality of fresh concrete – a new approach", Magazine of Concrete Research, 52(5), 353-63.

[5] de Larrard F., 1999. Concrete mixture proportioning: a Scientific Approach, Spon Press, London, 320pp.

[6] Ferraris, C.F., 1999. "Measurement of the rheological properties of high performance concrete: state of the art report", Journal of Research of the National Institute of Standards and Technology, 104(5), 461-478.

[7] Chidiac S.E. and Habibbeigi F., 2005. "Modelling the rheological behaviour of fresh concrete: an elasto-viscoplastic finite element approach", Computers and Concrete Journal, 2(2), 97-110.

[8] Chidiac S.E. and Mahmoodzadeh F., 2009. "Plastic viscosity of fresh concrete – A critical review of predictions methods", Cement and Concrete Composites, 31(8), 535–544.

[9] Chidiac S.E. and Mahmoodzadeh F., 2010. "Yield stress of fresh concrete: a critical review of prediction methods", Cement and Concrete Composites, To be submitted for publication.

[10] ASTM C39-05, 2005. "Standard test method for compressive strength of cylindrical specimens", American Society for Testing of Materials, West Conshohochen, PA, USA.

[11] Moutassem F. and Chidiac S.E., 2010. "Assessment of Concrete Compressive Strength Predictions Methods", Cement and Concrete Composites, To be submitted for publication.

[12] Chidiac S.E., Moutassem F., and Mahmoodzadeh F., 2010. "Compressive strength model for concrete - II: calibration and validation", Cement and Concrete Composites, To be submitted for publication.

[13] Chidiac S.E., Moutassem F., and Mahmoodzadeh F., 2010. "A new compressive strength model for concrete – I: theory", Cement and Concrete Composites, To be submitted for publication.

[14] Johansen V. and Andersen P.J., 1996. "Particle packing and concrete properties", Materials Science of Concrete II, American Ceramic Society, Westerville, Ohio, 111-147.

[15] Wong H. and Kwan A., 2005. "Packing density: a key concept for mix design of high performance concrete", Proceedings of Materials Science and Technology in Engineering Conference (MaSTEC), Hong Kong.

[16] Tasi C.T., Li S., Hwang C.L., 2006. "The effect of aggregate gradation on engineering properties of high performance concrete", Journal of ASTM International, 3(3), 1-12.

[17] Shilstone Sr., J.M. and Shilstone Jr., J.M., 1993. "High performance concrete mixtures for durability", Proceedings of the Symposium on High Performance Concrete in Severe Environments, ACI SP-140, P. Zia, ed., American Concrete Institute, Farmington Hills, Michigan, USA, 281-306.

[18] ASTM C29-97, 1997. "Standard test method for bulk density and voids in aggregate", American Society for Testing of Materials, West Conshohochen, PA, USA.

[19] Moutassem F. and Chidiac S.E., 2008. "Evaluation of packing density models for concrete applications", 2nd Canadian Conference on Effective Design of Structures, McMaster University, Hamilton, Ontario, Canada.

[20] Chidiac S.E., Maadani O., Razaqpur A.G., Mailvaganam N.P., 2003. "Correlation of rheological properties to durability and strength of hardened concrete", Journal of Materials in civil engineering ASCE, 15(4), 391-399.

[21] Laskar A.I. and Sudip, T., 2007. "Correlation between compressive strength and rheological parameters of high-performance concrete", Research Letters in Materials Science, 10.1155/2007/45869.

[22] Laskar A.I. and Sudip, T., 2008. "A new mix design method for high performance concrete", Asian Journal of Civil Engineering, 9(1), 15-23.

[23] ASTM C127-04, 2004. "Standard test method for specific gravity and absorption of coarse aggregate", American Society for Testing of Materials, West Conshohochen, PA, USA.

[24] ASTM C128-04, 2004 "Standard test method for specific gravity and absorption of fine aggregate", American Society for Testing of Materials, West Conshohochen, PA, USA.

[25] CSA A23.2-2A, 2000. "Sieve analysis of Fine and Coarse Aggegate", Concrete Materials and Methods of Concrete Construction/Methods of Tests for Concrete, Rexdale, ON., Canada.

[26] ASTM C260-04, 2004. "Air-entraining admixtures for concrete", American Society for Testing of Materials, West Conshohochen, PA, USA.

[27] Kosmatka S.H., Kerkhoff B., Panarese W.C., 2002. Design and control of concrete mixtures, Seventh Canadian Edition, Cement Association of Canada.

[28] CSA A23.2-4C, 2000. "Air content of plastic concrete by the pressure method", Concrete Materials and Methods of Concrete Construction/Methods of Tests for Concrete, Rexdale, ON., Canada.

[29] Goltermann P., Johansen V., Palbol L., 1997. "Packing of aggregates: an alternative tool to determine the optimal aggregate mix", ACI Material journal, 94 (5), 435-443.

[30] CSA A23.2-5C, 2000. "Slump of concrete", Concrete Materials and Methods of Concrete Construction/Methods of Tests for Concrete, Rexdale, ON., Canada.

[31] ASTM C192-02, 2002. "Making and curing concrete specimens in the laboratory", American Society for Testing of Materials, West Conshohochen, PA, USA.

[32] Mahmoodzadeh F. and Chidiac S.E., 2010. "New models for predicting plastic viscosity and yield stress of fresh concrete", Cement and Concrete Composites, To be submitted for publication.

[33] Frankel N.A. and Acrivos A., 1976. "On the viscosity of concentrated suspension of solid spheres", Journal of Chemical Engineering Science, 22(6), 847-53.

[34] Schindler A. K. and Folliard K. J., 2005. "Heat of hydration models for cementitious materials", ACI Materials Journal, 102(1), 24–33.

[35] Rasmussen R.O., Ruiz J.M., Rozycki D.K., McCullough B.F., 2002. "Constructing high-performance concrete pavements with FHWA HIPERPAV systems analysis software", Transportation Research Record 1813, Transportation Research Board, Washington, DC, 11-20.

[36] Montgomery D.C. and Runger G.C., 2003. Applied statistics and probability for engineers, Third edition, NewYork: John Wiley and Sons Inc.

[37] Quiroga P, 2003. The effect of the aggregate characteristics on the performance of portland cement concrete, Ph.D. Dissertation, The University of Texas at Austin.

[38] Kolias S. and Georgiou C., 2005. "The effect of paste volume and of water content on the strength and water absorption of concrete", Cement and Concrete Composites 27(2), 211–216.

Table 5.1 Chemical and physical properties of hydraulic cement GU-type 10

SiO_2 (%)	19.7
Al_2O_3 (%)	4.9
Fe_2O_3 (%)	2.4
CaO (%)	62.2
MgO (%)	3.1
SO_3 (%)	3.4
Na_2O (%)	1.3
Loss of Ignition (%)	2.9
Equivalent Alkalies (%)	0.75
Specific Surface Area (Blaine) (cm^2/g)	4280
% Passing 325 (45um) Mesh (%)	90.7
Time of Setting-Initial (min)	115
Compressive Strength – 28 Day (MPa)	41.9

Table 5.2 Concrete mix design composition

Mix #	w/c	Size	Water (kg/m^3)	Cement (kg/m^3)	Coarse aggregate (bulk volume)	Coarse aggregate (kg/m^3)	Sand (kg/m^3)	%Air
1	0.40	14	193	483	0.50	794	851	5.9
2	0.60	14	193	322	0.62	971	815	5.3
3	0.40	14	205	513	0.62	971	618	4.8
4	0.60	14	205	342	0.50	794	939	5.1
5	0.40	20	184	460	0.69	1134	563	4.6
6	0.60	20	184	307	0.57	928	898	5.6
7	0.40	20	197	493	0.57	928	703	4.8
8	0.60	20	197	328	0.69	1134	641	3.1
9	0.50	14	193	386	0.504	794	934	5.7
10	0.70	14	175	250	0.504	794	1100	8.8
11	0.50	14	205	410	0.504	794	881	5.1
12	0.70	14	193	276	0.504	794	1029	7.5
13	0.50	14	193	386	0.616	971	759	5.1
14	0.70	14	175	250	0.616	971	925	8.7
15	0.50	14	205	410	0.616	971	706	4.8
16	0.70	14	193	276	0.616	971	854	5.6
17	0.50	14	199	398	0.560	883	820	5.0
18	0.50	14	199	398	0.448	706	994	7.8
19	0.50	14	199	398	0.672	1059	645	6.7
20	0.50	14	199	398	0.560	883	820	5.8
21	0.40	14	216	540	0.50	794	807	2.1
22	0.60	14	216	360	0.62	971	787	1.0
23	0.40	14	228	570	0.62	971	574	1.8
24	0.60	14	228	380	0.50	794	912	1.2
25	0.40	20	205	513	0.69	1134	542	1.6
26	0.60	20	205	342	0.57	928	892	1.5
27	0.40	20	216	540	0.57	928	692	1.4
28	0.60	20	216	360	0.69	1134	643	1.5

Table 5.3 Experimental and predicted rheological properties and compressive strength results

Mix #	$(\phi/\phi^*)_{agg}$	$(\phi/\phi^*)_{conc}$	τ_{oexp} (Pa)	τ_{omodel} (Pa)	Error (%)	μ_{exp} (Pa.s)	μ_{model} (Pa.s)	Error (%)	$f'c_{exp}$	$f'c_{model}$	Error (%)
1	0.741	0.880	1763	1398	21	49	34	30	37.8±2.3	36.5	3
2	0.803	0.863	1046	918	12	12	9	25	23.1±1.2	24.3	5
3	0.716	0.883	1530	1525	0	31	40	31	36.4±1.0	38.1	5
4	0.790	0.855	645	761	18	6	7	17	27.2±1.1	24.9	9
5	0.752	0.895	2228	2200	1	80	84	5	35.7±1.8	37.9	6
6	0.810	0.865	887	962	8	11	10	13	23.9±2.0	23.7	1
7	0.721	0.885	2105	1610	23	56	45	20	38.4±1.4	38.0	1
8	0.796	0.873	600	1182	97	9	13	42	23.8±2.3	27.3	15
9	0.783	0.867	738	1011	37	8	13	63	30.4±0.8	30.0	1
10	0.839	0.864	1391	946	32	-	-	-	14.9±0.8	14.7	2
11	0.762	0.862	565	902	60	5	11	121	32.9±1.0	31.1	5
12	0.815	0.850	720	680	6	8	5	34	18.4±0.7	16.7	9
13	0.778	0.871	876	1103	26	9	15	66	30.7±2.6	30.6	0
14	0.827	0.856	841	779	7	9	6	30	13.6±0.6	14.8	9
15	0.756	0.865	864	950	10	10	12	19	32.5±0.2	31.4	3
16	0.818	0.861	604	863	43	8	7	11	18.6±2.0	18.7	0
17	0.770	0.867	922	1005	9	9	13	44	31.9±0.6	31.0	3
18	0.761	0.844	759	592	22	7	6	13	26.3±1.0	27.7	5
19	0.755	0.853	742	718	3	9	8	12	25.5±1.3	28.9	13
20	0.763	0.859	794	840	6	-	-	-	33.1±2.2	30.0	9
21	0.729	0.904	1208	1210	0	20	25	29	42.6±1.5	41.7	2
22	0.803	0.884	607	649	7	-	-	-	31.0±0.3	30.3	2
23	0.702	0.902	1464	1138	22	26	22	14	43.8±3.5	42.1	4
24	0.788	0.873	728	463	36	6	5	16	29.7±0.3	30.2	2
25	0.744	0.915	2131	2027	5	48	47	2	40.5±2.4	42.4	5
26	0.816	0.888	679	732	8	7	8	22	31.9±2.3	29.8	7
27	0.719	0.910	1134	1560	38	-	-	-	43.3±1.4	42.9	1
28	0.786	0.877	597	546	8	9	5	40	27.3±0.7	29.8	9

Table 5.4 Calibration of models and goodness of fit

	Plastic Viscosity (Pa-s)				Yield Stress (Pa)				Strength (MPa)	
Air consideration	**C_1**	**η_i**	**σ**	**R^2**	**C_1**	**η_i**	**σ**	**R^2**	**σ**	**R^2**
Air entrained	-0.0079	2.75	6.1	0.92	8.8×10^{-7}	0.73	269	0.74	1.8	0.96
Non-air entrained	-0.0048	1.67	3.9	0.95	-5.3×10^{-4}	0.25	250	0.83		

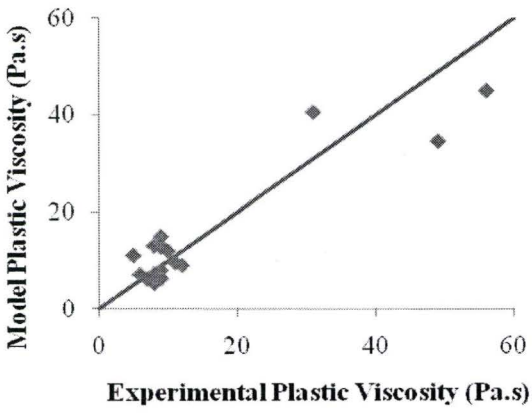

(a) Plastic Viscosity, air entrained

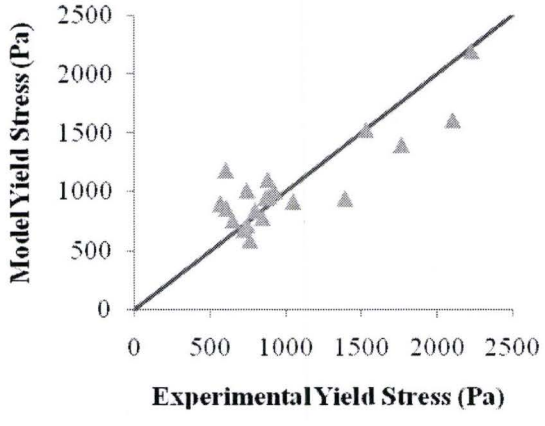

(b) Yield Stress, air entrained

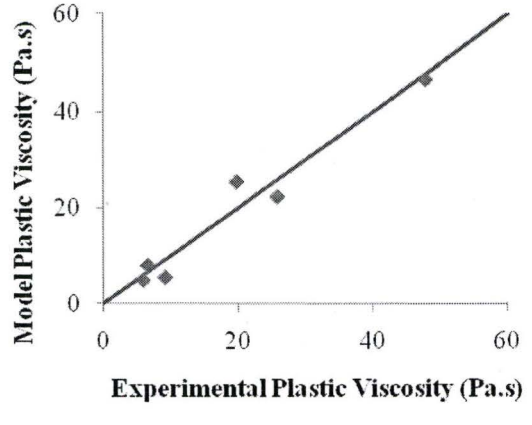

(c) Plastic Viscosity, non-air entrained

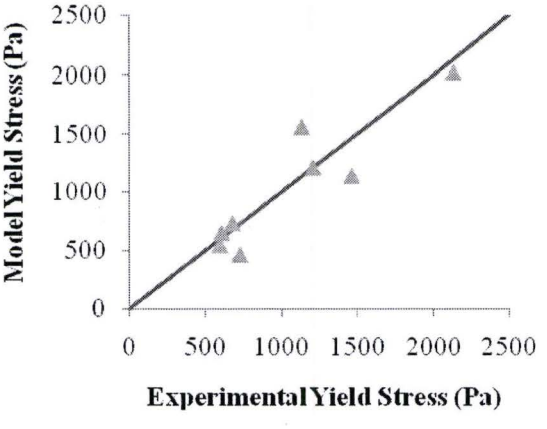

(d) Yield Stress, non-air entrained

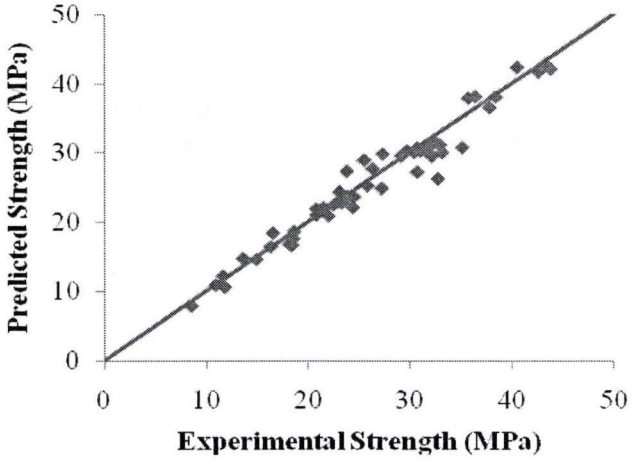

(e) Compressive Strength

Figure 5.1 Prediction capability of the yield stress, plastic viscosity, and strength models

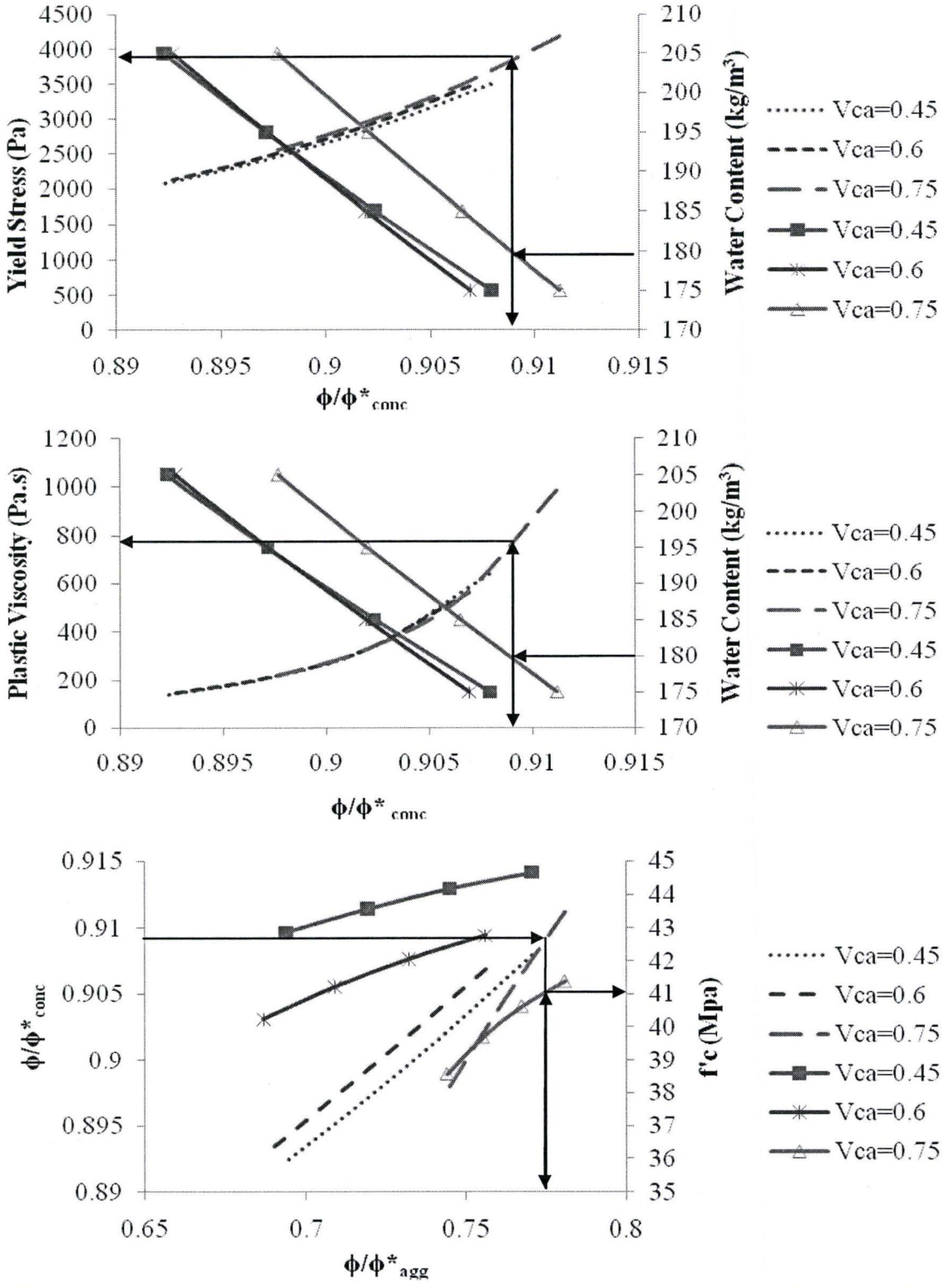

Figure 5.2. Linking the rheological properties to strength Nomograph - w/c = 0.35, 14 mm, air entrained (5% air)

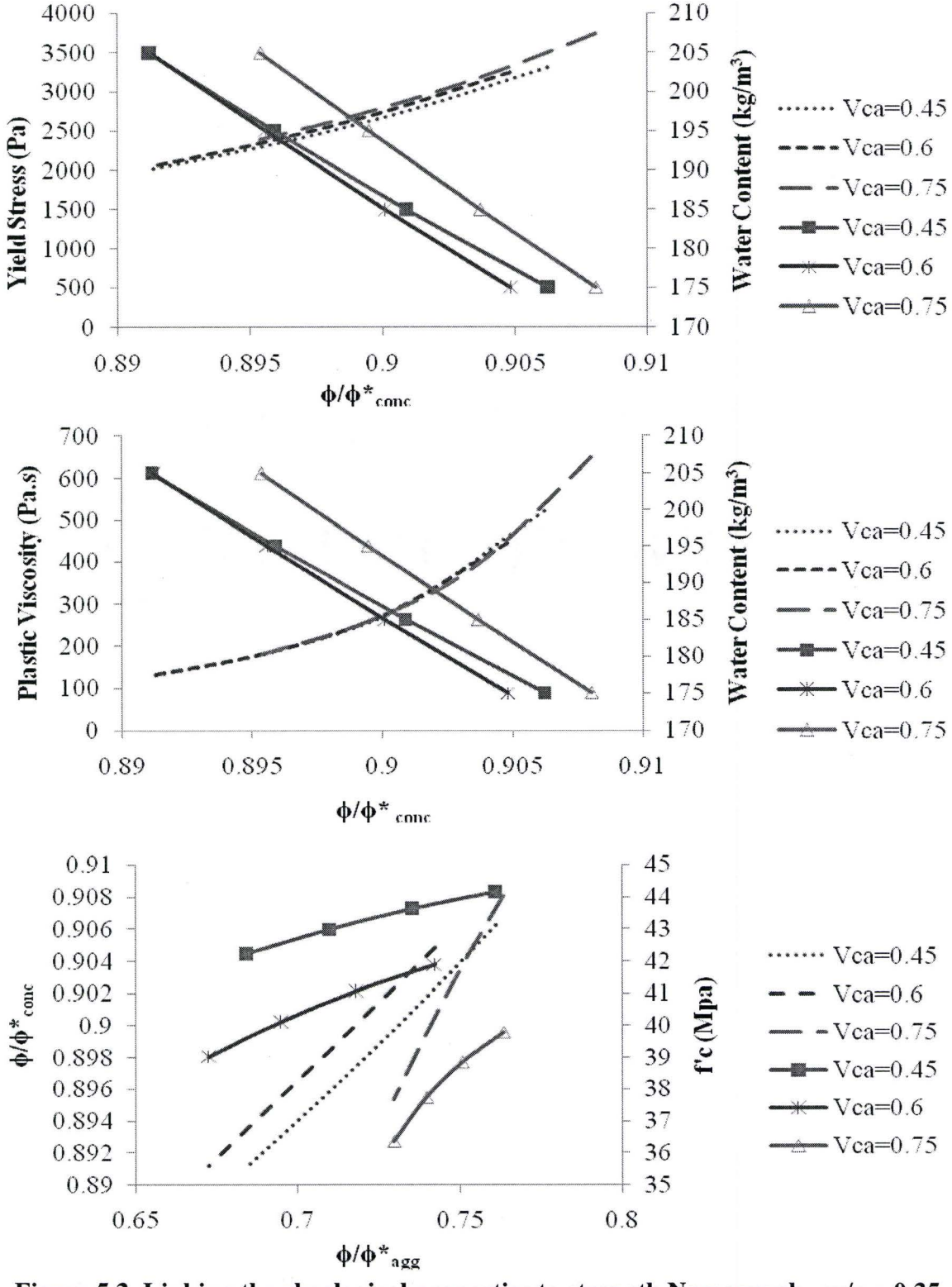

Figure 5.3. Linking the rheological properties to strength Nomograph - w/c = 0.35, 20 mm, air entrained (5% air)

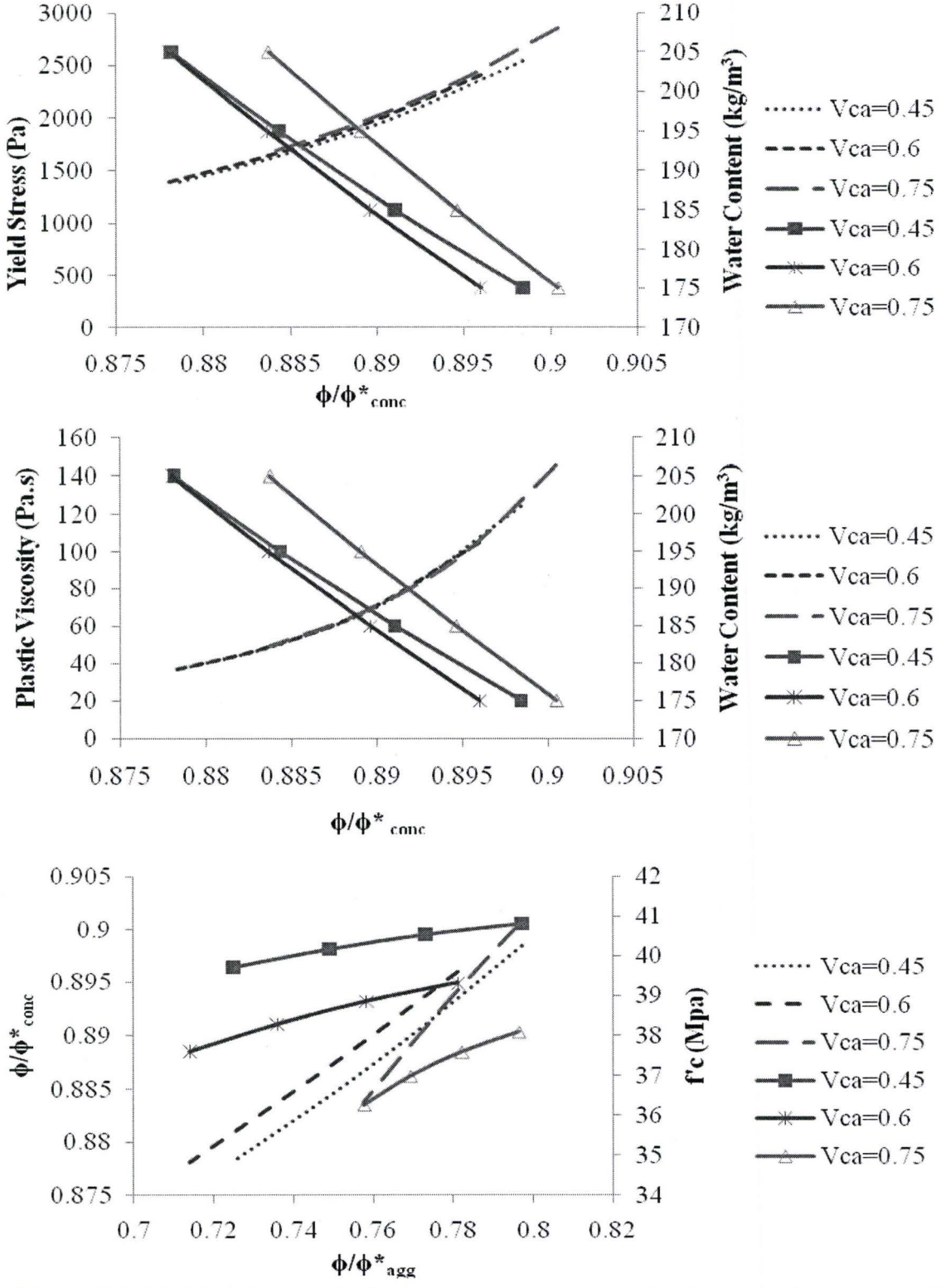

Figure 5.4. Linking the rheological properties to strength Nomograph - w/c = 0.40, 14 mm, air entrained (5% air)

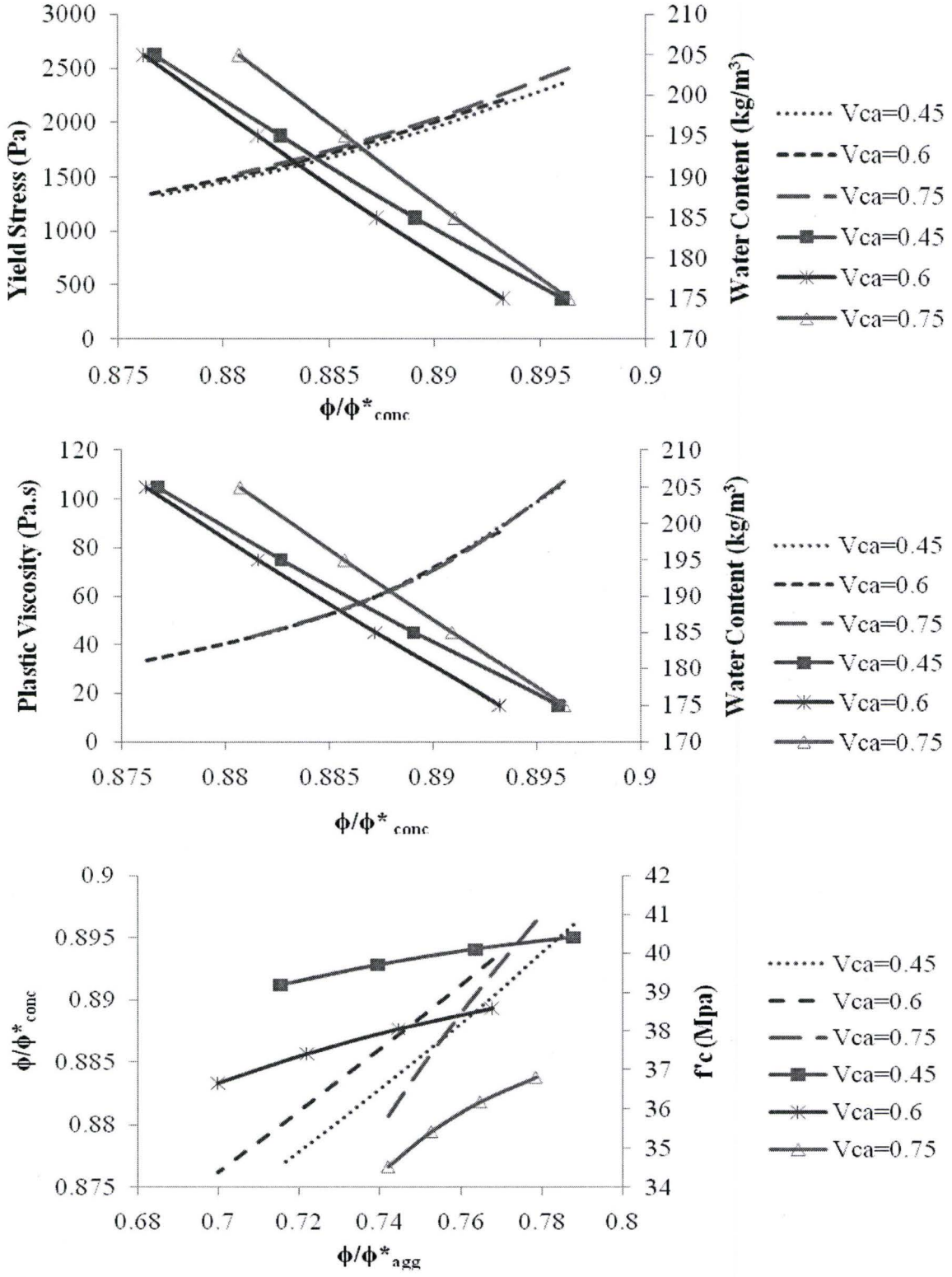

Figure 5.5. Linking the rheological properties to strength Nomograph - w/c = 0.40, 20 mm, air entrained (5% air)

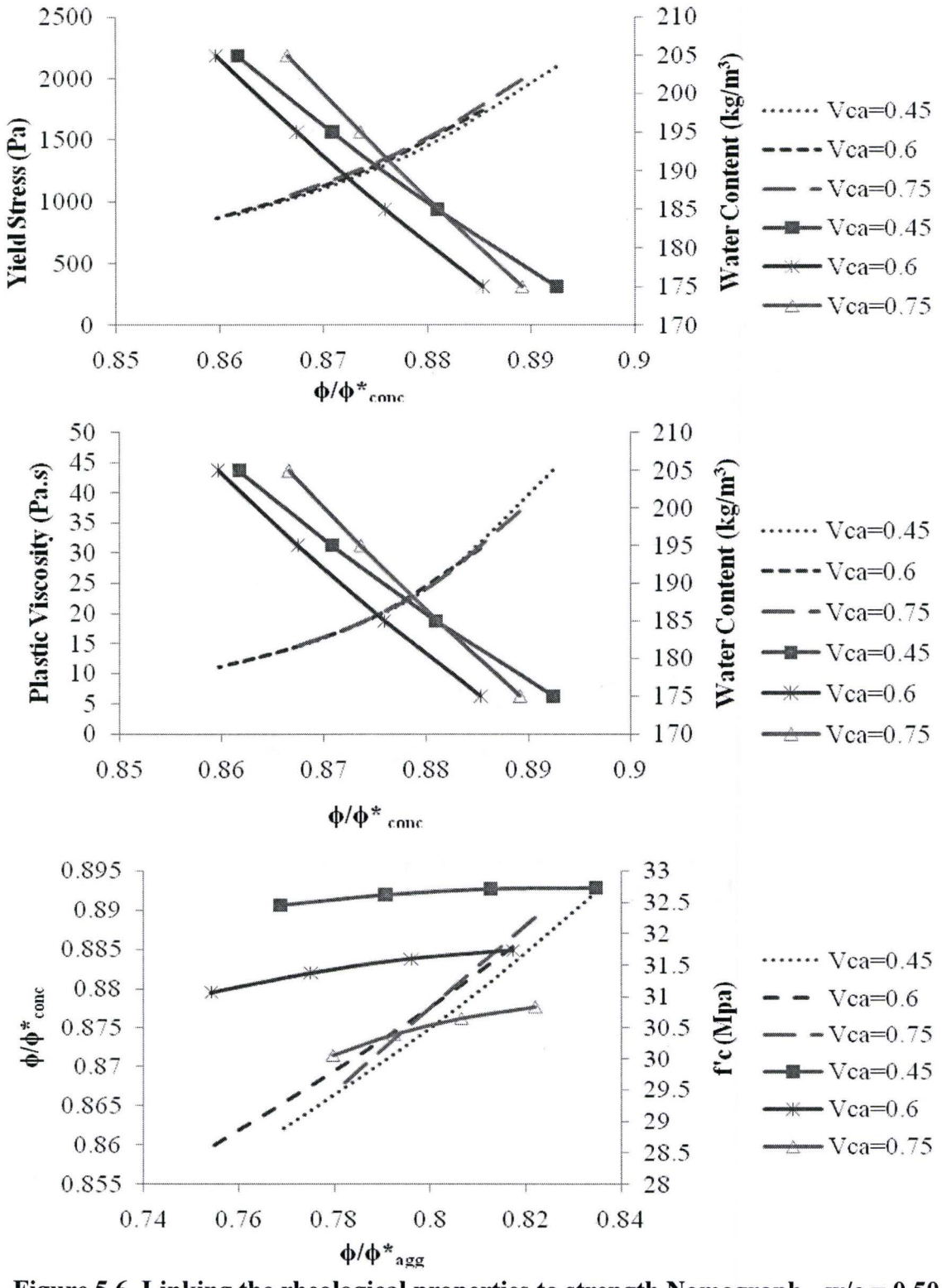

Figure 5.6. Linking the rheological properties to strength Nomograph - w/c = 0.50, 14 mm, air entrained (5% air)

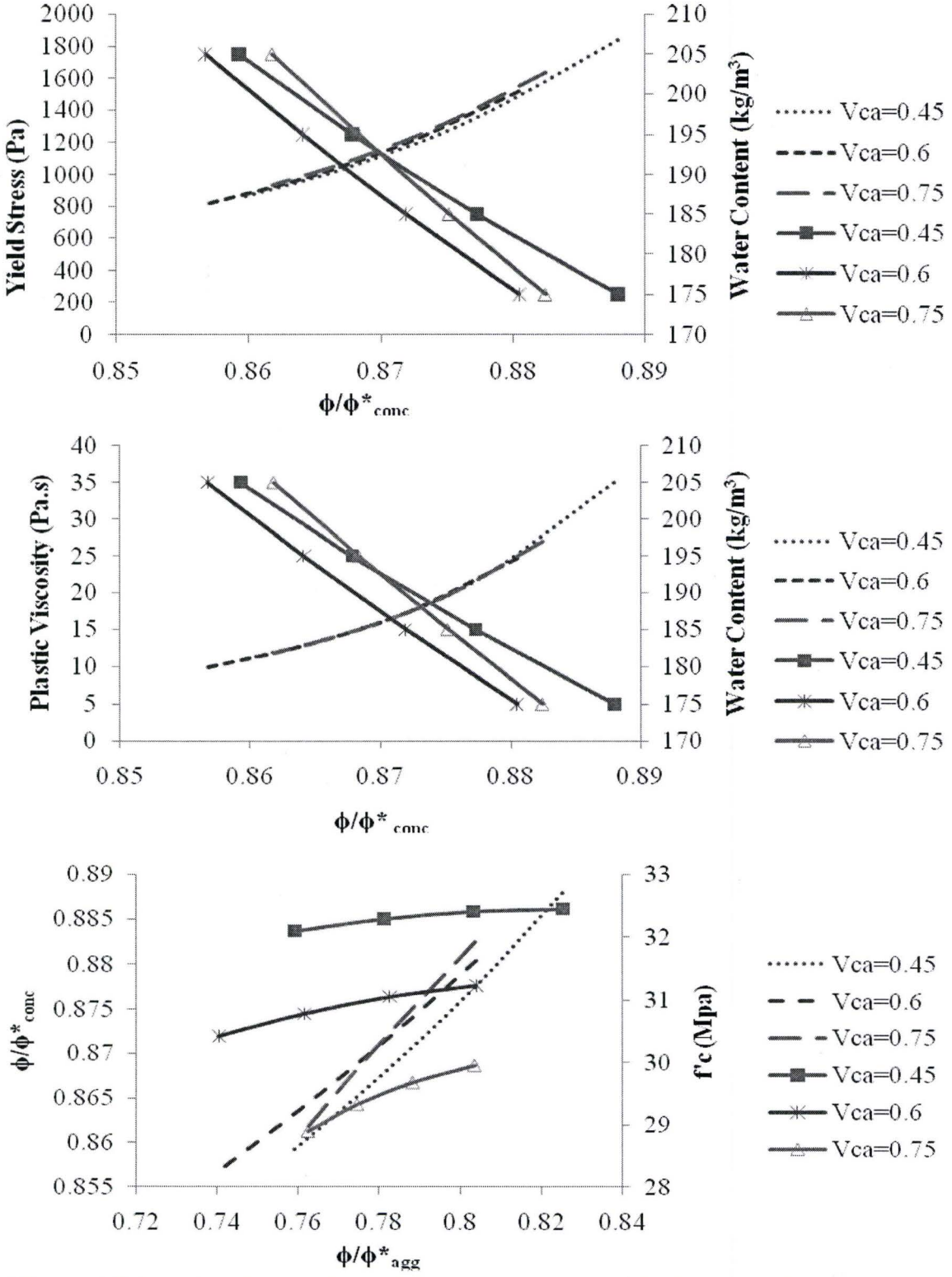

Figure 5.7. Linking the rheological properties to strength Nomograph - w/c = 0.50, 20 mm, air entrained (5% air)

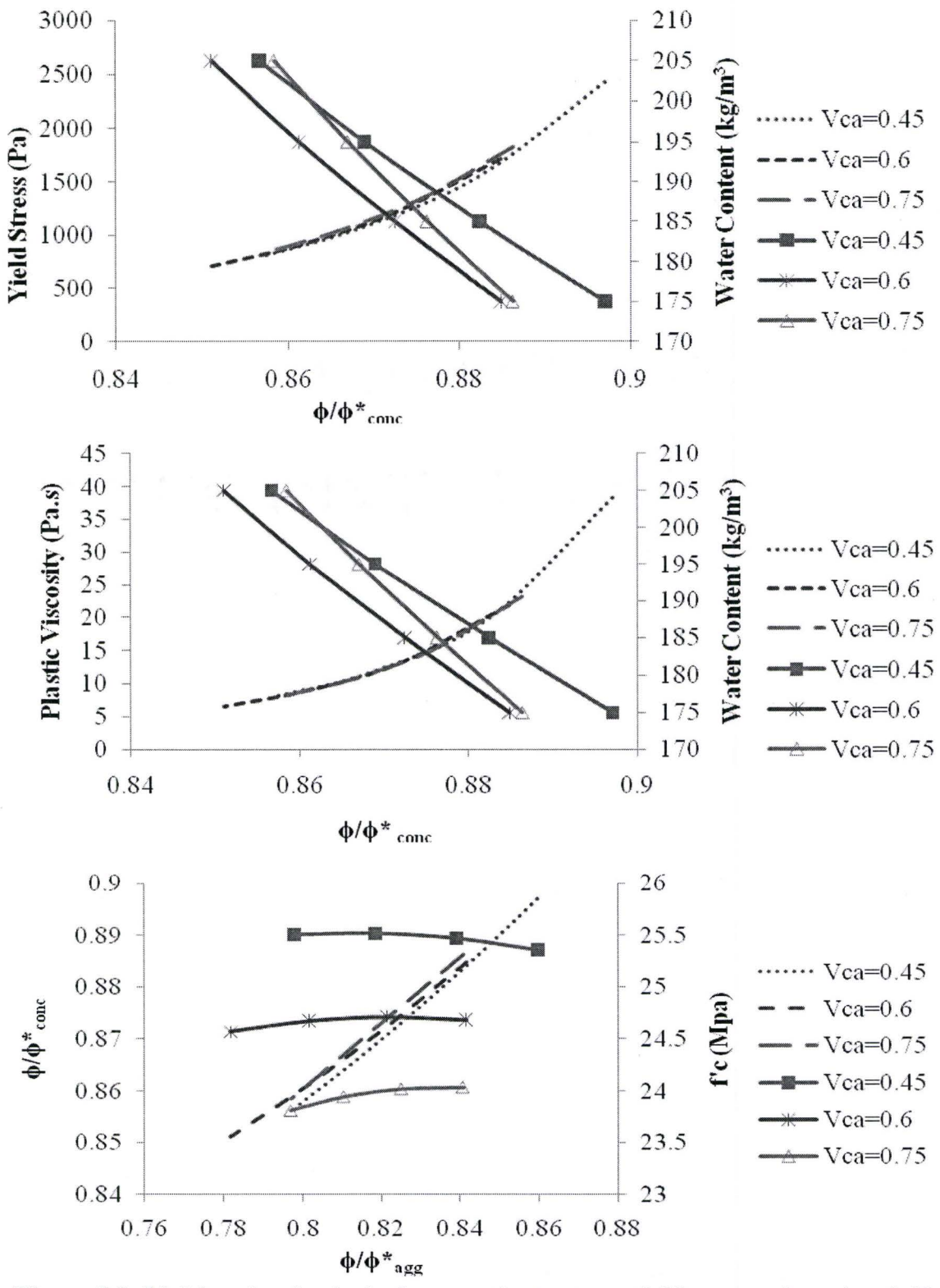

Figure 5.8. Linking the rheological properties to strength Nomograph - w/c = 0.60, 14 mm, air entrained (5% air)

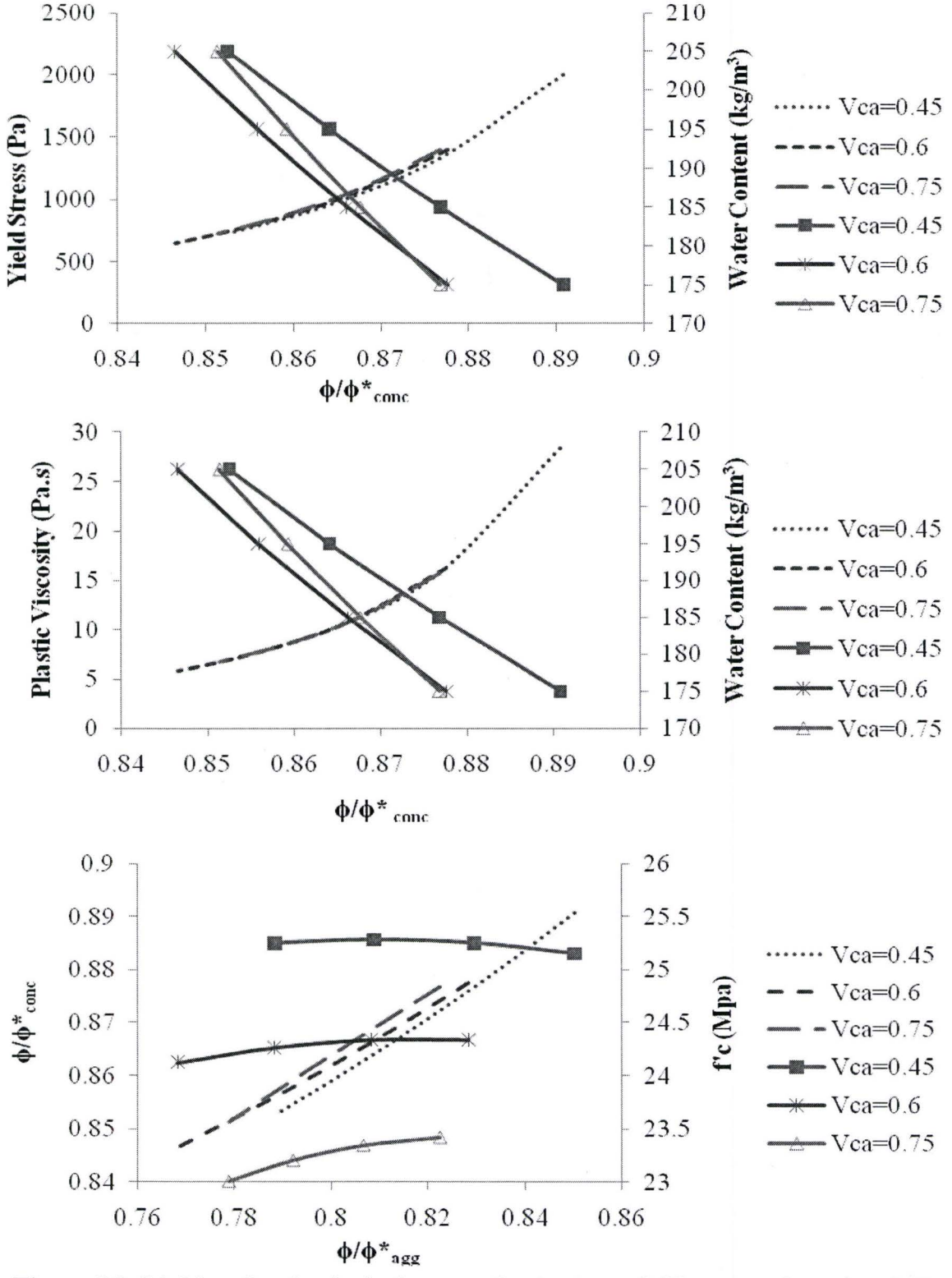

Figure 5.9. Linking the rheological properties to strength Nomograph - w/c = 0.60, 20 mm, air entrained (5% air)

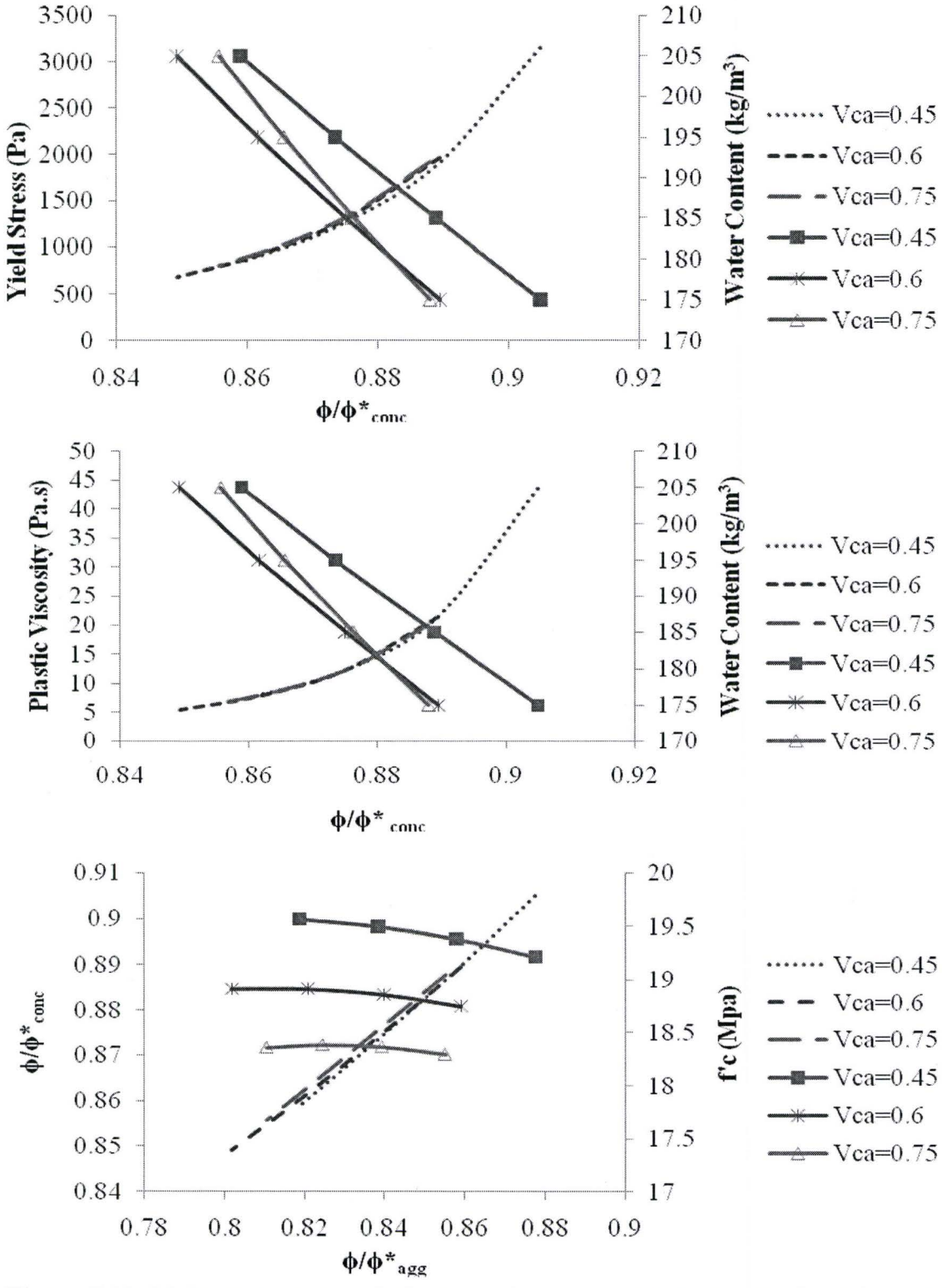

Figure 5.10. Linking the rheological properties to strength Nomograph - w/c = 0.70, 14 mm, air entrained (5% air)

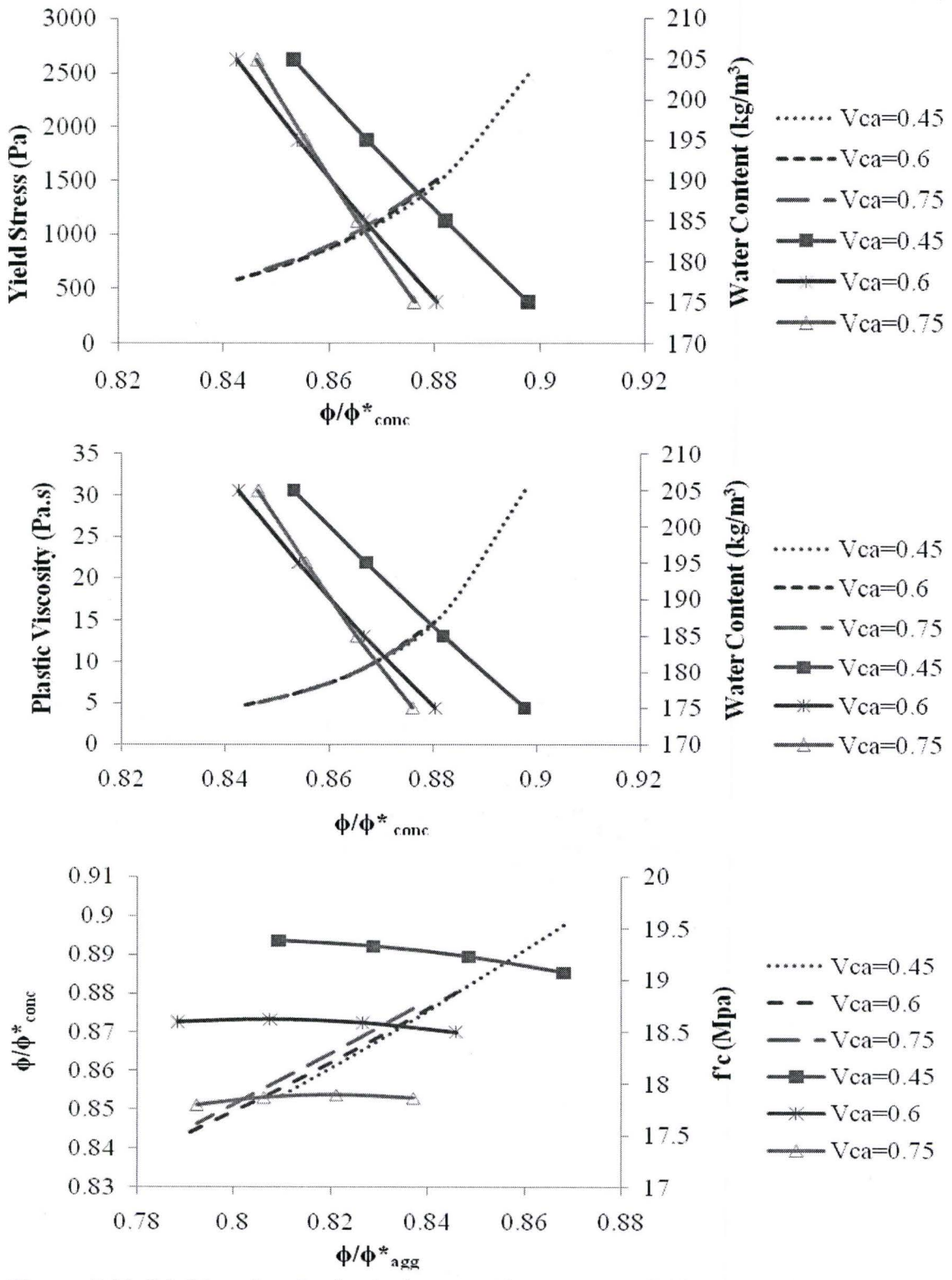

Figure 5.11. Linking the rheological properties to strength Nomograph - w/c = 0.70, 20mm, air entrained (5% air)

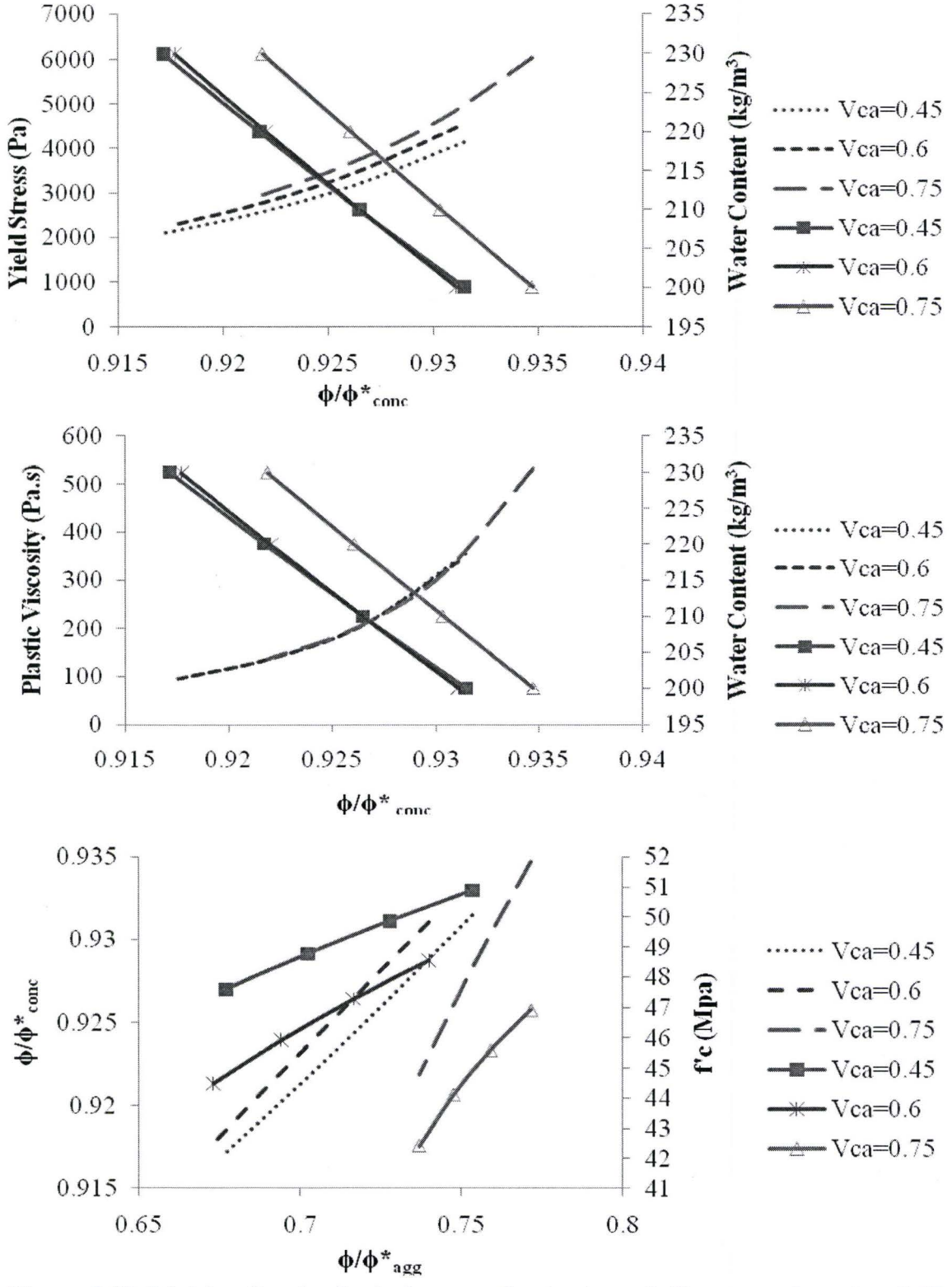

Figure 5.12. Linking the rheological properties to strength Nomograph - w/c = 0.35, 14 mm, non-air entrained (1.5% air)

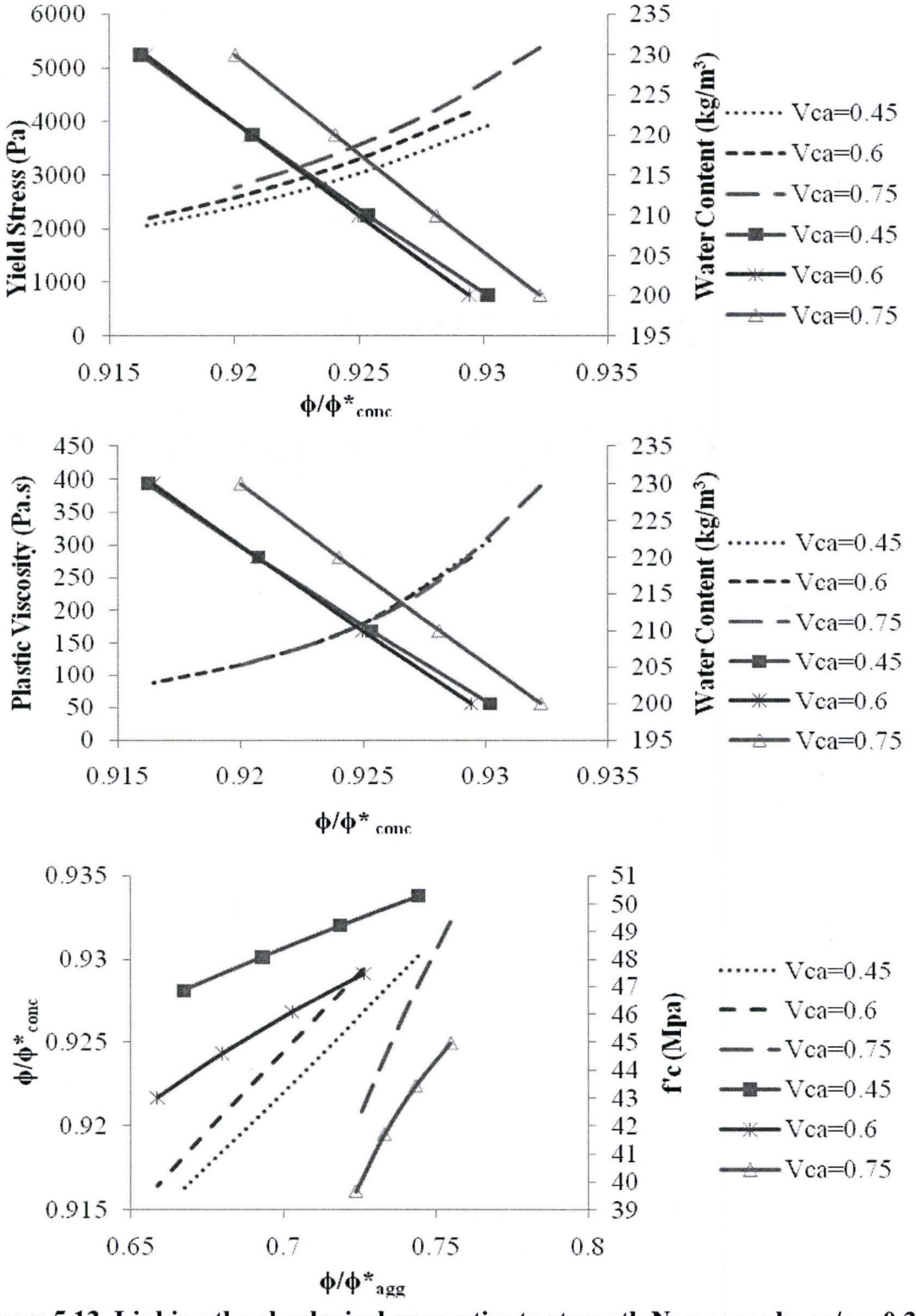

Figure 5.13. Linking the rheological properties to strength Nomograph - w/c = 0.35, 20 mm, non-air entrained (1.5% air)

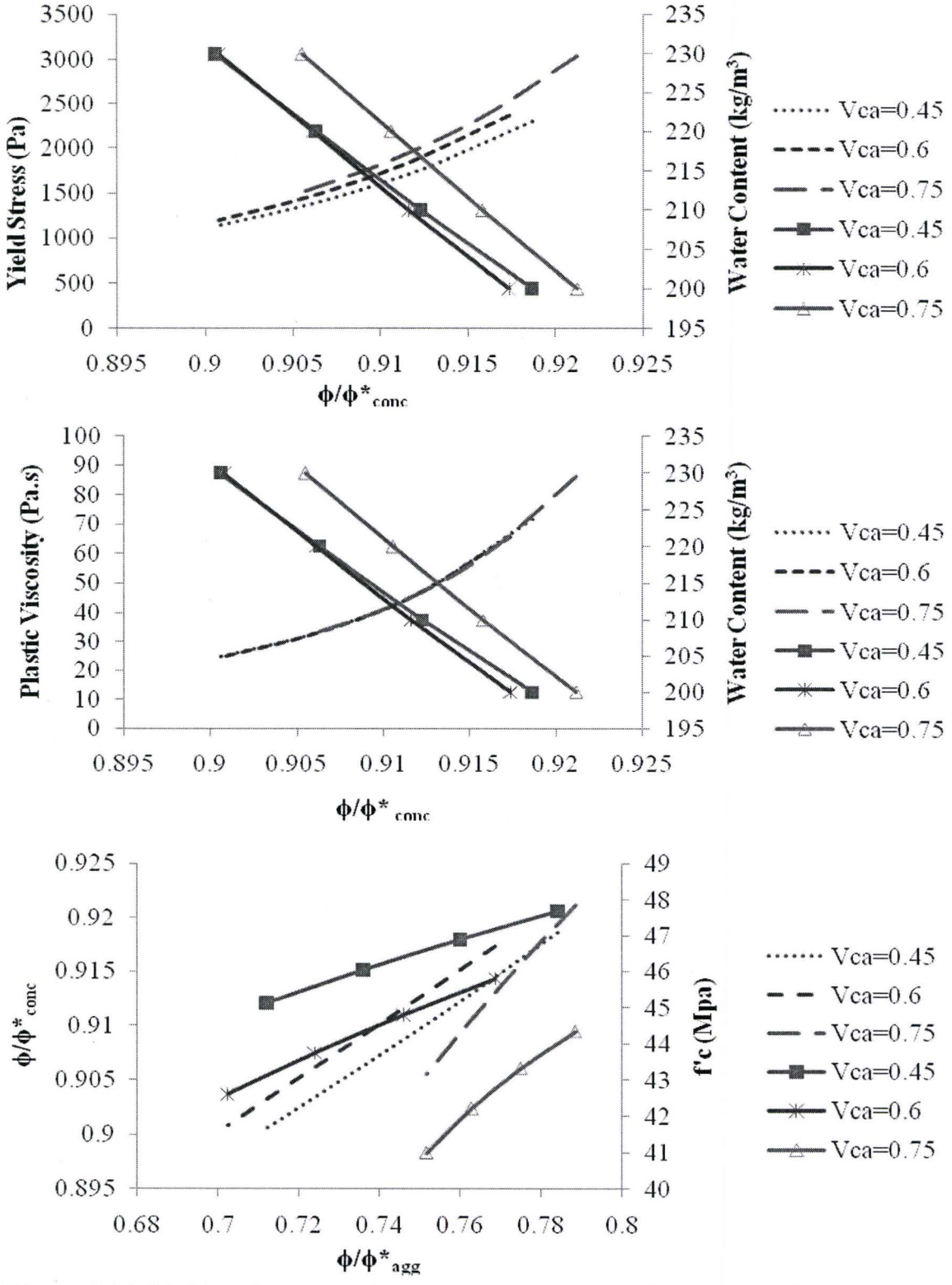

Figure 5.14. Linking the rheological properties to strength Nomograph - w/c = 0.40, 14 mm, non-air entrained (1.5% air)

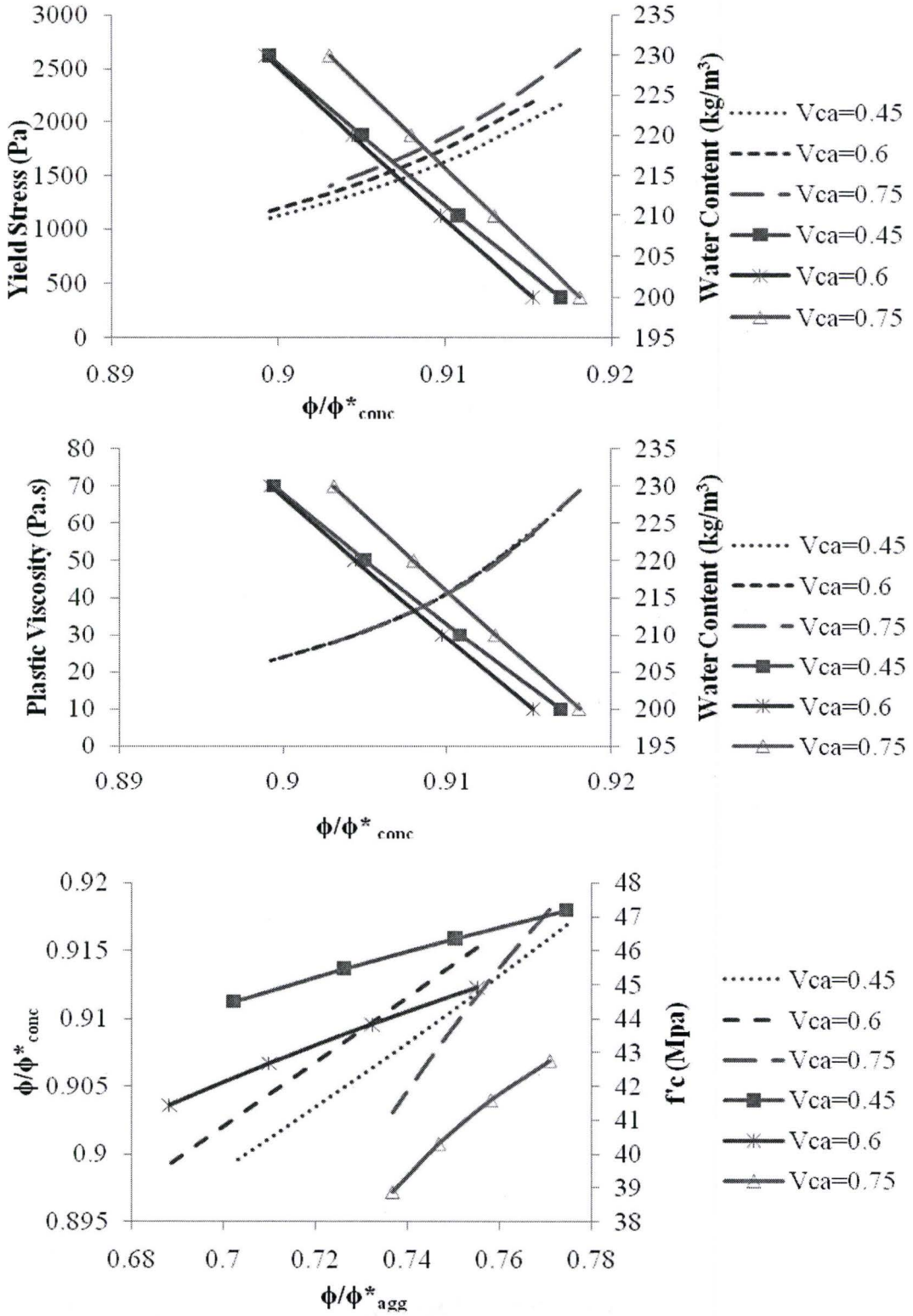

Figure 5.15. Linking the rheological properties to strength Nomograph - w/c = 0.40, 20 mm, non-air entrained (1.5% air)

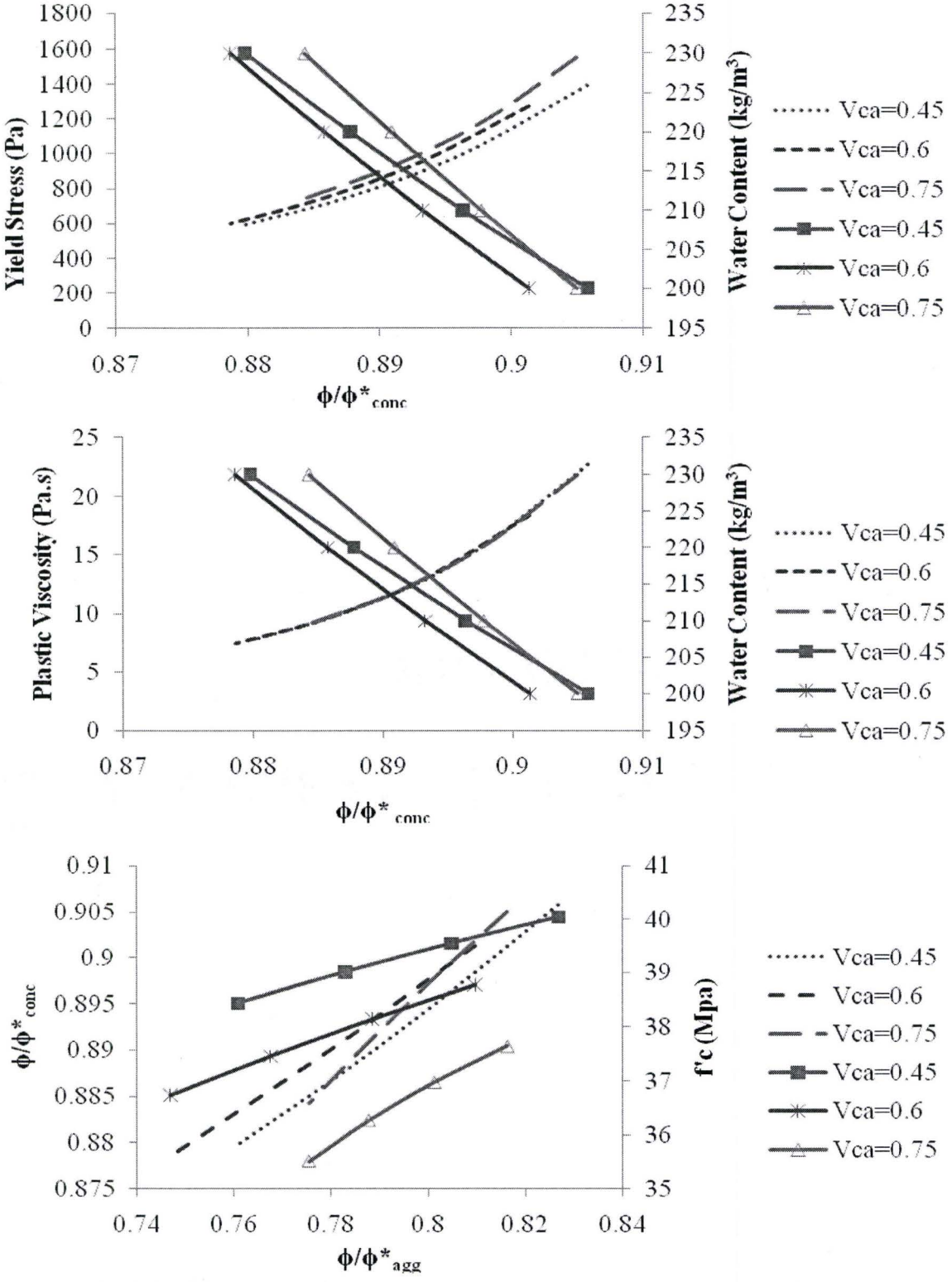

Figure 5.16. Linking the rheological properties to strength Nomograph - w/c = 0.50, 14 mm, non-air entrained (1.5% air)

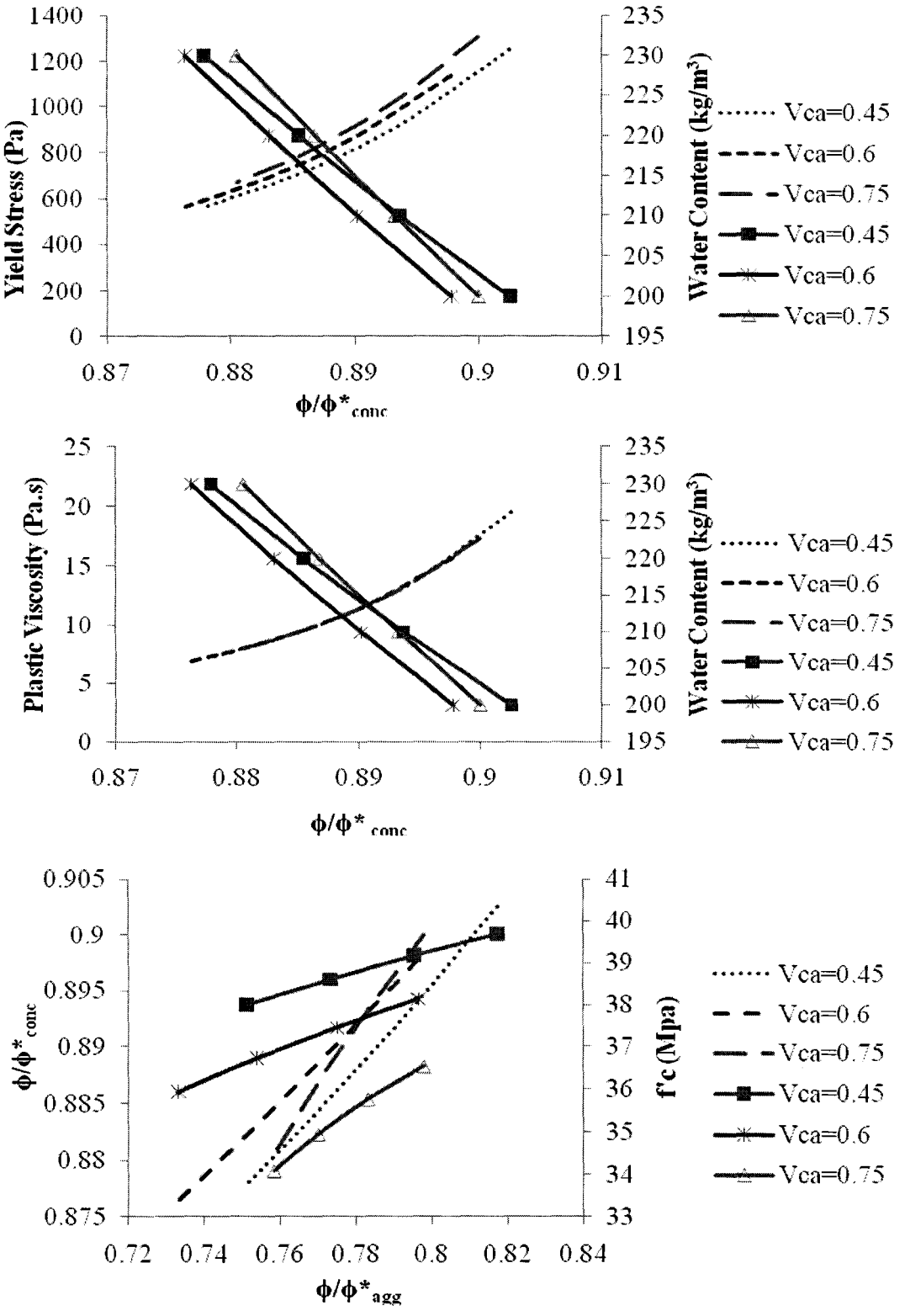

Figure 5.17. Linking the rheological properties to strength Nomograph - w/c = 0.50, 20 mm, non-air entrained (1.5% air)

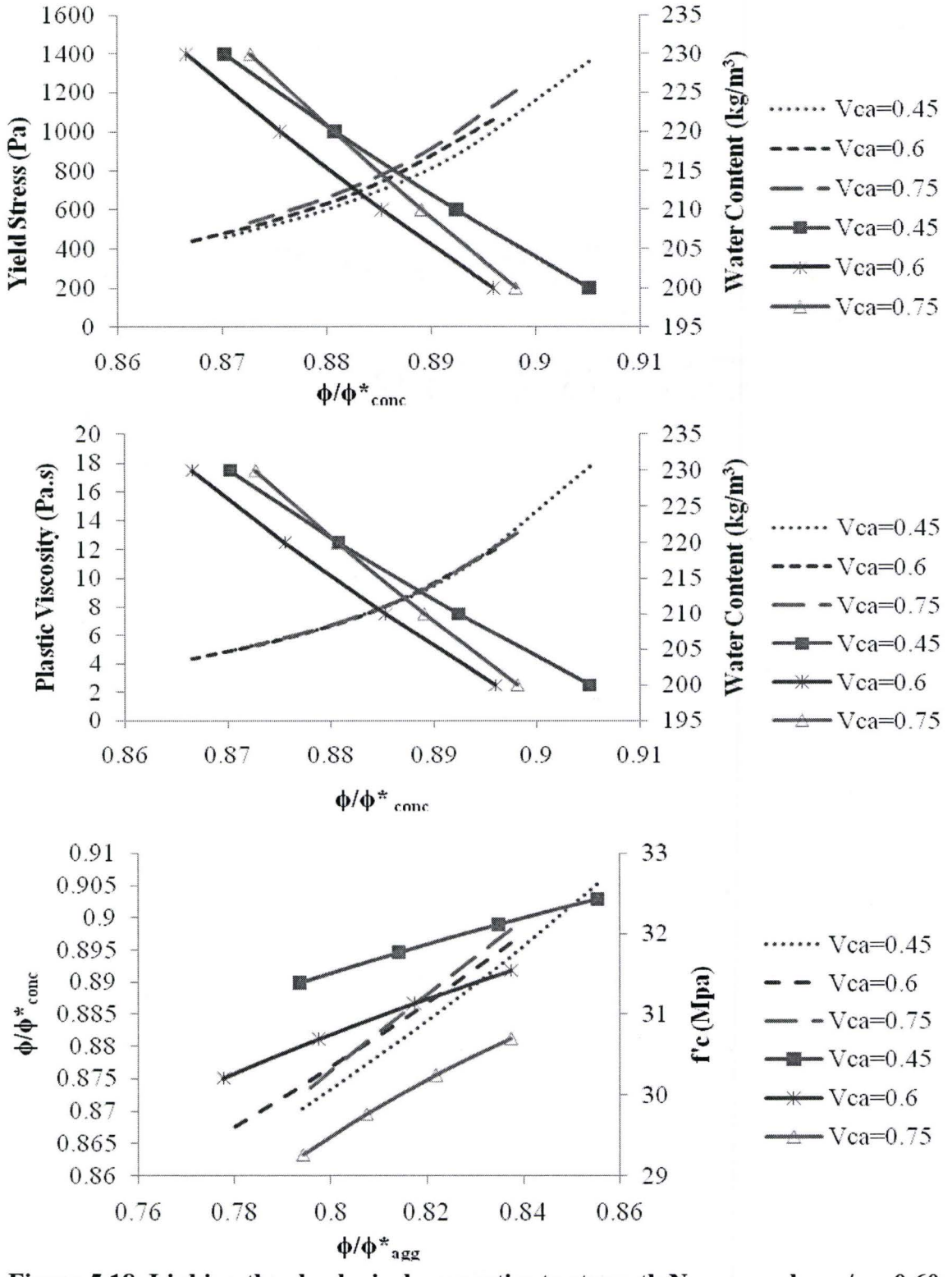

Figure 5.18. Linking the rheological properties to strength Nomograph - w/c = 0.60, 14 mm, non-air entrained (1.5% air)

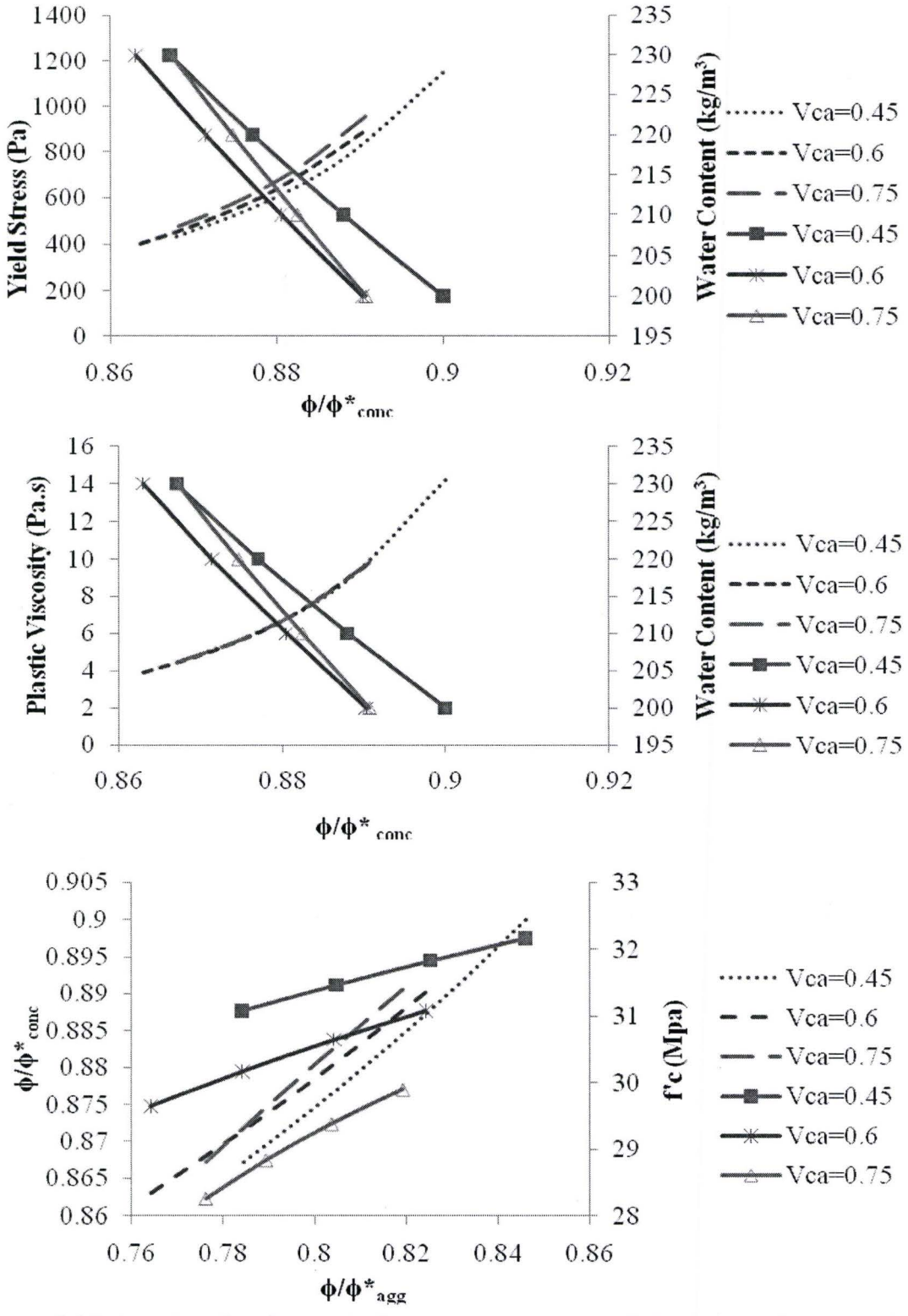

Figure 5.19. Linking the rheological properties to strength Nomograph - w/c = 0.60, 20 mm, non-air entrained (1.5% air)

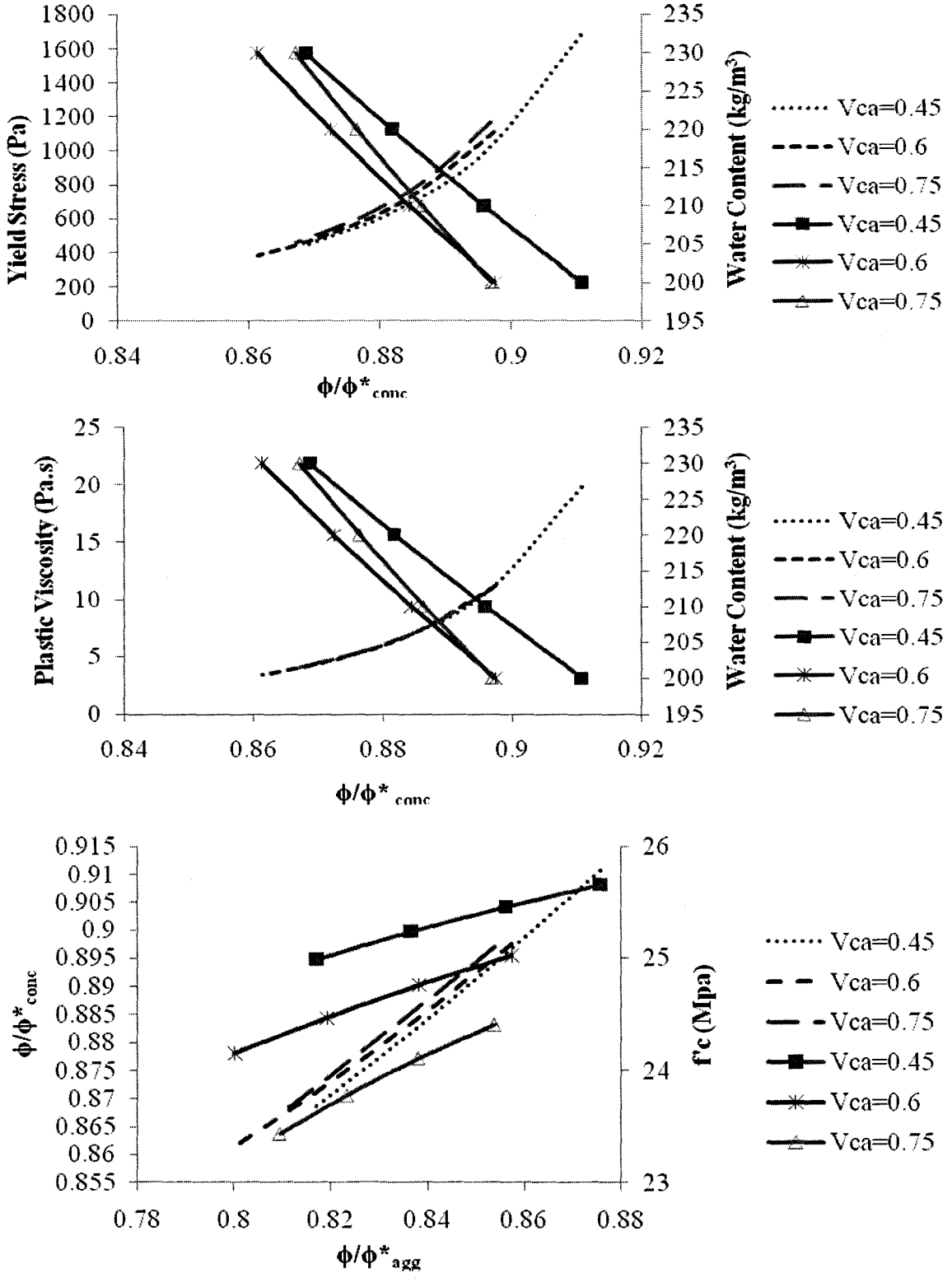

Figure 5.20. Linking the rheological properties to strength Nomograph - w/c = 0.70, 14 mm, non-air entrained (1.5% air)

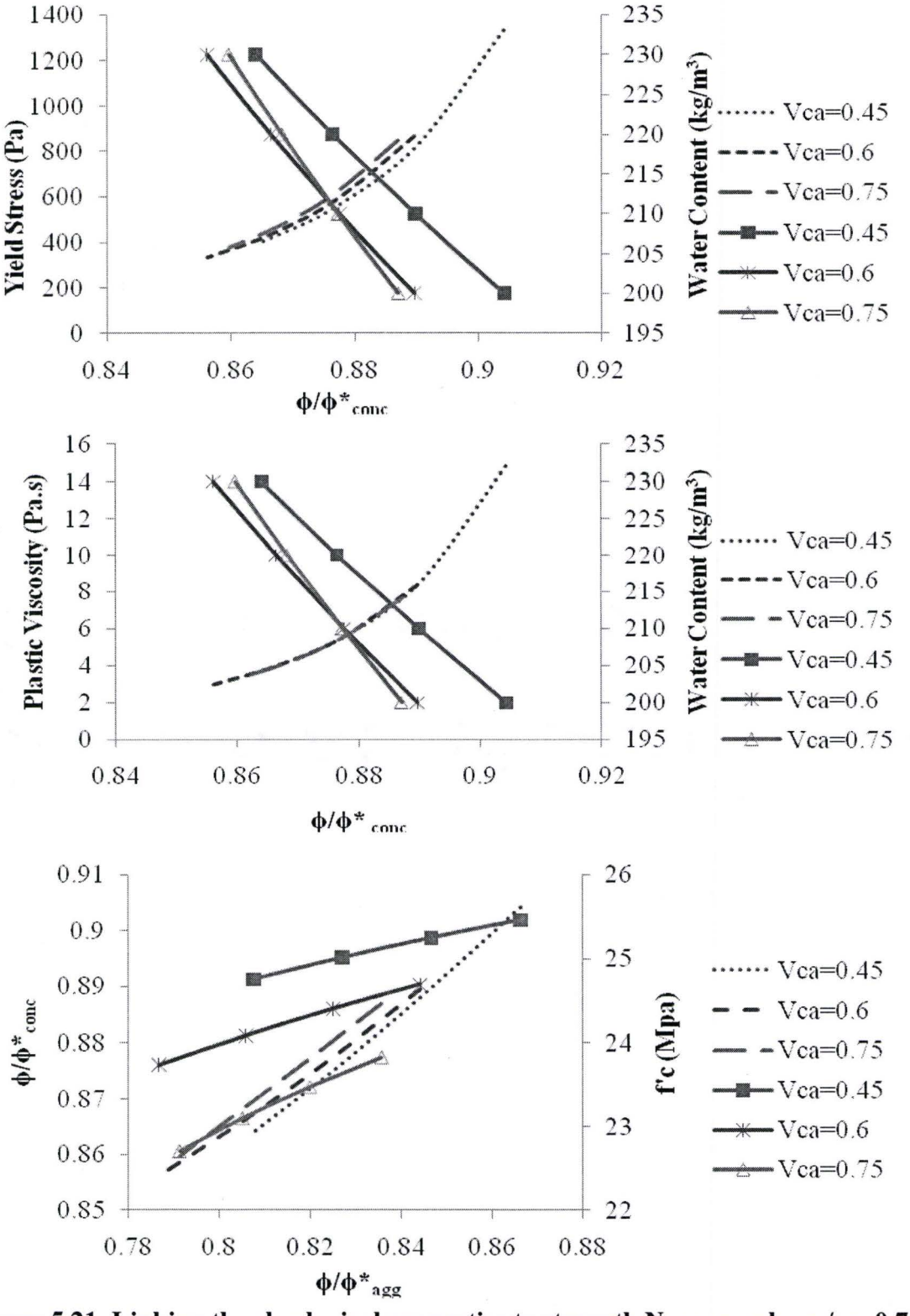

Figure 5.21. Linking the rheological properties to strength Nomograph - w/c = 0.70, 20 mm, non-air entrained (1.5% air)